Condensed Phase Membrane Introduction Mass Spectrometry

by

Kyle Daniel Duncan

B.Sc., Vancouver Island University, 2010

A Dissertation Submitted in Partial Fulfillment of the

Requirements for the Degree of

DOCTOR OF PHILOSOPHY

in the Department of Chemistry

Supervisory Committee

Condensed Phase Membrane Introduction Mass Spectrometry

by

Kyle Daniel Duncan

B.Sc., Vancouver Island University, 2010

Dr. Chris Gill, Co-Supervisor

(Department of Chemistry, Vancouver Island University)

Dr. Thomas Fyles, Co-Supervisor

(Department of Chemistry)

Dr. Dennis Hore, Departmental Member

(Department of Chemistry)

Dr. Erik Krogh, Departmental Member

(Department of Chemistry, Vancouver Island University)

Dr. Roberta Hamme, Outside Member

(Department of Earth and Ocean Sciences)

Abstract

Supervisory Committee

Dr. Chris Gill, Co-Supervisor
(Department of Chemistry, Vancouver Island University)

Dr. Thomas Fyles, Co-Supervisor
(Department of Chemistry)

Dr. Dennis Hore, Departmental Member
(Department of Chemistry)

Dr. Erik Krogh, Departmental Member
(Department of Chemistry, Vancouver Island University)

Dr. Roberta Hamme, Outside Member
(Department of Earth and Ocean Sciences)

Over the last few decades, membrane introduction mass spectrometry (MIMS) has been established as a robust tool for the on-line continuous monitoring of trace gases and volatile organic compounds. However, the range of amenable anlaytes has been limited by the need for molecules to pervaporate into a gaseous acceptor phase, or high vacuum environment of a mass spectrometer. This thesis expands the range of amenable analytes for MIMS to include larger, less volatile molecules (*e.g.,* 200 to 500 Da), such as pharmaceuticals, persistent organic pollutants, and small biomolecules. This was achieved through the use of a liquid|membrane|liquid interface. We distinguish the technique from conventional MIMS, which uses a gaseous acceptor phase, by inserting the prefix condensed phase to emphasize the use of a solvent acceptor phase — thus yielding CP-MIMS. An initial flow-cell interface with a methanol acceptor phase was characterized, yielding detection limits for model analytes in pptr to ppb, and analyte response times from 1-10 minutes. The flow cell interface was miniaturized into an immersion style CP-MIMS probe ($\sim$ 2 cm), which allowed for analysis of

smaller volume samples and improved membrane washing capabilities. Comparable detection limits were observed for the immersion probe, however, it was noticed that significant analyte depletion was observed for samples under 2 mL. In addition, each of the developed membrane interfaces were observed to suffer from ionization suppression effects from complex samples when paired with ESI. Several strategies for mitigating ionization suppression using CP-MIMS are presented, including the use of a continuously infused internal standard present within the acceptor solvent. The developed CP-MIMS system was challenged with the analysis of naphthenic acids (a complex mixture of aliphatic carboxylic acids) directly in contaminated real-world samples. The method used negative ESI to rapidly screen and mass profile aqueous samples for naphthenic acids (as $[M\text{-}H]^-$), with sample duty cycles $\sim$ 20 min. However, it was found that Negative ESI did not differentiate hydroxylated and carboxylated analytes, and both species contributed signal to the total naphthenic acid concentration. To increase method specificity for carboxylic acids, barium ion chemistry was used in conjunction with positive ion tandem mass spectrometry. Common product ions were used to quantify carboxylated analytes, while a qualifier ion was used to confirm the functionality. The increased selectivity afforded by the barium ion chemistry was at the cost of a modest increase in detection limits. CP-MIMS has been established as a technique capable of the direct analysis of real-world samples, and shows promise as a rapid screening method for amenable environmental contaminants and/or biomolecules.

Table of Contents

Supervisory Committee **ii**

Abstract **iii**

Table of Contents **v**

List of Tables **ix**

List of Figures **xi**

List of Abbreviations **xv**

Acknowledgements **xvii**

Dedication **xviii**

1 Introduction **1**

2 Initial characterization of a condensed phase membrane introduction mass spectrometry interface **6**

2.1 Introduction 6

2.2 Experimental 9

2.3 Results and Discussion 15

2.3.1 Parametric Studies 15

2.3.2 Sample Applications 26

2.4 Conclusion 32

3 A Miniature Condensed Phase Membrane Introduction Mass Spectrometry Probe for Measurements of Pharmaceuticals and Contaminants in Small Samples 34

3.1 Introduction 34

3.2 Experimental 37

3.3 Results and Discussion 42

3.3.1 Acceptor Phase Flow Rate Study 42

3.3.2 Membrane Washout Solvent Choice 43

3.3.3 Sample Mixing and Depletion Studies 45

3.3.4 Direct Calibration of Target Analytes 50

3.3.5 On-line Monitoring: Chlorination of Phenol 51

3.3.6 Automated Sample Introduction and Complex Sample Matrices 52

3.3.7 Direct, *In-vivo/In-Situ* Monitoring 56

3.4 Conclusion 58

4 Ionization suppression effects with condensed phase membrane introduction mass spectrometry: methods to increase the linear dynamic range and sensitivity 59

4.1 Introduction 59

4.2 Experimental 62

4.3 Results and Discussion 65

4.3.1 Ionization Suppression Studies 65

4.3.2 Linear Dynamic Range Studies 68

4.3.3 Measurements in Complex Sample Matrices 70

4.3.4 Stopped-Flow Quantitation 73

4.4 Conclusion 75

5 Semi-quantitative sceening and mass profiling of Naphthenic acids 77

5.1 Introduction 77

5.2 Experimental 81

5.2.1 Condensed phase membrane introduction mass spectrometry . 81

5.2.2 Mass spectrometry 82

5.2.3 Standard solutions and real world samples 83

5.2.4 Biochar adsorption studies 84

5.3 Results and Discussion 85

5.3.1 CP-MIMS verses dilution and direct infusion 85

5.3.2 Qualitative characterization of membrane permeable species in NA samples 87

5.3.3 Membrane performance characteristics 91

5.3.4 Semi-quantitative analysis of real world samples 93

5.3.5 Continuous monitoring of NAs in dynamic systems 97

5.4 Conclusion 99

6 Selective ionization and tandem mass spectrometric rapid screening of carboxylic acids from complex aqueous samples 101

6.1 Introduction 101

6.2 Experimental 104

6.2.1 Standard solutions and sample preparation 104

6.2.2 Mass Spectrometry method development 104

6.2.3 Condensed phase membrane introduction mass spectrometry . 105

6.3 Results and Discussion 106

6.3.1 Confirmation of diagnostic ions for quantitative screening purposes . . . 106
6.3.2 Direct analysis in wastewater effluent . . . 111
6.3.3 Non-targeted tandem MS screening of naphthenic acids . . . 113
6.4 Conclusion . . . 116

7 Conclusions **118**
7.1 Summary . . . 118
7.2 Recommendations for Future Work . . . 121

A Supplementary Figures **124**

Bibliography **128**

List of Tables

Table 2.1 Physical data and MS scan parameters for the target analytes studied. 13

Table 2.2 Instrumental detection limits and signal response times determined for a variety of analytes measured by CP-MIMS employing a PDMS HFM interface. 19

Table 2.3 Comparison of signal rise times and detection limits for selected target analytes obtained with Nafion and PDMS hollow fibre membranes 25

Table 2.4 Detection limits for MS/MS analysis of nonylphenol and estrone in DI, Nanaimo River water, and artificial urine. 28

Table 3.1 MS and physicochemical parameters. 41

Table 3.2 Comparison of membrane cleanup strategies 45

Table 3.3 Effect of sample mixing on signal response times and detection limits. 46

Table 3.4 Detection limit comparison for miniature probe verses flow cell type CP-MIMS interfaces 48

Table 3.5 Peak Height and Area Signal Relative Standard Deviations (RSD) for the Autosampler Implemented Miniature CP-MIMS Probe. . 56

Table 4.1 Analyte physicochemical properties and MS scan parameters. . . 64

Table 4.2 Aniline concentrations in complex aqueous samples determined by CP-MIMS, obtained using a continuously infused internal standard in the acceptor phase to correct for ionization efficiency variations. 72

Table 5.1 Selected water quality parameters for samples analyzed. 84

Table 5.2 Comparison of membrane geometries, response times, and detection limit estimates for selected NA isomer classes. 93

Table 6.1 Comparison of detection limits between negative mode ESI and positive tandem MS method or analytes in deionized water. . . . 113

List of Figures

Figure 2.1 Schematic diagram of the CP-MIMS experimental apparatus . . 11
Figure 2.2 Chemical structures of selected target analytes. 14
Figure 2.3 Plot of the signal to noise ratio versus CP-MIMS acceptor flow rate for signals obtained from 20 ppb aqueous solutions of 2,4-dichlorophenol using a PDMS HFM interface. 17
Figure 2.4 Representative calibration curve for aqueous nonylphenol analyzed by CP-MIMS (350 pptr–19 ppb) 18
Figure 2.5 Parametric investigation of the stopped flow acceptor phase enrichment of 2,4-dichlorophenol. 22
Figure 2.6 Typical analytical signals obtained for measurement of several target analytes using a Nafion membrane interface 24
Figure 2.7 Measurement of estrone and nonylphenol directly from complex matrices. 27
Figure 2.8 Full scan mass spectra for the measurement of 10 ppb nonylphenol and 800 ppb estrone in artificial urine by CP-MIMS and direct infusion ESI-MS of the same solution. 29
Figure 2.9 The use of CP-MIMS as a continuous on-line monitor for the bench scale chlorination of 2.5 μM (240 ppb) aqueous phenol buffered at pH 7. 31

Figure 3.1 Schematic diagram of the miniature CP-MIMS probe and experimental apparatus. 39
Figure 3.2 Plot of signal-to-noise (S/N) ratio versus CP-MIMS acceptor flow rate for signals obtained from aqueous solutions of 28 ppb 2,4,6-trichlorophenol and 78 ppb triclosan 43
Figure 3.3 Comparison of the signals for 78 ppb aqueous solutions of triclosan, including wash out times, using de-ionized water wash out and methanol wash out. 44
Figure 3.4 Demonstration of the continuous interrogation of smaller sample volumes of 70 ppb aqueous gemfibrozil with the miniature CP-MIMS probe. 49
Figure 3.5 Representative calibration curves for 2,4,6-trichlorophenol, triclosan, nonylphenol, and gemfibrozil in DI water 51
Figure 3.6 On-line monitoring of the chlorination of aqueous phenol at 25°C in an uncapped 40 mL glass vial. 53
Figure 3.7 Typical data for the miniature CP-MIMS probe when implemented in an automated analysis series of a variety of sample matrices spiked with ppb levels of target analytes. 55
Figure 3.8 Demonstration of continuous *in-situ* / *in-vivo* monitoring using the miniature probe. 57

Figure 4.1 Ionization supression caused by high concentration spikes of 2-methylquinoline (2-MQ) added to the sample. 67
Figure 4.2 CP-MIMS linear dynamic range for aniline, using APCI and ESI 69

Figure 4.3 Quantitation of aniline using a CP-MIMS immersion probe in spiked water samples (DI water; wastewater effluent; and artifical urine) at pH 8.5 using a continuously infused internal standard and ESI-MS 71

Figure 4.4 Stopped-flow mode quantitation of gemfibrozil at low pptr levels from aqueous DI samples. 74

Figure 5.1 Full scan negative ion mass spectrum of OSPW2 sample diluted a) 100× and b) 200× 87

Figure 5.2 CP-MIMS derived signal to noise ratios for three representative carboxylic acids (50 ppb) as a function of the sample pH 88

Figure 5.3 Kendrick mass defect plots for a standard Merichem naphthenic acid mixture obtained using direct infusion and CP-MIMS experiments 90

Figure 5.4 Selected ion monitoring chronogram of six water samples separated by a methanol wash between samples 95

Figure 5.5 Comparison NA quantification by full scan CP-MIMS and SPE-LC-MS/MS methods 97

Figure 5.6 Adsorption of Merichem naphthenic acids on aqueous suspensions of biochar samples A and B 99

Figure 6.1 CID mass spectra for lauric acid, lauric acid-d_2, and perfluorooctylethanoic acid in the presence of barium acetate. 107

Figure 6.3 CID mass spectra of 2-phenylethanoic acid, 3-phenylpropanoic acid, and 4-phenylbutanoic acid in the presence of barium acetate 109

Figure 6.4 Direct infusion of several carboxylated and hydroxylated compounds 110

Figure 6.6 Calibration of model compounds in wastewater effluent. 112
Figure 6.7 On-line tandem MS analysis of Merichem naphthenic acids spiked to a natural river water sample. 115

Figure A.1 High resolution full scan mass spectrum for direct infusion of 1 ppm refined Merichem (in methanol) 124
Figure A.2 Calibration curves for Merichem naphthenic acid mixture in aqueous solution 125
Figure A.3 Adsorption of Merichem naphthenic acids on aqueous suspensions of biochar samples A and B 126
Figure A.4 CID mass spectra of 2-ethyl-1,3-hexanediol in the presence of barium acetate 127

List of Abbreviations

2-MQ	2-methylquinoline
APCI	Atmospheric pressure chemical ionization
API	Atmospheric pressure ionization
APPI	Atmospheric pressure photoionization
CE	Capillary electrophoresis
CID	Collision induced dissociation
CP-MIMS	Condensed phase membrane introduction mass spectrometry
DCP	Dichlorophenol
DI	Deionized
ESI	Electrospray ionization
FTICR-MS	Fourier transform ion cyclotron resonance mass spectrometry
FTMS	Fourier transform mass spectrometry
GC	Gas chromatography
GW	Groundwater
HFM	Hollow fibre membrane
HPLC	High pressure liquid chromatography
LC	Liquid chromatography
LDR	Linear dynamic range
MIMS	Membrane introduction mass spectrometry

MS	Mass spectrometry
MS/MS	Tandem mass spectrometry
NA	Naphthenic acids
OSPW	Oil sands process water
PDMS	Polydimethylsiloxane
PPCP	Pharmaceuticals and personal care products
PyBA	Pyrenebutyric acid
QA/QC	Quality assurance and quality control
SIM	Selected ion monitoring
SPE	Solid phase extraction
SPME	Solid phase micro-extraction
SVOC	Semi-volatile organic compound
SW	Surface water
TFCM	Thin film composite membrane
TIC	Total ion current
TOC	Total organic carbon
VOC	Volatile organic carbon

ACKNOWLEDGEMENTS

I want to express my deepest thanks to both Dr. Chris Gill and Dr. Erik Krogh. Without either of you, I would never have found my interest for Chemistry in the first place. The opportunities you have afforded me have been incredible, and the guidance and support from both of you has made this project possible.

I would also like to thank Dr. Tom Fyles for grounding discussions, clear perspective, and time spent in making this document a cohesive package. In addition, appreciation is given to my committee members Dr. Dennis Hore and Dr. Roberta Hamme for their effort and critical insight.

Thank you to the AERL group members, who have made the years of this project extremely enjoyable. Particularly, I would like to acknowledge Nick Davey and Dr. Ryan Bell for their insightful comments and sarcastic remarks. The discussions shared within the office have both grown my cynicism, and added much needed perspective into the workings of our world.

I would also like to acknowledge my close Nanaimo friends for the much needed beverage breaks and activities, constantly reminding me to restore some sort of work/life balance. Further, I thank my Pine/Fry street family Brad Fraser and Lumi VanGrootheest for delicious family meals, and a wonderful place to live. Chelsea Klein — your continuing support, kindness, and lasting understanding has turned me around in times of difficulty, and given me the drive to keep moving — thank you. Lastly I would like to express my deepest acknowledgement to my Family: Lucie Thivierge; Randy Duncan; and Corrina Duncan. The support you have given me over the years has enabled me to keep studying and find my true passion.

DEDICATION

To Lucie and Randy

Chapter 1

Introduction

With the advent of new sensitive analytical methodologies and instrumentation, organic micro-pollutants have been observed in surface waters, wastewaters, and elsewhere throughout our natural environments [1,2]. These include compound subclasses such as pharmaceuticals, personal care products, pesticides, herbicides, and other persistent organic pollutants. Sampling protocol for these types of analytes typically entails filling discrete bottles at several locations to ascertain the concentration, fate, and spatial distribution of the contaminant in question. Further, proper sampling protocol dictates that a number of blank and/or spiked samples must be collected to ensure proper quality assurance and control (QA/QC). This can lead to an inordinate number of samples to transport to an appropriate analytical facility, which drives up the cost of field sampling campaigns.

Once the samples reach the lab, the majority of methods require significant sample clean-up before chromatographic separation, and often mass spectrometric detection. To reach desired detection limits, often litre size samples must be extracted and preconcentrated into mL or μL volumes. Standard lab protocols require further quality control measures, such as the addition of method blanks and/or spikes - often result-

ing in more than one QA/QC sample for each real sample. All of this sample work up and QA/QC requires time and highly trained personnel, which in turn increases the cost to the consumer for the analysis for organic micro-pollutants at commercial analytical facilities. In addition, while these methods are sensitive and precise, the data obtained represent snapshots in time, and may not be indicative of the actual spacial or temporal distribution of analytes. To better understand analytes in their natural dynamic systems, high throughput methods would be better suited – where many samples can be analyzed quickly, and without prohibitive cost.

This potential for increasing data density is a reason online analytical approaches have been growing in the literature. A quick Web of Science topic search for 'online method' in the analytical chemistry category returns a total of 3387 hits from 1985 to 2014. Each five year period shows an increase in the number of publications, with 10 papers published from 1985 to 1989, and 1243 published from 2011 to 2014. Online methods reduce labour and increase autonomy, which can decrease human error and increase method reproducibility. One of the most popular online methods for the analysis of organic micro-pollutants is online solid phase extraction (SPE) [3]. All sample work-up (including extraction, dilution, and measurement) can be done by a robotic autosampler. This method then requires chromatographic separation, prior to analytical detection. Chromatographic methods for the separation of multicomponent mixtures of analytes are often not trivial to develop. Even with the m/z discrimination afforded by mass spectrometric detection, co-eluting species can cause problems in quantitation, and matrix effects can interfere with method reproducibility.

An alternative technique, which eliminates chromatographic separation, is membrane introduction mass spectrometry (MIMS). This on-line approach utilizes a semi-permeable membrane (*e.g.,* polydimethylsiloxane, PDMS) to interface a mass spectrometer directly to a sample. Analytes partition into the membrane material, diffuse

through the membrane, and desorb into an acceptor phase(*e.g.,* flowing He), or high vacuum environment, where they are directed to the mass spectrometer for detection. With PDMS, the membrane acts to preclude charged species (*e.g.,* salts), and allow selective transport of amenable analytes (hydrophobic). Key advantages of this technique include minimal sample preparation, direct *in situ* measurements, and continuous monitoring capabilities. For the analysis of discrete samples, sample duty cycles are a function of membrane permeation kinetics. Method selectivity arises from membrane perm-selectivity and m/z discrimination and/or tandem mass spectrometric transitions. Currently, MIMS is primarily used for the direct analysis of volatile organic compounds (VOCs) from air and/or aqueous samples [4]. While this technique works well for VOCs, semi-volatile and non-volatile compounds typically suffer from lengthy membrane response times. This limitation arises because of the need for analytes to desorb from the inner surface of the membrane material into the gas phase.

The purpose of this thesis is to expand the range of MIMS amenable analytes to include larger, less volatile molecules (*e.g.,* 200 to 500 Da), such as molecules of environmental and bioanalytical concern (*e.g.,* pharmaceuticals, personal care products, fatty acids, and hormones). We propose to achieve this with a liquid–membrane–liquid interface, henceforth termed CP-MIMS (to highlight the use of a condensed, liquid, acceptor phase). Permeating analytes will then be solvated by the liquid acceptor, rather than desorb into a gaseous acceptor phase. Inclusion of a liquid acceptor solvent results in a shift of suitable ionization sources. Rather than conventional electron ionization, atmospheric pressure ionization sources are required (*e.g.,* electrospray ionization) to eliminate solvent. In addition, the use of a liquid acceptor phase enables easy modification (*e.g.,* addition of acid/base) to enhance membrane transport, ionization efficiency, and/or m/z discrimination.

CP-MIMS differs from conventional chromatographic methods in that multiple analytes may permeate the membrane and reach the mass spectrometer at one time. Therefore analyte discrimination is a result of unique m/z or tandem mass spectrometric transitions. Elution time as an added separation metric allows chromatographic methods greater specificity. However, direct sampling and the relatively short duty cycles of CP-MIMS could minimize the number of samples that are sent for conventional analysis by more robust separation techniques (*e.g.,* LC-MS/MS). In addition, with the recent advent of field portable atmospheric pressure ionization mass spectrometers, it is conceivable that CP-MIMS could be employed for the rapid on-site analysis of organic micro-pollutants. This method could greatly minimize the number of samples shipped for external analysis, and help researchers better understand the spatial and temporal distribution of environmental contaminants. Further, in circumstances where time is of the essence (*e.g.,* spill response), a portable CP-MIMS system could provide information in a more timely manner, informing better decision making regarding potential remediation.

Chapter 2 attempts to establish CP-MIMS in a lab setting, and characterize analytic performance measures such as detection limits, response times, and linear dynamic range. In addtion, the breadth and type of analytes which are able to be analyzed are explored. Once a working apparatus was characterized, Chapter 3 focuses on the construction and characterization of a CP-MIMS immersion probe more suitable for smaller samples. Chapter 4 identifies ionization suppression issues often observed in electrosrpay ionization as a potential problem, and provides potential strategies for their mitigation using CP-MIMS. In an effort to work with real-world samples, Chapter 5 discusses efforts to detect and quantify naphthenic acids (a complex assemblage of environmentally relevant analytes associated with oil sands process waters). Lastly, Chapter 6 presents a strategy to increase specificity for carboxylated

analytes (*e.g.,* naphthenic acids) through barium ion chemistry and tandem MS in positive ion mode.

This thesis comprises work that has been published. Each chapter is a stand alone paper that contains the pertinent introductory material, experimental details, and discussion of results. The final chapter of the thesis unifies each project and highlights challenges faced, avenues for further work, and some potential applications going forward.

Chapter 2

Initial characterization of a condensed phase membrane introduction mass spectrometry interface

Reproduced with permission from Duncan, K.; McCauley, E.; Krogh, E.; Gill, C. "Characterization of a condensed-phase membrane introduction mass spectrometry (CP-MIMS) interface using a methanol acceptor phase coupled with electrospray ionization for the continuous on-line quantitation of polar, low-volatility analytes at trace levels in complex aqueous samples." *Rapid Commun. Mass Spectrom.*, 25, 1141-1151 (2011). Data collection and preliminary analysis by K. Duncan. Erin McCauley was involved in preliminary work involving fluid handling and interface integrity. The publication was drafted by C. Gill, with additional editorial contribution from E. Krogh and K. Duncan.

2.1 Introduction

The technique of membrane introduction mass spectrometry (MIMS) has been used for decades as a method for directly monitoring analytes in air and water samples via mass spectrometry [5, 6]. The membrane acts as a semi-permeable barrier that rejects the sample matrix and allows analytes to pass through for direct analysis (as a mixture) by the mass spectrometer. Aside from differences in permselectivity at the membrane level, analyte species admitted to the mass spectrometer are discriminated by unique masses, ion chemistry (*e.g.,* selective chemical ionization for target

analytes) and/or by tandem mass spectrometry. Several reviews describe MIMS research trends [7], environmental applications [4] and its role in process analytical chemistry [8]. In this way, MIMS is part of a recent wave of MS-based techniques that minimize sample preparation and make it possible to carry out direct on-line analysis in complex samples.

The overall mass transfer of analyte across a semi-permeable membrane, on the molecular level, involves partitioning into the membrane material, diffusion through the membrane, and partitioning out of the membrane at the opposite surface. This process is driven by a concentration gradient, which is maintained by removing the analyte on the downstream (acceptor) side. Enrichments occur at the membrane level due to the relative solubility of analyte in the sample and membrane material. The overall mass transport is governed by Ficks Law [9]. To date, the majority of MIMS techniques involve polymer membranes (*e.g.,* polydimethylsiloxane) that separate samples (typically gaseous or liquid samples) from a gaseous acceptor phase for analyte transfer to the ion source of the mass spectrometer. The acceptor phase may be a specific carrier gas such as helium or simply the high vacuum environment of the MS.

With conventional MIMS, analytes are removed from the membrane by desorption into the gas phase (the overall process termed pervaporation). In principle, the pervaporation of analytes through a membrane can be limited by their physical-chemical properties that affect solubility, diffusivity and volatility. Conventional MIMS using PDMS interfaces is sensitive down to parts-per-trillion levels with measurement response times down to seconds for small, hydrophobic volatile analytes. Larger, semi-volatile analytes are slower to permeate the membrane and consequently suffer from somewhat longer measurement response times and lower sensitivity at ambient temperature. A number of researchers have improved the pervaporation of semi-

volatile analytes by using various heating strategies [10–17], laser desorption [18], plasma desorption [19, 20], ambient sonic spray ionization [21] and/or by using alternative membrane substrates [22–24]. The adaptation of conventional MIMS for the analysis of molecules with low volatility (*e.g.,* large, highly polar and/or charged species) has been accomplished by chemical derivatization of these analytes before measurement [15, 25, 26] or strategies that produce volatile fragment molecules from the analyte, including the use of enzymes immobilized on the membrane surface [27]. The on-line performance characteristics of conventional MIMS (favoring relatively volatile analytes) are seriously limited for many molecules of environmental and bioanalytical significance because many are large, polar and/or charged compounds. A powerful variant on the MIMS approach that can address this limitation is accomplished by using a condensed (liquid) acceptor phase and a suitable direct liquid ionization technique such as electrospray (ESI) or atmospheric pressure chemical ionization (APCI) [28]. Conventional MIMS with a gaseous acceptor phase uses physical gradients that are inherently dissipative. More powerful flux coupling mechanisms, such as those exploited in natural membrane systems, can only arise with a condensed (liquid) acceptor phase. The underlying principles of coupled membrane transport systems have been known for more than a decade [29], yet many novel directions have remained unexplored for lack of a suitable analytical tool. We refer to the hybrid approach, using a liquid acceptor phase, as condensed phase MIMS (CP-MIMS).

Although there is great potential for CP-MIMS as an analytical technique, there have been relatively few publications in this area to date. Tomlinson and Naylor presented a cartridge membrane based pre-concentrator for protein analysis by capillary electrophoresis-mass spectrometry (CE-MS) [30]. Lee and co-workers developed an elegant micro-membrane chromatography technique utilizing a capillary mounted, porous and hydrophobic polyvinylidene fluoride sheet membrane directly coupled with

an electrospray ionization (ESI) emitter for post digest protein separation [31–33] prior to MS detection. Creaser *et al.* also utilized a polyvinylidene fluoride sheet membrane interfaced with atmospheric pressure chemical ionization (APCI) to measure starting materials and products for injected 20 μL aliquots of a highly concentrated pharmaceutical reaction mixture [34]. VanHassel and Bier demonstrated a heated polydimethylsiloxane hollow fiber membrane interface directly attached to an ESI capillary for the ppb – pptr level analysis of volatile and semivolatile organic compounds (VOCs and SVOCs) in 250 μL loop injected aqueous samples [35].

We report the development of a CP-MIMS system, using methanol as an acceptor phase in the lumen of a capillary HFM, with improved performance characteristics over those published previously [34, 35]. We demonstrate the use of our on-line CP-MIMS system in a continuous monitoring mode or in a trap-and-release mode, which further enhances analytical sensitivity. The optimization of fluid handling parameters as well as the detection limits and signal response times for a range of analytes and sample matrices is examined, using negative ion electrospray ionization (ESI) with both selected ion monitoring (SIM) and tandem mass spectrometry (MS/MS) for analyte detection. A comparison between CP-MIMS and direct infusion ESI is presented for trace analytes in high ionic strength samples. Our improved CP-MIMS system has been used with both PDMS and Nafion polymer HFMs, and because of superior fluid handling characteristics, it will facilitate future investigations with more delicate membrane assemblies.

2.2 Experimental

The mass spectrometer used for this work was a triple quadrupole system (Micromass Quattro LC, Waters-Micromass, Altrincham, Cheshire, UK) equipped with a

high flow electrospray ionization (ESI) probe, Z-Spray source. Nitrogen gas for the ESI source (UHP grade, 99.999% pure) was supplied from a pressurized liquid nitrogen dewar and argon collision gas (also UHP) was supplied from a compressed gas cylinder (Praxair Inc., Nanaimo, BC, Canada). For these experiments, the vacuum system base pressure for the mass analyzer was $\sim$7 x 10^{-7} Torr. All experiments were performed in negative ion mode with an ESI capillary voltage of -2.2 kV and a cone voltage of -43 V. Desolvation gas flow was set to 750 L per hour at 350°C and the cone curtain gas was set to 60 L per hour. Selected ion monitoring (SIM) was used for the detection and quantification of most analytes used in this study, except where noted when MS/MS was used for greater specificity. For the MS/MS experiments, the collision cell was maintained at a pressure of 2 mTorr, using collision induced dissociation (CID) energies of 30 eV for nonylphenol and 36 eV for estrone under these conditions.

The CP-MIMS interface developed for this work is based upon a flow-over capillary hollow fiber membrane (HFM) design that we have described in previous work [36]. Figure 2.1 is a schematic diagram of the experimental apparatus. A 10 cm length of the desired HFM was mounted on two short lengths of stainless steel hypodermic tubing (22 Gauge, Vita Needle Company Inc., Needham, MA, USA). Membrane materials used for this work included HFM made from polydimethylsiloxane (PDMS, 0.94 mm OD, 0.51 mm ID, Silastic Brand, Dow Corning, Midland, MI, USA) and Nafion (0.84 mm OD, 0.64 mm ID, Perma Pure LLC, Toms River, NJ, USA). The membrane assembly was then mounted in a flow cell made from 0.25 stainless steel tubing and Swagelok compression fittings (Supleco, Bellefonte, PA, USA) using graphite-vespel chromatographic ferrules (Restek, Bellefonte, PA, USA). The exposed ends of the hypodermic tubing were attached to 1/16 OD PEEK tubing using low dead volume PEEK unions (VICI Valco, Brockville Ont., Canada). The solvent reservoir

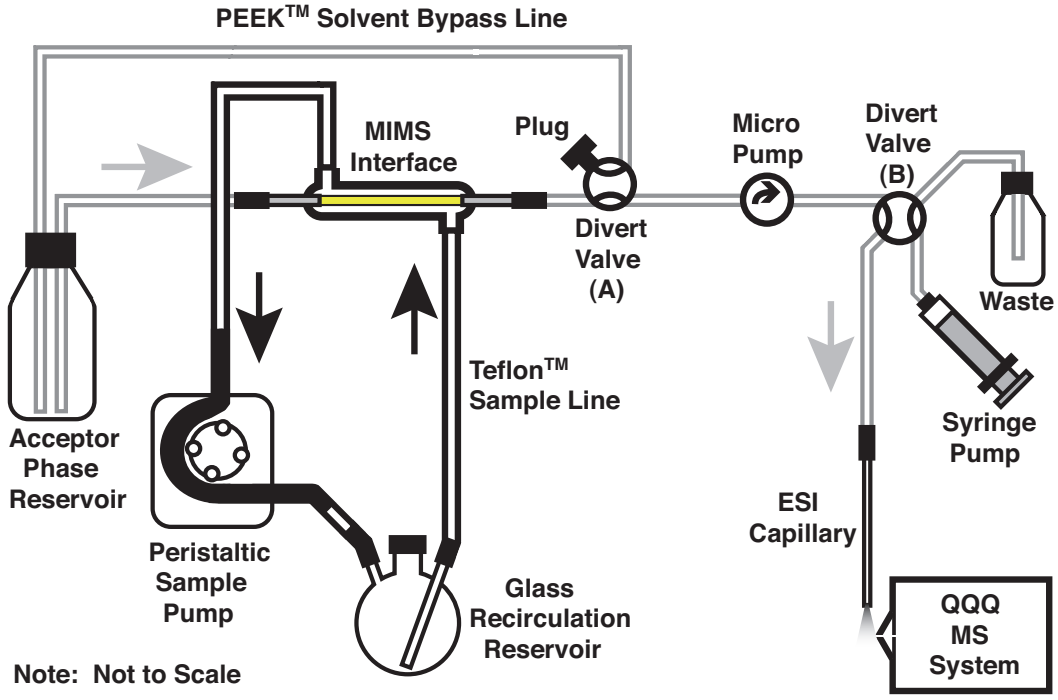

Figure 2.1: Schematic diagram of the CP-MIMS experimental apparatus. For stopped acceptor flow experiments, divert valve A was actuated so that the MIMS interface was off-line and the flow of acceptor stopped for prescribed intervals. The plug in one port of divert valve A prevented the incidental draining of the acceptor phase from the MIMS during the stopped-flow periods. To quantify analyte levels in the acceptor phase, standard solutions were directly infused from a syringe pump by actuating divert valve B.

was connected to the MIMS interface with large bore PEEK tubing (0.76 mm ID) to minimize reduced pressure at the membrane during operation. The remainder of the PEEK tubing used was 0.25 mm ID to reduce internal dead volume and achieve higher linear velocities in the transfer lines between the membrane interface and the electrospray ion source. The precision in-line pump used to deliver solvent from the interface to the electrospray source was a prototype four piston micro pump (Cheminert Model M6, VICI Valco Instruments Co. Inc., Houston, TX, USA). Control of the pump was accomplished with the manufacturer supplied interface hardware and software using the mass spectrometer data collection computer. A standard 500 mL HPLC glass solvent reservoir (Sigma Aldrich, Oakville, Ont., Canada) was used to supply the

methanol acceptor phase, which was degassed via helium gas (UHP grade, 99.999% pure, Praxair) sparging before and during operation. For stopped flow/enrichment studies, a four port 1/16 tubing divert valve (Model VE4WC, VICI Valco Instruments Co. Inc., Houston, TX, USA) was used to supply pure methanol to the electrospray source when the membrane acceptor solvent flow was stopped.

For direct calibration of analyte levels in the acceptor phase, dilute standards prepared in methanol were infused directly to the ESI probe at 500 μL per minute with a syringe pump (Model 70-2205 Econoflow Syringe Pump, Harvard Apparatus, St. Laurent, QC, Canada) via the mass spectrometer internal flow divert valve. Reagents, solvents and target analytes were obtained from a variety of suppliers and were ACS grade or better unless otherwise noted. Abietic acid (Tech grade, 70%), triclosan, ibuprofen, 4-bromobenzoic acid, phenol, 2-chlorophenol, 2,4-dichlorophenol, 2,4,6-trichlorophenol, nonylphenol, estrone, ethynylestradiol, sodium L-lactate, and sodium chloride were all obtained from Sigma Aldrich (Oakville, Ontario, Canada). HPLC grade methanol, sodium citrate, urea, sodium bicarbonate, sodium hypochlorite (as 5% active chlorine solution), magnesium sulfate, sodium sulfate, potassium dihydrogen phosphate and dipotassium hydrogen phosphate were obtained from Fisher Scientific (Ottawa, Ontario, Canada). Calcium chloride and ammonium chloride were both purchased from BDH Chemicals, Mississauga, Ontario, Canada. Table 2.1 lists the target analytes studied, relevant MS scan parameters and pertinent physical properties. Figure 2.2 gives the chemical structures of selected target analytes.

Aqueous samples and standards were circulated at ambient conditions (1 atm, 25 C) through the CP-MIMS interface using a peristaltic pump system (Model 77200-62 Masterflex Easy-Load II with LS-25 Viton pump tubing, Cole-Parmer, Vernon Hills, IL, USA). The 500 mL glass sample reservoir used (Figure 2.1) was constructed in house, and was equipped with a Teflon faced septum port for injecting small aliquots

Table 2.1: Physical data and MS scan parameters for the target analytes studied.

Target Analyte	CAS #	Molar mass (g mol^{-1})	Vapour Pressure [a] (Pa @ 25^oC)	Log K_{ow} [a]	Molar Volume [b] cm^3	MS Scan Parameters m/z
Abietic acid	514-10-3	302.45	4.3 x 10^{-5}	6.46	270	SIM 301
4-Bromobenzoic acid	586-76-5	201.02	1.3 x 10^{-3}	2.86	120	SIM 199+201
2-Chlorophenol	95-57-8	128.56	316	2.19	100	SIM 127
2,4-Dichlorophenol	120-83-2	163	15.8	3.09	112	SIM 161+163
2,4,6-Trichlorophenol	88-06-2	197.45	2.3	3.67	124	SIM 195+197+199
Estrone	53-16-7	270.37	3 x 10^{-8}	3.25	230	SIM 269 MS/MS 269 $\rightarrow$ 145
Ethynylestradiol	57-63-6	296.44	3.6 x 10^{-7}	3.67	245	SIM 295
Ibuprofen	5687-27-1	206.28	2.5 x 10^{-2}	3.97	200	SIM 205
Nonylphenol	25154-52-3	220.35	1.15	5.76	236	SIM 219 MS/MS 219 $\rightarrow$ 133
Phenol	108-95-2	94.11	61.7	1.44	88	SIM 93
Triclosan	3380-34-5	289.54	8.6 x 10^{-5}	4.76	195	SIM 287

[a] Obtained from SRC Physical Properties Database [37]
[b] Calculated using ACD Software [38]

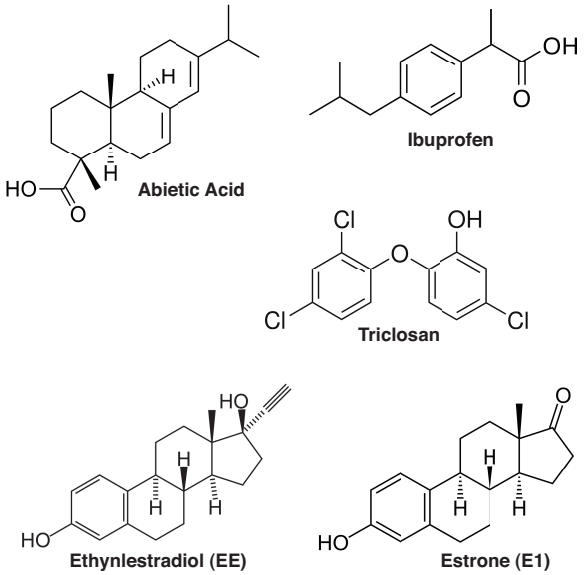

Figure 2.2: Chemical structures of selected target analytes.

of standards prepared in methanol or de-ionized (DI) water via analytical syringes. The flow path of the aqueous sample system was constructed with short lengths of 0.25 OD Teflon tubing (Cole-Parmer, Vernon Hills, IL, USA), using short lengths of LS-25 Viton pump tubing as unions at the glass reservoir. All aqueous standards were prepared from high purity DI water (Model MQ Synthesis A10, Millipore Corp., Billerica, MA, USA). For all aqueous experiments, the interface was flushed with DI water between runs until a stable baseline signal was observed. Signals for standards were characterized by their background subtracted intensities at steady state for analytical calibration and by their 10-90% signal rise times. All detection limits presented are based on a signal-to-noise ratio (S/N) of 3. Sample matrices used for this work included natural water and a surrogate biological sample (artificial urine), prepared as follows. Nanaimo River water (a clear, oligotrophic freshwater supply typical of surface waters in coastal British Columbia sampled in June 2010) was filtered through a 0.45 μm membrane filter (Durapore, Millipore Corp. Billerica, MA, USA) before use. This natural water sample was pH 6.9 ± 0.1 (Model AR25 Accumet Research

pH Meter, Fisher Scientific, Ottawa, Ontario, Canada), had a specific conductivity of 40 ± 5 μS/cm (or $\sim$20 ppm total dissolved solids, measured using a Model AR20 Accumet Research Conductivity Meter, Fisher Scientific, Ottawa, Ontario, Canada), and a total dissolved organic carbon content of 1.1 ± 0.1 ppm (as non-purgeable organic carbon, measured using a TOC-V Total Organic Carbon Analyzer, Shimadzu Scientific Instruments Columbia, MD, USA). Artificial urine solution was prepared with DI water and contained 25 mM ammonium chloride, 2.5 mM calcium chloride, 2.0 mM magnesium sulfate, 25 mM sodium bicarbonate, 7.0 mM potassium dihydrogen phosphate, 7.0 mM dipotassium hydrogen phosphate, 90 mM sodium chloride, 10 mM sodium sulfate, 2.0 mM citric acid, 1.1 mM lactic acid and 170 mM urea, with pH of 6.0 adjusted by the addition of 1.0 M hydrochloric acid [39, 40]. For the chlorination of phenol, DI water was buffered at pH 7 by adding 10 mL of a 0.5 M phosphate buffer [41]. This solution was re-circulated over a PDMS HFM in a closed loop at 300 mL per minute and fortified with a standard solution of phenol to a final concentration of 240 ppb. After 5 mins, a stock solution of sodium hypochlorite was added to yield an initial dose of active chlorine of 5 ppm as Cl_2.

2.3 Results and Discussion

2.3.1 Parametric Studies

Acceptor and Sample Flow Rate

We have evaluated the influence of both the acceptor and sample flow rates on sensitivity and signal response time using a 20 ppb aqueous solution of 2,4-dichlorophenol. For all the work presented, the membrane interface was operated at ambient pressures and temperatures (1.00 ± 0.05 atm, 25 ± 2 °C). We do not observe substantial variations in either sensitivity or signal response time resulting from minor day-to-

day fluctuations in either parameter. Figure 2.3 shows that the signal to noise ratio increases with increasing acceptor flowrates up to 500 μL/min. At lower acceptor phase flows, signal noise was much more pronounced because of flow pulsing from the micro pump, leading to instability in the ESI source, producing erratic signals. At the higher flow rates, the noise is greatly diminished, but at the same time the signal intensity also decreases. This is the result of increased dilution of the permeant in the acceptor phase. During this study, it was also noted that the signal response time (as measured by time required for the analyte signal to rise from 10-90% of the steady state value) was longer at low acceptor flow rates and decreased to constant value (t_{10-90} = 1.2 minutes, data not shown) at acceptor flows greater than 200 μL per min. This suggests that the observed signal response times above this threshold flow rate were mainly due to membrane transport phenomena rather than post-membrane diffusional broadening and mixing resulting from slower linear velocities in the solvent handling system. An acceptor phase flow rate of 500 μL/min was used in subsequent studies to minimize solvent consumption while maintaining optimum performance. Varying the aqueous sample re-circulation flow rate over the interface from 220–370 mL per minute did not alter the observed CP-MIMS signal intensity. Thus, a sample flow rate of 300 mL per min was used for all subsequent experiments.

Quantification, Signal Response Times and Detection Limits for Selected Target Analyte

The analytical performance of the interface was evaluated for a variety of relatively non-volatile target analytes (see Table 2.1 for physical properties). Figure 2.4 represents a typical analytical calibration curve for aqueous nonylphenol at the pptr–ppb level, illustrating excellent linearity. The inset in this figure shows the analytical

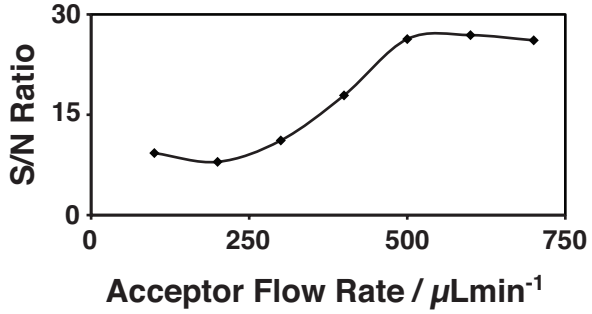

Figure 2.3: Plot of the signal to noise ratio versus CP-MIMS acceptor flow rate for signals obtained from 20 ppb aqueous solutions of 2,4-dichlorophenol using a PDMS HFM interface. At $\sim$ 500 μL per minute, an optimum in the signal to noise exists. This acceptor phase flow rate was used for all subsequent work.

signal for a 5 ppb standard re-circulated over the membrane. Each point in the calibration curve was determined by averaging $\sim$ n>100 background subtracted measurements obtained for the maximum signal levels for each respective standard. It should be noted that the signal rise time (t_{10-90} = 8.2 minutes) is indicative of the analytical response for this analyte. The signal fall time is slightly longer, which is the result of the wash out between samples, including rinsing the entire aqueous recirculation apparatus (Figure 2.1). This would be reduced by the incorporation of a sample/rinse switching valve near the membrane, easily incorporated in the next generation of this device. Detection limits and signal response times using a PDMS HFM interface and a methanol acceptor phase for the target analytes studied were determined for standard solutions using signal averages as described above for Figure 2.4, and are summarized in Table 2.2. We report our detection limits based upon S/N = 3 (one significant figure) and signal rise times (two significant figures), to facilitate comparisons with the work of others. Replicate experiments (n = 3–5) were performed in all cases to ensure reproducibility for the quoted values. Target analytes for this study were selected based upon their environmental or biological relevance and upon their observed poor analytical performance (either impractically long signal rise times and/or lack of analytical sensitivity) using isothermal MIMS systems employ-

ing a gaseous acceptor phase [10]. It should be noted that some of these compounds listed in Table 2.2 can be measured using gas phase MIMS techniques at elevated temperatures [10–20] or by chemical derivatization followed by MIMS analysis at ambient temperatures [15, 25, 26]. However, the use of the CP-MIMS approach is less harsh or involved, achieves superior results and can be chemically tuned with the appropriate combination of membrane material and solvent. The vapour pressures of target analytes at ambient temperature (Table 2.1) range from several hundred Pa (chlorophenol) to $\sim 10^{-8}$ Pa (estrone). Analytes with vapour pressures less than $\sim 10^{-3}$ Pa (*e.g.,* abietic acid, triclosan) are difficult to desorb into a carrier gas even with thermal assistance.

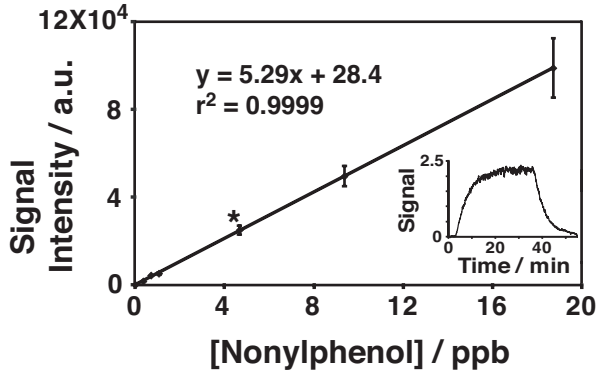

Figure 2.4: Representative calibration curve for aqueous nonylphenol analyzed by CP-MIMS (350 pptr–19 ppb). The analytical signal for the 4.7 ppb standard (*) is shown in the inset. Error bars represent ± 1 standard deviation for the average of each signal measurement.

Table 2.2: Instrumental detection limits and signal response times determined for a variety of analytes measured by CP-MIMS employing a PDMS HFM interface.

Target Analyte	Measured Conc. ppb	t_{10-90}	Detection Limit * ppb
Abietic Acid	37	5.9	10
4-Bromobenzoic acid	247	2.1	5
2-Chlorophenol	20	0.70	1
2,4-Dichlorophenol	20	1.2	0.1
2,4,6-Trichlorophenol	20	1.7	0.05
Estrone	302	8.1	10
Ethynylestradiol	607	11	100
Ibuprofen	274	3.3	5
Nonylphenol	23	8.2	1
Phenol	349	1.8	100
Triclosan	20	7.4	1

* All DLs are based on Signal/Noise equal to 3

Detection limits of our CP-MIMS system are governed by enrichment factors at the membrane level (which are largely driven by analyte specific solubilities) and factors that influence ionization efficiency at the ESI. We report detection limits ranging from 50 pptr for 2,4,6-trichlorophenol to 100 ppb for phenol. We attribute this difference to increased ionization efficiencies of the ESI anticipated in negative ion mode. On the other hand, the two orders of magnitude difference we observe in the detection limits of nonylphenol over phenol are likely due to differences in the their respective solubility parameters, as reported by the octanol-water partition coefficients (K_{ow}) listed in Table 2.1 for the target analytes used in this study. The

detection levels we report are consistent with work presented for an earlier generation of CP-MIMS type interface developed by the Bier group based on a flow injection sampling system, where 250 μL sample plugs are flowed over the outside of a HFM with the acceptor phase in the lumen entrained to a mass spectrometer for analyte detection [35]. Because we are interested in developing continuous on-line monitoring capabilities to temporally resolve analyte concentrations, we have also characterized the signal response times for target analytes.

The signal response time is measured by the time required for the analytical signal to rise from 10-90% of its steady-state value in response to a slug injection of analyte into an aqueous sample, which is continuously flowed over the outer surface of our HFM in the interface assembly. The response time is largely governed by the diffusion rate of the analyte through the membrane, which to a first approximation is related to its molar volume. In general, smaller molecules will diffuse through PDMS faster than larger ones, as can be seen by the t_{10-90} response times reported in Table 2.2. Our response times range from $\sim$1 to 10 minutes for the target analytes. Generally, the longest response times are associated with the largest analytes (ethynylestradiol, estrone, nonylphenol, triclosan and abietic acid), which have molar volumes of $\sim$200 cm^3 mol^{-1} or greater (Table 2.1). To study dynamic chemical processes (*e.g.,* chemical reaction kinetics, such as those illustrated in Figure 2.7 below), the signal rise times must be faster than the process being studied, otherwise valuable temporal resolution for the measurement(s) is lost or complicated by membrane transport kinetics.

Stopped Acceptor Flow Mode

Because the CP-MIMS system can be operated with a continuous flow of acceptor phase (continuous monitoring mode) or with a static plug of acceptor phase in the membrane lumen (stopped flow mode), we have undertaken a comparison of the relative enrichment factors. In this study, an aqueous solution containing 8.5 ppb of 2,4-dichlorophenol (DCP) was re-circulated over a PDMS HFM containing methanol. When the methanol was continuously flowed to the ESI at 500 μL min^{-1}, the concentration of DCP in the acceptor phase was determined to be 0.58 ppb. The acceptor phase concentrations were quantified directly by using a series of DCP standards in methanol introduced at divert valve B (see Figure 2.1). However, when the acceptor phase is stopped and allowed to equilibrate with the membrane interface, the enrichment of DCP increases dramatically. Figure 2.5a shows intensity of the DCP signal as a function of the acceptor phase stop time. This is accomplished in our system by actuating divert valve A (Figure 2.1). In Figure 2.5b, we convert the signal intensity to an enrichment factor by dividing the concentration of analyte in the acceptor phase with that in the aqueous sample. As can be seen, a 12-fold enrichment is observed for DCP when the acceptor phase is stopped for $\sim$15 minutes. No further analyte enrichment was observed beyond 15 min. The stopped acceptor flow mode acts to greatly improve sensitivity for analytes measured via CP-MIMS, in this case, by enriching the analyte concentration in the methanol acceptor phase. If the ratio of analyte concentration in the acceptor phase during continuous flow is compared with that in the 15 min stopped flow, we achieve 1–2 orders of magnitude improvement in detection limits. Our detection limit for DCP in stopped acceptor flow mode decreases to 5 pptr, a 20$\times$ improvement over the data reported in Table 2.2. This is consistent with our observed enrichment factors. Increased sensitivity in stopped flow mode comes at the expense of a longer duty cycle (*e.g.,* >15 min/measurement),

but is useful when increased sensitivity is required for ultra trace measurements.

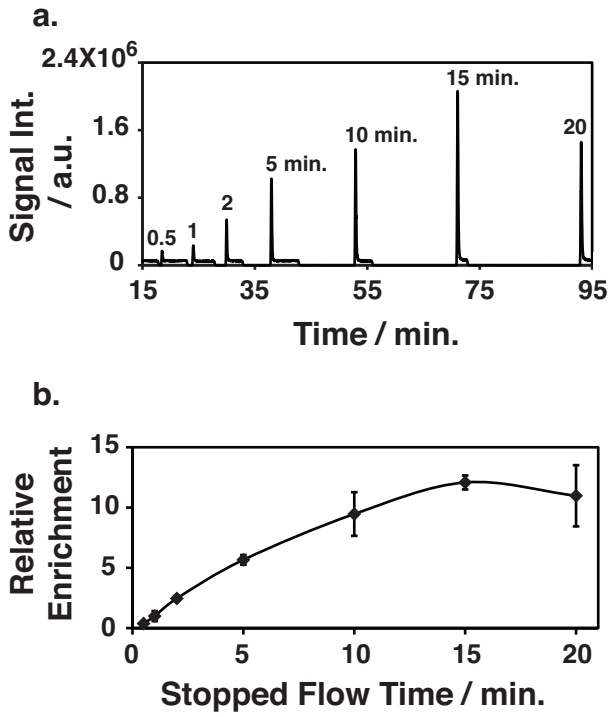

Figure 2.5: Parametric investigation of the stopped flow acceptor phase enrichment of 2,4-dichlorophenol. This data was obtained during the recirculation of an aqueous 8.5 ppb 2,4-dichlorophenol solution. In figure 2.5a, one series of typical stopped flow data is depicted, although the experiment was performed in triplicate. Analytical signals presented were quantified based upon the concentration in the methanol acceptor phase. Figure 2.5b illustrates the average results from the three replicate experiments (error bars represent ± 1 standard deviation).

Nafion Membrane Studies

Our group (and others) are interested in applying different membrane materials in order to change analyte permselectivity and thus extend the applicability of MIMS as an on-line monitoring platform. For example, Nafion sheet membranes have been employed by Gernatova *et al.* with a gas phase acceptor MIMS system [24]. Nafion is a commercially available copolymer of perfluoro-3,6-dioxa-4-methyl-7-octene-sulfonic acid and tetrafluoroethylene (Teflon). This ionomer has rather unique properties,

including being highly conductive for ions (acting as a cation exchange membrane), polar/hydroxylated species, and displays a propensity for water and alcohol transport, making it of great interest for a wide variety of fields ranging from fuel cell research to water treatment membranes [42]. We have evaluated the operation of our CP-MIMS interface with a Nafion HFM. Because Nafion expands substantially when wetted with both water and alcohol [43] (∼25% linear expansion of the HFM in methanol in our case), we pre-wetted the membrane with methanol (the acceptor phase) during assembly, and kept it immersed in methanol (by simply filling the interface) until use. This eliminated previous problems we experienced with membrane folding in the interface casing resulting from this excessive linear expansion – a situation that led to membrane rupture and/or blockages during earlier investigations. The Nafion HFM membranes used for this work (in the described manner) exhibited similar robustness to mechanical stresses (*e.g.,* 300 mL per minute samples flows in a 0.25 diameter tube) to that observed for PDMS HFM membranes. Over the course of our work described in this manuscript, we observed no failures in either type of membrane from substantial on-line use.

For the Nafion membrane study presented in Figure 2.6, the target analytes 2,4-dichlorophenol (40 ppb), triclosan (41 ppb), ethynylestradiol (302 ppb) and estrone (303 ppb) were spiked in a re-circulating aqueous sample at different times to give the indicated final concentrations. The signal traces given in Figure 2.6 indicate that all compounds were detected at the levels introduced, with a range of sensitivities and signal rise times. Further, the chosen target analytes do not seem to have any significant interference upon each other. This suggests that at least for the chosen analytes, there is negligible alteration of membrane transport properties (and ESI ionization efficiencies) for trace level CP-MIMS measurements, consistent with observations for similar target analytes made using gaseous acceptor phase MIMS [10].

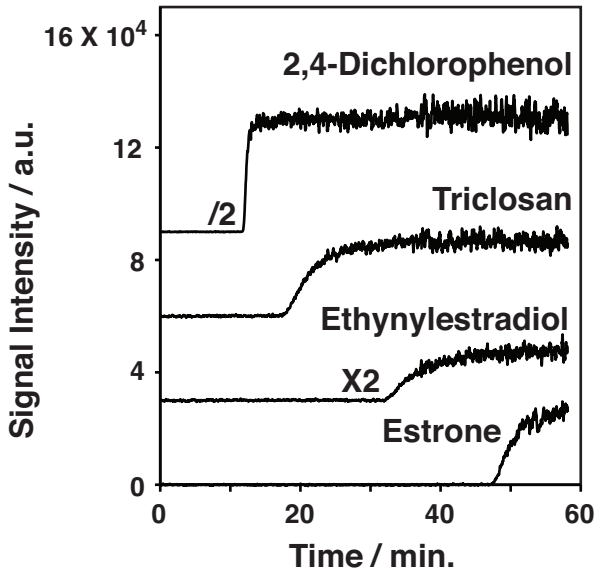

Figure 2.6: Typical analytical signals obtained for measurement of several target analytes using a Nafion membrane interface. For clarity, the signal intensity for 2,4-dichlorophenol is reduced by a factor of 2 and the signal for ethynylestradiol is increased by a factor of 2. Additionally, each signal trace in is offset by 3×10^4 a.u.

Because these analytes were also tested using a PDMS membrane interface, a direct comparison of the performance of both membranes for CP-MIMS is given in Table 2.3. Upon inspection, some of the target analytes (*e.g.,* 2,4-dichlorophenol and triclosan) display essentially the same performance regardless of the membrane used, evidenced by similar detection limits and signal response times. Other species (*e.g.,* estrone and ethynylestradiol) display complimentary behavior, in that better detection limits are achieved for each species with a specific membrane type. The sensitivity for ethynylestradiol improves from 100 ppb in our PDMS interface to 10 ppb in the Nafion case, whereas the detection limits for estrone increase from 2 ppb to 4 ppb (Table 2.3). We suggest that the sensitivity improvements associated with ethynylestradiol in Nafion are due to the greater affinity of this membrane material for the more hydroxylated analyte. These observations are promising, suggesting that Nafion may indeed provide a route to improved selectivity and sensitivity for polar

Table 2.3: Comparison of signal rise times and detection limits for selected target analytes obtained with Nafion and PDMS hollow fibre membranes

Membrane Type		2,4-Dichlorophenol	Estrone	Ethynylestradiol	Triclosan
Nafion	t_{10-90} (min)	1.3	5.9	9.5	7.7
	Detection Limit (ppb)	0.1	4	10	1
PDMS	t_{10-90} (min)	1.2	8.1	11	7.4
	Detection Limit (ppb)	0.1	2	100	1

* All DLs are based on Signal/Noise equal to 3

(poly)hydroxylated analytes with CP-MIMS.

2.3.2 Sample Applications

To illustrate the utility of the system for continuous on-line monitoring, several sample applications were examined including: the measurement of contaminants and/or bio-molecules in fortified natural waters and artificial urine sample; and the in-situ reaction monitoring during the chlorination of phenol.

Natural Water and Surrogate Biological Samples

In a series of experiments to demonstrate the utility, selectivity and sensitivity of CP-MIMS, several complex aqueous samples of estrone (89 ppb) and nonylphenol (1.3 ppb) were analyzed using a PDMS HFM and utilizing MS/MS for improved selectivity and sensitivity. Sample matrices used for this study included DI water (for comparison), filtered Nanaimo river water and a high ionic strength solution of undiluted artificial urine. Experiments were conducted by re-circulating each sample matrix over the membrane for $\sim$ 20 min, followed by an injection of an aqueous combined standard to yield the final concentrations indicated above. Figure 2.7 illustrates the MS/MS signal rise for both analytes in a) water, b) river water and c) artificial urine. At the end of each run, deionized water was used to wash out the analyte and re-establish baseline levels. It is clear that MS/MS signals are obtained for all analytes in each of the sample matrices. Table 2.4 summarizes the detection limits of nonylphenol and estrone in each matrix. The sensitivity of the technique for both analytes appears to be the same in DI water and river water. The slight reduction in the signal intensities observed in the artificial urine sample (Figure 2.7) is presumably due to matrix effects caused by this rather complex sample. We have not yet attributed this slight signal suppression to a specific cause, although we speculate it

is either due to a membrane transport change and/or ESI ionization efficiency change due to component(s) in the complex artificial urine sample.

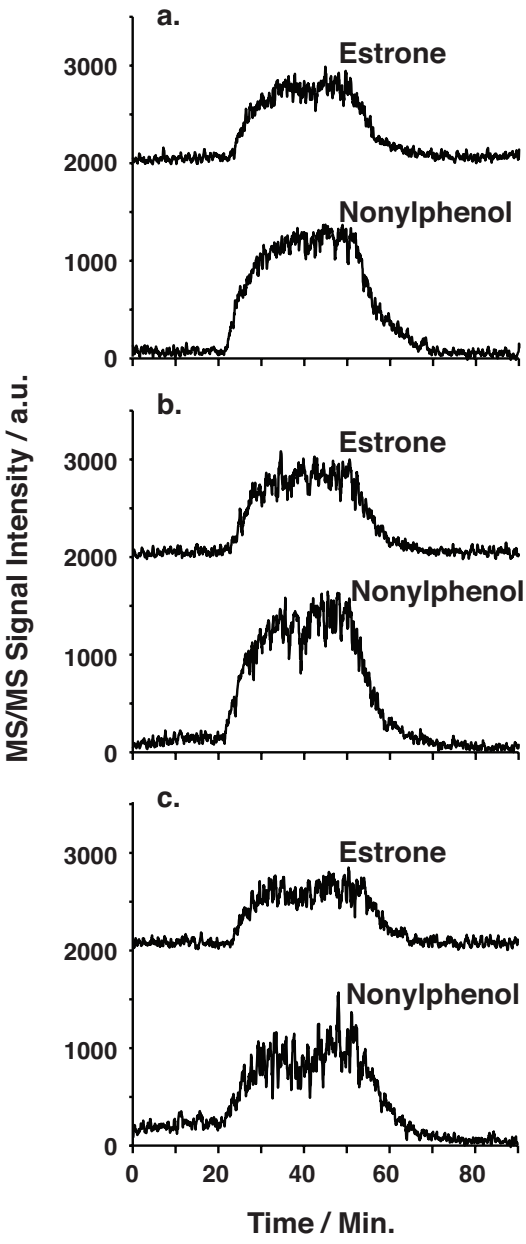

Figure 2.7: Measurement of estrone (89 ppb) and nonylphenol (1.3 ppb) for a sample challenge re-circulated for 20 min in: a. deionized water, b. Nanaimo river water and c. artificial urine. Following each experiment, the PDMS interface was rinsed with DI water to re-establish baseline signals. In each experiment, the estrone MS/MS signal is offset by 2000 a.u. for clarity.

Table 2.4: Detection limits for MS/MS analysis of nonylphenol and estrone in DI, Nanaimo River water, and artificial urine.

Target Analytes	Detection Limit (ppb)		
	Deionized Water	Nanaimo River Water	Artificial Urine
Nonylphenol	0.1	0.1	0.1
Estrone	10	10	20

* All DLs are based on Signal/Noise equal to 3

To illustrate the utility of CP-MIMS for direct, trace-level measurements in complex sample matrices over measurements made by direct infusion ESI-MS, an experiment was conducted in which nonylphenol (10 ppb) and estrone (800 ppb) were spiked in artificial urine and analyzed in the same manner as presented in Figure 2.7, except that full scan (m/z = 100–300) mode was used instead of MS/MS. In addition, an aliquot of this spiked urine sample was also analyzed by direct infusion ESI-MS (introduced at 500 μL per minute, via the syringe pump and divert valve B, see Figure 2.1). The resulting background subtracted mass spectra for both measurements are presented in Figure 2.8.

It is clear that the analytes are readily detected by the full scan CP-MIMS experiment, and that the profound signal suppression caused by the artificial urine (and its concomitant high levels of salts) does not allow the detection of the analyte species by direct infusion ESI-MS. Further experiments were also conducted at lower direct infusion rates (80 μL per minute) and for diluted sample aliquots (1:4 vol/vol dilution of the spiked artificial urine in methanol). Even with reduced infusion rates and for the diluted sample, no analyte signals above background noise were observed (data not shown). Direct infusion ESI-MS can indeed provide meaningful snap-shot information about the composition of complicated samples [44]. However, for direct, on-line, trace level analyte measurements (*e.g.,* ppb-pptr) in complicated samples with high milli-molar concentration of salts and other compounds (such as biological

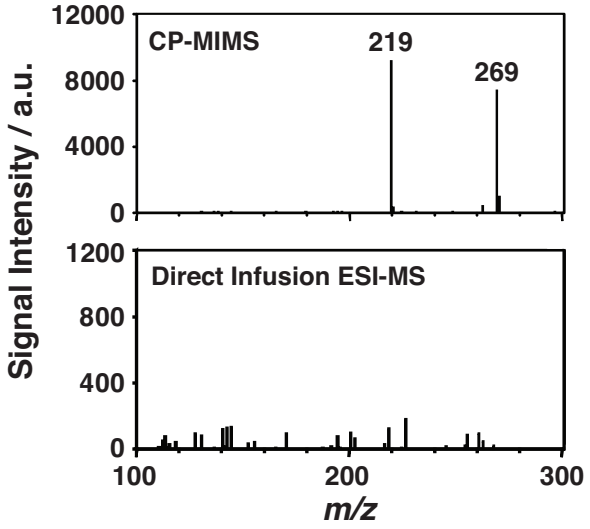

Figure 2.8: Full scan mass spectra for the measurement of 10 ppb nonylphenol and 800 ppb estrone in artificial urine by CP-MIMS and direct infusion ESI-MS of the same solution. The y-axis scale for the direct infusion experiment is expanded by 10× to illustrate the lack of signals at $m/z = 219$ (nonylphenol) and $m/z = 269$ (estrone).

fluids), CP-MIMS appears to offer advantages over direct infusion ESI-MS methods.

In summary, the results presented in Figures 2.7 and 2.8 above suggest that CP-MIMS coupled with MS/MS is not only providing a novel on-line analytical method, but also a potential new route to reduce or eliminate signal suppression effects that often occur for direct measurements in complex sample matrices, especially biological fluids [45]. Hydrophobic membranes such as PDMS allow the selective rejection of salts and other ionic species present in these samples, facilitating direct measurements by CP-MIMS for trace level analyte species that may not be possible by direct infusion ESI-MS methods. In this way, CP-MIMS is acting as an on-line clean-up/extraction step, eliminating the need for sample handling, dilutions and/or chromatographic separations often employed for bio-analytical measurements.

On-line Monitor of the Chlorination of Phenol

The on-line continuous monitoring of a bench scale chlorination reaction of dilute aqueous phenol (2.5 μM, or 240 ppb) is presented in Figure 2.9. Upon the addition of active chlorine, the phenol concentration immediately drops with a concomitant increase in the signal for monochlorophenol. Subsequent loss of monochlorophenol occurs as it continues to react with active chlorine to yield di and trichlorophenols at progressively slower rates as the aromatic ring becomes progressively deactivated by the added chlorine substituents. The 2,4,6-trichlorophenol continues to react via chlorinated quinones to ultimately yield trichloromethane, a commonly observed disinfection by-product. Although not presented in this study, we and others [46] have observed the production of trichloromethane as a final product, verified by both conventional MIMS (using a gaseous acceptor phase) and by off-line GC-MS experiments. The traces in Figure 2.9 were quantified using aqueous standards of the appropriate analytes. It should be noted that the 2-chlorophenol isomer was used to quantify monochlorophenol products although the reaction mixture would presumably contain a mixture of 2- and 4-chlorophenol products. Similarly, 2,4-dichlorophenol was employed to quantify dichlorophenol species, although the chlorination product would be expected to contain both 2,4- and 2,6-dichlorophenols.

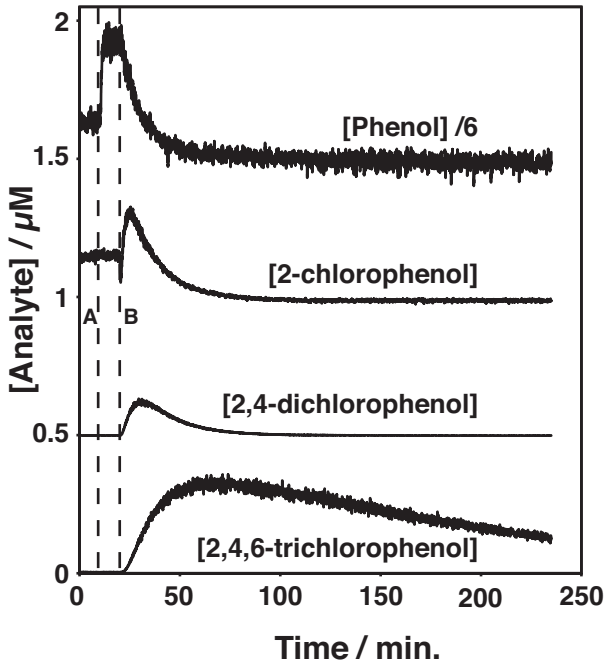

Figure 2.9: The use of CP-MIMS as a continuous on-line monitor for the bench scale chlorination of 2.5 μM (240 ppb) aqueous phenol buffered at pH 7. Phenol was added at dashed line A (10 min) and 5 ppm active chlorine (as Cl_2) was added at dashed line B (15 min). The signal for phenol is scale reduced by a factor of 6 and the traces for each component are offset by 0.5 μM for clarity purposes.

The kinetics for this chlorination example are not extensively interpreted, as this chemical reaction system is presented for illustrative purposes, but we do note the maxima for the observed production of each species is consistent, with the appearance/disappearance of each in the anticipated order (*e.g.,* the mono, then di, then trichloro analogs). It is interesting to note that for the signal for the monochlorophenols, we observe a reproducible baseline shift (drop) in the signal upon addition of the active chlorine. We have not characterized this fully, although it is presumably due to the transport of HOCl across the membrane into the methanol acceptor phase, subsequently altering the ESI ionization characteristics. Although this chlorination system has been studied by others [46] using gas phase MIMS at low mM levels, we are demonstrating the use of CP-MIMS at low μM levels, an improvement of about 3

orders of magnitude for on-line MIMS reaction monitoring of this particular reaction, and at neutral, environmentally relevant pH levels. We also note that the observed kinetic data is representative of the reactions taking place in solution and is not limited by membrane transport phenomena, evidenced by the fact the analytical rise times for each species (Table 2.2) are considerably faster (∼1–2 minutes) than the observed production and decay rates presented.

2.4 Conclusion

This work presents and characterizes an improved condensed phase membrane introduction mass spectrometry interface developed for the continuous monitoring of low volatility polar analytes and non-volatile analytes in aqueous solutions with HFMs. The system employs a methanol acceptor phase and an in-line micropump for solvent delivery from the membrane to an electrospray ionization tandem mass spectrometer (ESI-MS/MS). The system demonstrates detection limits in the low pptr-ppb range, and can be operated in either continuous acceptor flow mode or in stopped acceptor flow mode, where the acceptor phase is stopped for prescribed intervals to allow analyte preconcentration in the acceptor phase prior to MS analysis. Stopped acceptor flow operation results in an observed enhancement of sensitivity of an order of magnitude. We have evaluated the use of both polydimethylsiloxane (PDMS) and Nafion HFMs and have observed complementary behavior for certain classes of analytes. Notably, we observe improvements in sensitivity using a Nafion HFM for the trace determination of polar hydroxylated species (*e.g.,* ethynylestradiol) in aqueous samples. We have demonstrated the use of the presented CP-MIMS system for the sensitive and selective direct measurement of environmentally and biologically relevant target analytes in natural river water and artificial urine, and its potential

advantages over direct infusion ESI-MS methods. Furthermore, we present data illustrating the continuous on-line monitoring of the chlorination of a dilute aqueous solution of phenol, following the fate of reactants and chlorinated intermediates. Although the membrane interface necessarily introduces a bias as a result of inherent permselectivity properties, we achieve improved detection limits for those analytes which do permeate and can readily quantify analyte concentrations by using conventional calibration techniques (*e.g.,* direct calibration, standard additions and/or and internal standard methods in either the sample or directly in the acceptor phase).

The improved CP-MIMS interface maintains the HFM at ambient hydrostatic pressures, making it suitable for investigations involving delicate membrane systems. The system has been characterized for use as a continuous on-line monitor, and has distinct advantages in this application over earlier generations of CP-MIMS type interfaces in the literature. Future work includes the investigation of application specific acceptor phases, the use of the system to study membrane transport phenomena and the further exploration of the use of Nafion and other HFM systems for increased permselectivity of target species in complex (*e.g.,* environmental and biological) samples.

Chapter 3

A Miniature Condensed Phase Membrane Introduction Mass Spectrometry Probe for Measurements of Pharmaceuticals and Contaminants in Small Samples

Reproduced with permission from Duncan, K; Willis, M.; Krogh, E.; Gill, C. "A miniature condensed-phase membrane introduction mass spectrometry (CP-MIMS) probe for direct and on-line measurements of pharmaceuticals and contaminants in small, complex samples." *Rapid Commun. Mass Spectrom.*, 27, 1213-1221 (2013). Experiments were designed and carried out by K. Duncan, C. Gill, and M. Willis. Data analysis was carried out by K. Duncan. Drafting of the manuscript was done by C. Gill with contributions from K. Duncan, with editorial contributions from all authors.

3.1 Introduction

The use of membranes is becoming increasingly important for the separation and purification of a wide range of molecules from complex samples, including the production of high purity gases, their use in water treatment strategies, industrial scale chemical purifications, fuel cell development and medical applications [47–53]. Membrane introduction mass spectrometry (MIMS) is the extension of membrane separation to

the field of mass spectrometry. MIMS uses a membrane to directly interface samples with mass spectrometers, obviating an intermediate step such as chromatographic separation, utilizing the membrane as a semi-selective means of analyte isolation. The material properties of the membrane, the permeate carrier (*e.g.,* gas or liquid), the mode of ionization used and tandem mass spectrometric techniques all confer additional degrees of selectivity for different analytes with MIMS. Because of the rapid nature of MIMS measurements (typically limited by the membrane transport of the analyte) and the lack of sample pretreatment, the technique is well suited for on-line, real-time type measurements directly in complex samples. The selectivity of the membrane will limit the range of possible analyte species (*e.g.,* hydrophobic analytes are preferentially selected by hydrophobic membrane materials), and because analytes are transferred as a mixture to the mass spectrometer, they must be ionized effectively and resolvable by either m/z or by MS/MS for MIMS measurements. For additional background regarding MIMS, a recent review has been published [54], and two earlier reviews are also recommended [4, 7].

Condensed Phase MIMS (CP-MIMS) uses a condensed (liquid) acceptor phase to transfer analyte molecules crossing a membrane interface directly to a mass spectrometer. There are a few variants of the CP-MIMS technique in the literature, using Electrospray Ionization (ESI) [35, 55], Atmospheric Pressure Chemical Ionization (APCI) [34] and Sonic Spray Ionization (SSI) [21]. Because the MIMS membrane imparts selectivity for target analytes over the bulk matrix, it is possible to directly measure trace level analytes in complex samples, while rejecting potential interferences. For example, polydimethylsiloxane (PDMS) selects for neutral, hydrophobic analytes, and effectively excludes ionic species (*e.g.,* salts), which can suppress ionization in direct flow injection analysis scenarios [45].

The CP-MIMS systems published to date have predominantly focused on the use

of membranes for analyte separations (*e.g.,* materials) or the type of mass spectrometry and/or ionization mode used [21,34,35,55]. Membrane interface designs explored by our group have been predominantly on-line, continuous sampling flow cells (*e.g.,* 0.25 OD tubing flow cells) requiring either rapid sample recirculation (∼300 mL/min) and/or relatively large (*e.g.,* 100–1000 mL) sample sizes [55]. An obvious disconnect exists when applying our flow cell geometry for small sample volumes, such as those commonly encountered in bio-analytical measurements in blood or urine samples. The ESI based CP-MIMS flow cell probe developed by the Bier group [35] used a 250 μL sample loop injection strategy for successful trace analyte detection. The CP-MIMS system reported by Creaser and co-workers utilized APCI for ionization, employed a smaller (20 μL) sample loop to inject aliquots of concentrated pharmaceutical process reaction samples, and was not developed for trace contaminant measurements [34]. Although both of these techniques use smaller sample volumes, sampling loop methods consume a portion of the sample to make a measurement, and because the sample must pass through fluid handling systems, there is also potential risk for analyte dilution or cross contamination.

Although not designed for CP-MIMS, the pioneering work of the Lloyd group developing miniature probes for *in-situ* gaseous acceptor phase MIMS [56,57] helped to inspire the CP-MIMS probe design presented by this work. Additional influences were adapted from the miniature sampling probe designs utilized for *in-vivo* micro-dialysis [58,59]. Micro-dialysis probes, however, use microporous membranes, which are permeable to ionic species (*e.g.,* salts *etc.*). Thus, commercially available micro-dialysis probes are not suitable for CP-MIMS applications involving high salt samples (such as bio-fluids) because of the ionization suppression that would occur when using techniques such as electrospray ionization (ESI) [60–63].

Solid phase micro-extraction (SPME) is powerful analytical sampling approach

and can be effectively used as a direct sample introduction method with mass spectrometry (*e.g.,* fibre MS) [64, 65], although the bulk of the SPME literature has focused on its power as a sample preparatory step for chromatographic separations [66]. SPME with coated fibres [66], typically integrates the analyte concentration over a specified exposure time. Recently, an off-line hollow fibre membrane based extraction assembly designed for 4 mL sample sizes was developed by Manso *et. al.*, optimizing analyte extraction from liquid samples for subsequent chromatographic analysis [67]. Although both SPME and Manso *et al.*s hollow fibre assembly approach minimize reagent use and boast low limits of detection, they do not allow for the continuous on-line monitoring of analytes.

This work presents the development and characterization of a miniature CP-MIMS probe to address the goal of continuous on-line measurements for trace level analytes in small volumes of complex samples. We have incorporated this sample probe into an autosampler to demonstrate the feasibility of conducting high-throughput measurements and/or sample pre-screening on multiple, small volume samples and demonstrate that analytes can be non-exhaustively analyzed in small volumes, allowing subsequent application of other analytical techniques (*e.g.,* HPLC-MS). Because we are continuously flowing the methanol acceptor phase through the lumen of our hollow fibre membrane (HFM) probe, we are able to monitor dynamic changes in analyte concentration over time.

3.2 Experimental

The acceptor phase flow characteristics of the miniature CP-MIMS membrane probe were designed to facilitate minimal dead volumes within the probe itself while simultaneously maximizing the linear velocity of the acceptor phase on the permeate side of

the membrane. Based upon our experience with PDMS CP-MIMS systems, we have developed several miniature PDMS HFM based MIMS probes in-house, with each generation improving upon the last in terms of reducing membrane size/diameter and minimizing the internal acceptor phase dead volume within the HFM lumen. A schematic diagram of the miniature CP-MIMS probe assembly and associated experimental apparatus used for this work is shown in Figure 3.1. The final working PDMS HFM dimensions used for this work were 0.94 mm OD, 0.51 mm ID and 20 mm long (Silastic brand; Dow Corning, Midland, MI, USA). The outer body of the probe stem was constructed from 22 gauge stainless steel hypodermic stock (Vita Needle Co., Needham, MA, USA). The coaxially arranged acceptor phase delivery capillary was made from a short length of deactivated Siltek capillary column (0.25 mm ID, 0.37 mm OD, Restek Corporation, Bellefonte, PA, USA). The membrane was mounted over the hypodermic probe stem and a stainless steel end plug using hexane (ACS grade, Fisher Scientific, Ottawa, Ontario, Canada) as a membrane-swelling agent. A few turns of 30 gauge copper wire (GC Electronics Ltd., Rockford, IL, USA) over the membrane at the end plug and on the probe stem were used to ensure that the membrane was not dislodged during preliminary testing and subsequent use. The probe was assembled using a 0.75 mm bore stainless steel tee union for 1/16 diameter tubing (Valco Instruments Company Inc, Brockville, ON, Canada), which also acted as a connection point for acceptor phase delivery and its subsequent transport to the mass spectrometer.

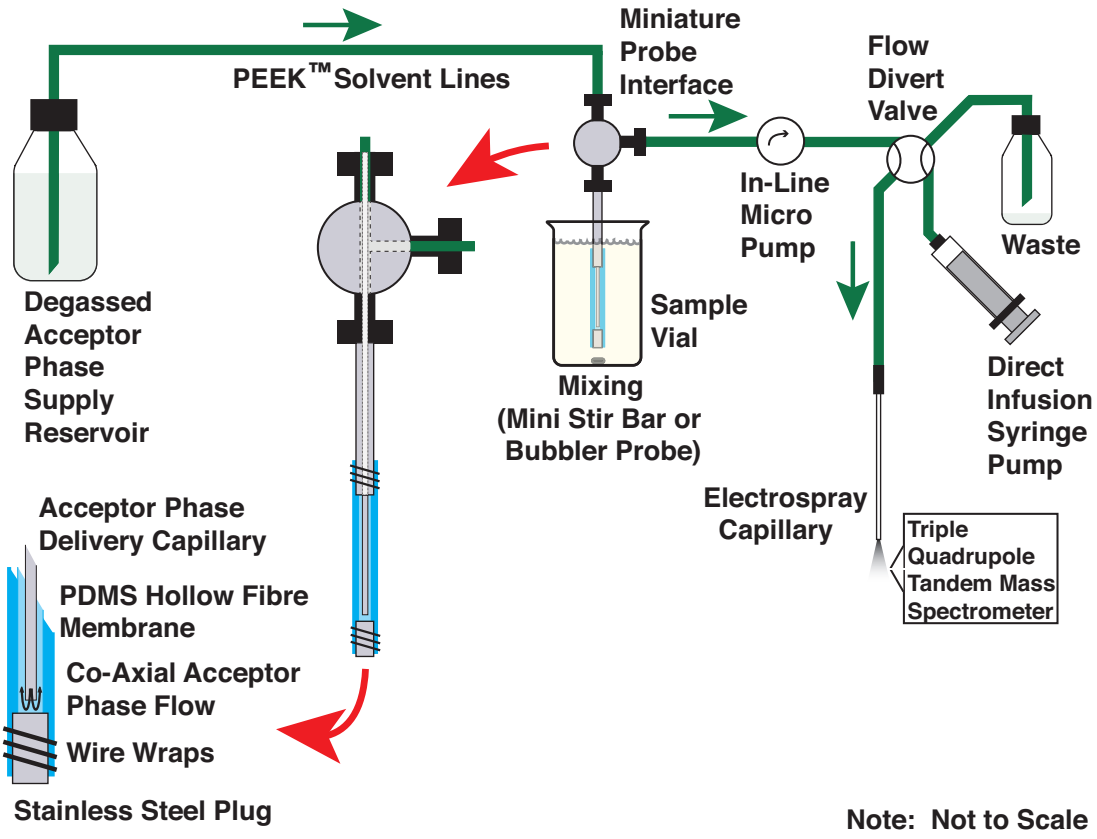

Figure 3.1: Schematic diagram of the miniature CP-MIMS probe and experimental apparatus.

For this work, HPLC grade methanol (Fisher Scientific) was used as supplied, and was degassed using helium sparging (UHP Grade, Praxair Inc., Nanaimo) when employed as an acceptor phase. Acceptor phase delivery to the membrane probe assembly was accomplished using 1/16" PEEK tubing (0.75 mm ID, Chromatographic Specialties, Brockville, ON, Canada), while acceptor phase transfer to the mass spectrometer used a smaller ID (0.25 mm) piece of PEEK tubing from the same supplier. The diameter of the tube used between the probe and the ESI source was intentionally smaller than the acceptor phase delivery tube to minimize any unintended dilution or signal broadening effects. Preliminary work (data not given) showed that minor changes in the length of the probe to mass spectrometer tubing did not adversely affect the signal rise time or maximum intensities observed.

A triple quadrupole tandem mass spectrometer equipped with a low dead volume in-line micro-pump and ESI was used for this work. This part of the CP-MIMS system has been described previously [55]. Target analytes for this work included phenol, 2-chlorophenol, 2,4-dichlorophenol, 2,4,6-trichlorophenol, triclosan (2,4,4'-trichloro-2'-hydroxydiphenyl ether), gemfibrozil (5-(2,5-dimethylphenoxy)-2,2-dimethyl-pentanoic acid) and nonylphenol (Sigma Aldrich, Oakville, ON, Canada). The chlorophenols and nonylphenol are representative drinking water contaminants [68, 69], triclosan is an antifungal/bacterial agent shown to have endocrine disruptive capabilities [70], and gemfibrozil is a fibrate drug used to lower lipid levels [71]. Stock analyte solutions were prepared at ppm levels in methanol, followed by dilution in deionized water (DI, Model MQ Synthesis A10, Millipore Corp., Billerica, MA, USA) or in other indicated matrices to low ppb levels for the presented work. For the chlorination experiment, a 20 000 ppm (as Cl_2) working stock of sodium hypochlorite (Sigma Aldrich, Oakville ON, Canada) was prepared in DI water, and a 0.5 M phosphate buffer (pH = 7.0) was used for pH adjustment [55]. Artificial urine [55], water from a closed system decorative Koi Fish Pond, lager beer with 5% alcohol by volume and primary sewage treatment effluent from a small municipal treatment plant were used without dilution or filtration for complex sample matrices in this study. Selected chemical, physical and the mass spectrometric scan parameters used for the target analytes are given below in Table 3.1.

Samples were contained in either 40 mL clear glass sample vials (Scientific Specialties Inc., Hanover, MD, USA), 4 mL HDPE autosampler cups (Pulse Instrumentation Inc., Milwaukee, WI, USA), 1.8 mL clear glass chromatography vials (Agilent Technologies, Mississauga, ON, Canada) or custom made 0.5 mL vials fashioned by cutting standard NMR tubes (Norell NMR Tubes, Landisville, NJ, USA), to shorter lengths, as indicated. All were washed 3× with HPLC Grade methanol and dried in air before

Table 3.1: MS and physicochemical parameters.

Target Analyte	Molar mass (g mol^{-1})	Vapour Pressure [a] (Pa @ 25^{o}C)	Log K_{ow} [a]	MS Scan Parameters m/z	Collision Energy eV
Phenol	94.11	61.7	4.76	93	-
2-Chlorophenol	128.56	316	2.19	127	-
2,4-Dichlorophenol	128.56	15.8	3.09	161	-
2,4,6-Trichlorophenol	197.45	2.3	3.54	195	-
Triclocan	289.54	8.6 x 10^{-5}	5.34	289	-
Gemfibrozil	250.33	8.1 x 10^{-5}	4.30	$249 \rightarrow 120$[c]	15
Nonylphenol	220.35	1.2	6.04	$219 \rightarrow 133$[c]	30

[a] Obtained from SRC Physical Properties Database [37].
[b] Negative ion mode used for all scans, and SIM except where noted.
[c] Selective reaction monitoring.

use. Samples were either unstirred, stirred with a miniature Teflon stir bar and magnetic stirrer (LAB DISC S56, Fisher Scientific, Vancouver, BC, Canada) or mixed by helium bubbled through the sample via a short length of 22 gauge stainless steel hypodermic tube. All measurements were made for samples at ambient temperature (25°C) and pressure (101 kPa). For the automation experiments, a commercial autosampler from a flow injection analysis system (Alpchem Corporation, Model 301, Clackamas, OR, USA) was used, modifying it by mounting the miniature CP-MIMS probe assembly in the sampling turret.

3.3 Results and Discussion

3.3.1 Acceptor Phase Flow Rate Study

After preliminary optimization experiments, characterization of the initial performance of the miniature CP-MIMS probe was conducted. The optimum acceptor phase flow was determined by measuring the signal-to-noise ratio (S/N) obtained for the steady state signals of ppb level aqueous solutions of 2,4,6-trichlorophenol and triclosan at methanol acceptor phase flow rates ranging from 50–300 μL/min. These measurements were made in 40 mL aqueous samples, using a magnetic stirrer and Teflon stir bar for mixing. After each measurement, the miniature probe was washed clean by immersing it in 40 mL of stirred DI water until the signal returned to baseline levels. The results are given in Figure 3.2, and show that the signal to noise ratio improves from $\sim$50–150 μL /min, level off between $\sim$150–250 μL/min and then decrease at flow rates $>$250 μL/min. A methanol acceptor phase flow rate of $\sim$200 μL/min provided the best signal-to-noise ratio for the miniature CP-MIMS probe and therefore was employed for all subsequent work.

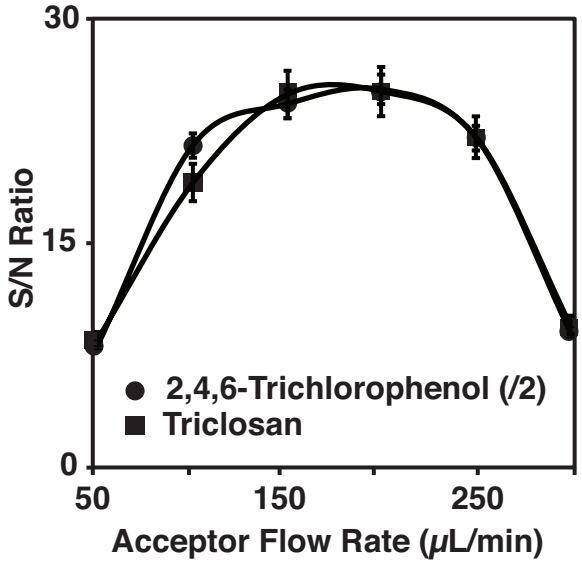

Figure 3.2: Plot of signal-to-noise (S/N) ratio versus CP-MIMS acceptor flow rate for signals obtained from aqueous solutions of 28 ppb 2,4,6-trichlorophenol and 78 ppb triclosan. Error bars represent the RSD (n > 100) of the signal measurements. For scaling purposes, the S/N ratios for 2,4,6-trichlorophenol were divided by two.

3.3.2 Membrane Washout Solvent Choice

In earlier investigations of CP-MIMS by our group, a high volume flow cell type MIMS interface assembly has been presented [55]. To wash this flow cell after a measurement or on-line monitoring experiment, DI water was flowed through the interface until the signals for target analytes returned to baseline levels. As noted above, the miniature CP-MIMS probe can be cleaned between measurements by simply dipping it in a small quantity of any suitable wash solvent. This can be DI water, or any other (membrane compatible) solvent, such as methanol. Changing the wash solvent provides faster membrane cleaning times between samples (than possible with water), decreasing the wait time needed between samples. Although our previously discussed flow cell interface could also be cleaned with organic solvent, it would require much greater quantities of solvent, increasing both the cost and waste produced by each measurement.

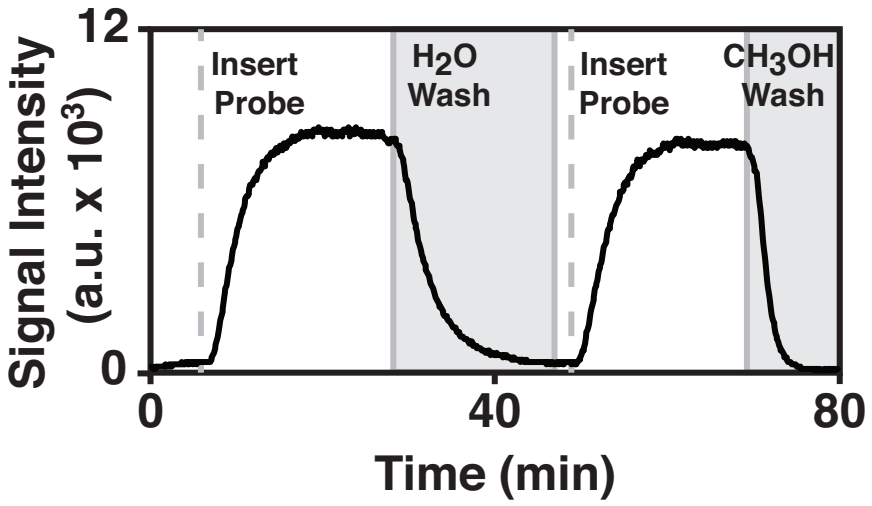

Figure 3.3: Comparison of the signals for 78 ppb aqueous solutions of triclosan, including wash out times, using de-ionized water wash out (left) and methanol wash out (right). Return to baseline signal levels for triclosan is achieved approximately three times faster in methanol than in water.

An experiment was conducted to compare the analyte wash out time after monitoring a 78 ppb aqueous triclosan solution. A 40 mL aliquot of stirred DI water was spiked with triclosan and monitored via direct insertion of the mini CP-MIMS probe. After the signal reached steady state, the probe was transferred to 40 mL of a stirred wash solvent (DI water or methanol). Depletion of the residual triclosan analyte was monitored as it is washed out of the PDMS membrane. Figure 3.3 illustrates the advantage of using methanol rather than water as the wash solvent. Methanol removes the triclosan from the PDMS membrane nearly 3× faster, allowing a shorter duty cycle than would be possible using a DI water wash. For all of the target analytes tested, the time required for the signal to decrease from 90 to 10 % of the steady state levels was determined for both DI water and methanol and is summarized in Table 3.2. Observed membrane wash out Improvement Factors range from 1.2 for less hydrophobic 2,4,6-trichlorophenol (log $K_{\mathrm{ow}} = 3.54$) to 4.1 for the more hydrophobic nonylphenol (log $K_{\mathrm{ow}} = 6.04$). Since the neutral form of the analyte partitions out

of the aqueous sample and diffuses through the PDMS membrane, we observe the greatest wash out improvements for the more hydrophobic analytes. We note a linear relationship between the analyte wash-out Improvement Factor (IF, Table 3.2) for methanol/water and the log K_{ow} values for the four compounds studied (IF = log K_{ow} + 2.4, R = 0.95, data not shown).

Table 3.2: Comparison of membrane cleanup strategies

Target analyte	Water wash (min)	Methanol wash (min)	Improvement factor [a]
2,4,6-Trichlorophenol	2.4	1.8	1.3
Gemfibrozil	7.8	3.5	2.2
Triclosan	7.8	2.8	2.8
Nonylphenol	14.6	3.6	4.1

[a] Improvement factor = water wash / methanol wash

3.3.3 Sample Mixing and Depletion Studies

In the flow cell geometries used in other MIMS systems, our group (as well as others) have observed that high sample flow rates must be maintained for optimum analytical performance [72]. At lower flow rates, laminar flow at the membrane surface creates a boundary layer that adds resistance to mass transport across the membrane. This phenomenon typically results in longer signal rise-times, reduced sensitivity and less reproducible quantitative results. Recognizing this, all of the previous investigations involved samples that were continuously mixed using a stir bar/magnetic stirrer arrangement. To implement the probe type CP-MIMS interface in smaller sample volumes (*e.g.,* < 5 mL) and/or in an autosampler (*vide supra*) may require alternate mixing strategies. This could be achieved by vibrating the membrane probe (analogous to patented SPME systems) [73] or by bubbling a stream of inert gas in the sample vial.

Table 3.3: Effect of sample mixing on signal response times and detection limits.

	Response time (min)			Detection limit (ppb)		
Target Analyte	No mixing	Helium bubbler	Stir bar	No mixing	Helium bubbler	Stir bar
Trichlorophenol	20.4	2.5	2.2	0.1	0.04	0.02
Triclosan	23.4	7.7	5.8	4	0.7	0.5
Gemfibrozil	21.1	8.3	5.9	7	5	2
Nonylphenol	35.5	9.5	9.5	3	0.5	0.7

* Reported response times represent $t_{10-90\%}$
* Detection limits are based on a S/N=3

A comparison study was conducted in which aqueous solutions (40 mL) containing 2,4,6-trichlorophenol (28 ppb), triclosan (77 ppb), gemfibrozil (78 ppb) and nonylphenol (53 ppb) were prepared by spiking with the appropriate quantity of stock solutions, followed by measurement with the miniature CP-MIMS system. One solution was not mixed, one mixed with the stir bar/stirrer, and the remaining solution was mixed by bubbling helium through the sample during the measurement. Although He bubbling provides an approach to mix samples in small volumes (not amenable to stir bar mixing), the potential for loss of volatile analytes exists. However, it should be noted that CP-MIMS is well suited for the analysis of low volatility analytes. The data collected was analyzed for the signal response times ($t_{10-90\%}$) and 3× S/N detection limits (Table 3.3). The unmixed solution yielded the longest response times and poorest detection limits, whereas both the helium bubbler and stir bar mixing gave comparable results. The increased analyte diffusion path length created by a depleted boundary layer developed at the membrane surface in unmixed samples adds mass transport resistance, reducing the permeability and increasing the transport time as predicted by Ficks law [9]. Mixing by mechanically vibrating the membrane probe was not attempted for this study, although it is anticipated that it would also be effective, based upon its commercial success with SPME methods [73]. The results of this study yielded $t_{10-90\%}$ response times of 2-10 minutes for the target analytes tested, and detection limits from pptr to low ppb levels. These detection limits compare well with those obtained from flow cell type CP-MIMS interfaces used with the same mass spectrometer [55], as illustrated by the detection limit comparison presented in Table 3.4. It should be noted that the current mini-probe takes advantage of improved MS scan parameters (*e.g.,* longer dwell times for each analyte ion) and benefits from less analyte dilution in the methanol acceptor phase, because of the slower acceptor flow rates here over the flow cell geometry [55]. Further, the lumen volume of the

Table 3.4: Detection limit comparison for miniature probe verses flow cell type CP-MIMS interfaces

	Detection limits [a] (ppb)	
Target analyte	Flow cel [b]	Miniature probe [c]
Trichlorophenol	0.05	0.02
Triclosan	1	0.05
Gemfibrozil	2[d]	2
Nonylphenol	1	0.7

[a] Based on a S/N=3.
[b] Obtained with the same mass spectrometer as above, using a 10 cm length of the same HFM as presented in a previous study [55]
[c] 40 mL sample mixed with a magnetic stir bar
[d] Measured at the time of this study

HFM in the mini-probe is partially filled with the acceptor phase delivery capillary (Figure 3.1), which alters the acceptor flow dynamics and yields increased linear velocities of methanol at the membrane lumen surface in the probe. Taken together, these factors give rise to detection limits for the 2 cm HFM mini-probe system reported here that are comparable to those obtained with the 10 cm HFM flow-cell interface [55].

We have investigated the depletion of analyte concentrations in small sample volumes to test if sample pre-screening using the miniature CP-MIMS probe could be followed by a second measurement (*e.g.,* HPLC-MS), using the same sample for both. Using previously published acceptor phase calibration methodologies [55], when 40 mL of 70 ppb aqueous gemfibrozil was interrogated with the miniature CP-MIMS probe, a gemfibrozil concentration of 9 ppb was observed in the methanol acceptor phase. At an acceptor phase flow rate of 200 μL/min, this corresponds to a total gemfibrozil mass transfer of $\sim$2 ng/min from the sample under steady-state conditions. To examine potential analyte depletion effects in small samples, 70 ppb aqueous gemfibrozil samples (1.8 mL and 400 μL) were continuously monitored with the miniature CP-

MIMS probe for a one-hour period. The results of this study are shown in Figure 3.4.

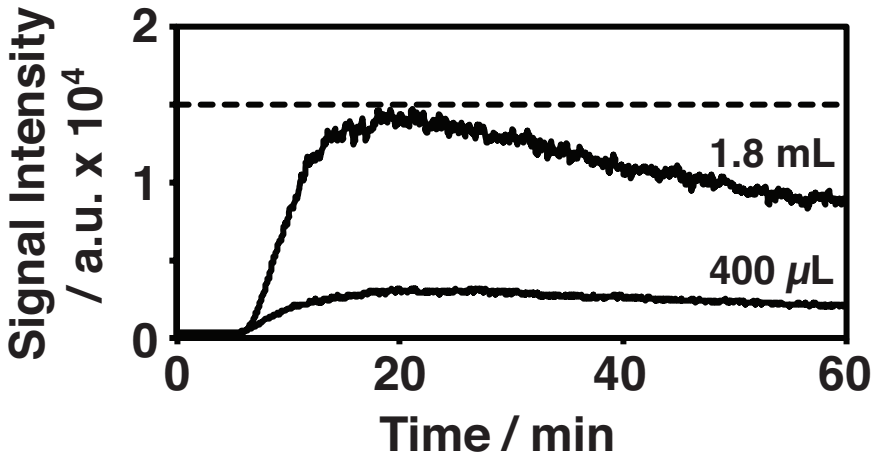

Figure 3.4: Demonstration of the continuous interrogation of smaller sample volumes of 70 ppb aqueous gemfibrozil with the miniature CP-MIMS probe. The dashed line represents the steady state signal level achieved for 70 ppb gemfibrozil in bulk samples (*e.g.,* 40 mL). It is evident that as sample size is reduced, the effects of signal depletion become more pronounced.

The dashed line represents the averaged steady-state signal level achieved for six replicate measurements of 70 ppb gemfibrozil in bulk samples (*e.g.,* 40 mL). It is evident from the figure that as sample size is reduced, the effects of signal depletion become more pronounced. The 1.8 mL sample (containing 130 ng of analyte) showed essentially the same maximum signal level as that obtained for larger sample volume measurements. The observed analytical signal begins to decline upon extended measurement times. This is because the analyte permeation had reached a steady-state before the depletion analyte became significant. However, in the case of the 400 μL sample (containing 28 ng of analyte), it is evident that the rate of analyte depletion is occurring on a time scale that competes with the rate of analyte permeation through the membrane. Consequently, the signal does not reach the same maximum level (5$\times$ lower than those obtained in 1.8 mL or larger samples). It is noted that the overall mass flux of analyte across the membrane is reduced for the 400 μL sample, resulting

in the observed lower sensitivity. In this case, analyte depletion lowers the concentration which governs mass transport according to Ficks laws [9]. In the case of the 1.8 mL sample signals depicted in Figure 3.4, there is a greater loss of relative signal over extended time periods because of the higher mass flux. This preliminary work suggests that although extended interrogation of small sample volumes can indeed deplete analyte from the sample, subsequent measurements can still possibly be made in small volumes by secondary measurement strategies, as long as the probe immersion time is kept to a minimum. By further reducing the size of the exposed membrane surface area, or by using non-steady state signals for quantitation (*e.g.,* less sample exposure time, as seen below in section 3.3.6), the amount of analyte extracted from the sample can be further reduced, mitigating analyte depletion effects.

3.3.4 Direct Calibration of Target Analytes

To illustrate the use of the miniature CP-MIMS probe for quantitative measurements, a series of combined aqueous standards in the ppb range were interrogated with the mini CP-MIMS probe, using a magnetic stir bar for sample mixing. The background subtracted steady-state signals for each of the target analytes were subsequently used to generate calibration curves, which are shown in Figure 3.5.

As can be seen from the plots, good linearity is observed over the low ppb concentration range examined. The calibration slopes range from 30 ppb^{-1} for gemfibrozil to 738 ppb^{-1} for trichlorophenol, demonstrating that we are $\sim$25$\times$ more sensitive to trichlorophenol than gemfibrozil on a per mass basis. Triclosan and nonylphenol exhibit intermediate response with sensitivities that are 6.0 and 5.2 times greater than gemfibrozil. These variations in sensitivity can be attributed to differences in both the permeation of the molecules through the membrane as well as their relative ionization efficiencies in the electrospray source.

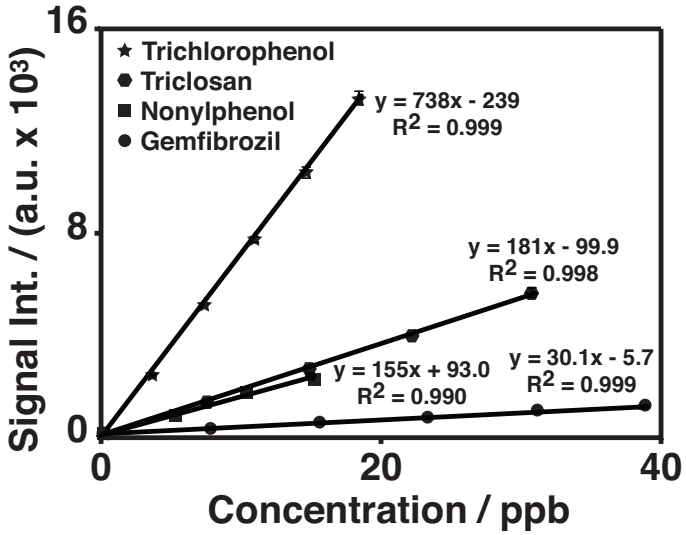

Figure 3.5: Representative calibration curves for 2,4,6-trichlorophenol (3–20 ppb), triclosan (7–40 ppb), nonylphenol (5–15 ppb), and gemfibrozil (7–40 ppb) in DI water using the miniature PDMS hollow fibre probe CP-MIMS interface. Each point represents an average of at least 100 steady state signal data points, and error bars represent 3 standard deviations.

3.3.5 On-line Monitoring: Chlorination of Phenol

On-line reaction monitoring by ambient ionization techniques, including ESI, is gaining increased popularity, and a recent review surveying a variety of mass spectrometric approaches has been published [74]. The use of a miniature CP-MIMS probe also allows the same potential applications for on-line monitoring as flow cell MIMS counterparts, including its use in flowing streams, but it also can be employed in confined spaces and in smaller volumes of sample than would be practical with flow cell type interfaces. As an illustrative (and comparative) example, the chlorination reaction of aqueous phenol was monitored with the probe system in a 40 mL vial. A sample of DI water, buffered at pH 7, was stirred and spiked to a final concentration of 250 ppb phenol. After the phenol signal reached steady-state, an aliquot of sodium hypochlorite was added to achieve an active chlorine concentration of 10 ppm (as Cl_2), and the reaction allowed to proceed at 25°C in an uncapped vial. The resulting signals for

reactants and chlorinated phenols are illustrated in Figure 3.6 as a function of time. No attempt is made to differentiate the structural isomers for mono and dichlorophenols (*i.e.,* both 2- and 4-chlorophenols are monitored by SIM at m/z 127) nor was any attempt made to monitor subsequent chlorination intermediates/products. The signal for phenol is observed to decrease upon addition of active chlorine simultaneous with an increase in the signal for monochlorophenol. The subsequent progression of intermediates through di and trichlorophenol intermediates is similar to that observed when using a flow cell interface plumbed in a closed re-circulation loop with a 500 mL reaction flask [55]. The results suggest that the miniature CP-MIMS probe could be applicable for the monitoring of a wide range of chemical systems, environmental testing scenarios and industrial processes. Because the miniature CP-MIMS probe can readily be implemented in small volume samples or be directly inserted in a continuously flowing sample stream (*e.g.,* a pipeline in an industrial scenario) it offers a simpler alternative for *in-situ* reaction monitoring when compared to a flow cell interface, which requires additional hardware (*e.g.,* plumbing and pumps).

3.3.6 Automated Sample Introduction and Complex Sample Matrices

One of the rationales for a miniature CP-MIMS probe is its facile use for on-line monitoring scenarios, although the utility of CP-MIMS as a rapid analytical screening tool can also be exploited in an automated sample introduction system. To demonstrate automated use, a rotary tray autosampler system from a flow injection analyzer was adapted to use the miniature CP-MIMS probe. The PEEK transfer lines employed were flexible enough that the probes movement in the autosampler system was unhindered. For this study, the autosampler was equipped with 4 mL sample cups and used a maximum programmable sampling time of 99 sec/sample. Trichlorophenol

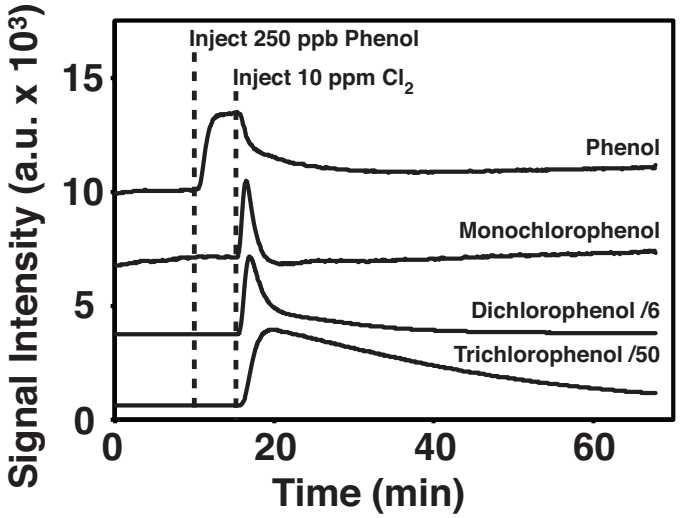

Figure 3.6: On-line monitoring of the chlorination of aqueous phenol at 25°C in an uncapped 40 mL glass vial. Mixing of the reaction was accomplished using a miniature magnetic stir bar. The signal traces for each analyte are offset for clarity, and the traces for the di- and trichlorophenols have been re-scaled by dividing them by the indicated factors.

(50 ppb) and nonylphenol (100 ppb) were analyzed in a wide variety of sample matrices. Sample matrices, including DI water, Koi pond water, beer, artificial urine, and primary sewage wastewater effluent. Samples were well mixed before filling the autosampler cups, and measured as part of a continuous sample sequence by a 99 second miniature CP-MIMS probe immersion in each sample. The probe was rinsed by automated immersion in clean methanol for 99 seconds between replicate samples and for 197 seconds between sample types. All samples were directly analyzed without dilution, pretreatment or filtration. Figure 3.7 gives the observed signal traces for the detection of the target analytes.

In evaluating the use of this simple autosampler system, it should be noted that samples were not mixed during the probe immersion. Although the exposure time of the membrane probe to the sample was very reproducible (because of the automation), it was not long enough to allow for steady-state signal development (Table 3.3). Analysis of the data showed similar relative standard deviations for both peak height

and peak area measurements at ∼10% for three replicates within the same sample matrix (Table 3.5. Fitting the autosampler with a mechanism to agitate the probe or to mix the samples would undoubtedly improve this precision. The signals observed for trichlorophenol (50 ppb) are much stronger than those for nonylphenol (100 ppb), but appear to be slightly less reproducible. This analyte dependent sensitivity/precision is readily explained by the fact that CP-MIMS is 5× more sensitive to trichlorophenol than nonylphenol (see Table 3.3). Furthermore, the signal response time for nonylphenol to reach steady-state is 4× longer than trichlorophenol. Taken together, these factors both contribute to the greater sensitivity observed for trichlorophenol over nonylphenol (Figure 3.7) in this application. Increasing the probe immersion time to let the signals reach their steady state levels, or operating in a stopped acceptor flow trap and release mode [55] would further improve sensitivity.

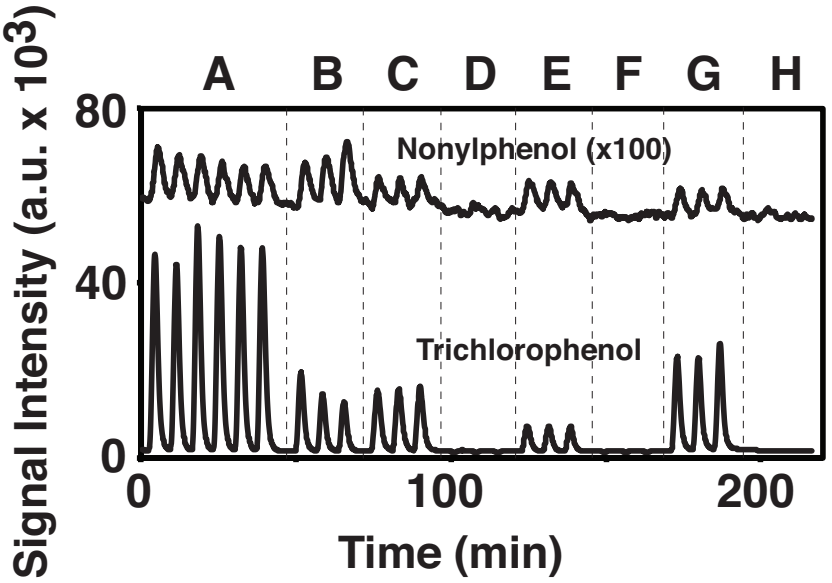

Figure 3.7: Typical data for the miniature CP-MIMS probe when implemented in an automated analysis series of a variety of sample matrices spiked with ppb levels of target analytes. The top trace (offset for clarity) is the signal for nonylphenol (100 ppb, signal × 100 for scaling purposes) and the bottom trace is for trichlorophenol (50 ppb). In each peak, a 4 mL unstirred sample was analyzed for 99 sec with the probe. All samples were analyzed as is without dilution or pre-filtration. The sample matrices evaluated included DI water (A), Koi pond water (B), beer (C spiked, D unspiked), artificial urine (E spiked, F unspiked) and primary sewage wastewater effluent (G spiked, H unspiked). All samples were analyzed in triplicate, except the DI water (6 replicates).

Although we observe some signal suppression effects for the complex samples, with analyte signal levels ranging from 13-120% when compared to those obtained for DI water samples, the effect appears to be both analyte and matrix dependent (Figure 3.7). In earlier work we have noted similar effects [55] and we are still in the process of characterizing the signal suppression source(s). However, the observations in Figure 3.7 suggest that CP-MIMS, even with signal suppression effects, allows direct measurements for trace level analytes in complex samples that would otherwise require substantial cleanup, preconcentration and/or chromatographic separations prior to analysis, and that would not be detected in direct infusion flow injection experiments [55]. Considering the crude autosampler system used and the wide range of

complex sample types tested, these proof-of-concept experiments demonstrate potential for CP-MIMS as a rapid, automated pre-screening technique to identify positive samples for subsequent quantitation by conventional methods (*e.g.,* HPLC-MS). This would allow better allocation of time and reagent costs in laboratories performing high throughput work-up and measurement of samples by conventional high sensitivity methods. If implemented as part of a modern autosampler system, the possibility of a logic driven, automated pre-screen prior to more time-consuming sample cleanup and chromatographic analyses is foreseeable.

Table 3.5: Peak Height and Area Signal Relative Standard Deviations (RSD) for the Autosampler Implemented Miniature CP-MIMS Probe.

	Target analyte signal % RSD			
	Trichlorophenol		Nonylphenol	
Matrix	Height	Area	Height	Area
DI water	6.8	8.8	13	11
Koi pond water	22	31	19	8.7
Beer	2.4	1.7	0.97	9.4
Artificial urine	2.6	5.1	4.2	3.4
1^o Effluent	8.3	3.8	2.8	4.2
average % RSD	8.4	10	7.9	7.2

3.3.7 Direct, *In-vivo/In-Situ* Monitoring

As a final demonstration of the applicability of the miniature CP-MIMS probe, its use in an *in-vivo* insertion probe was examined. A large, freshly cut celery plant stalk (*Apium graveolens*) was carefully pierced 1 cm from its base with a small twist drill bit to allow direct, horizontal insertion of the miniature CP-MIMS probe, such that the active membrane surface was completely inside the stem. The stalk with embedded

probe was mounted vertically with 1 mm of its base immersed in 50 mL of 130 ppm aqueous gemfibrozil solution. The system was left undisturbed, and the subsequent osmotic transport of gemfibrozil up the celery stalk recorded using the miniature CP-MIMS probe system for nearly an hour (Figure 3.8). Although no attempt is made to quantify the transport rate for the analyte in the live plant stem, this demonstrates that there is potential for the use of the miniature CP-MIMS probe in continuous monitoring *in-vivo* studies, similar to those currently employing micro-dialysis [75].

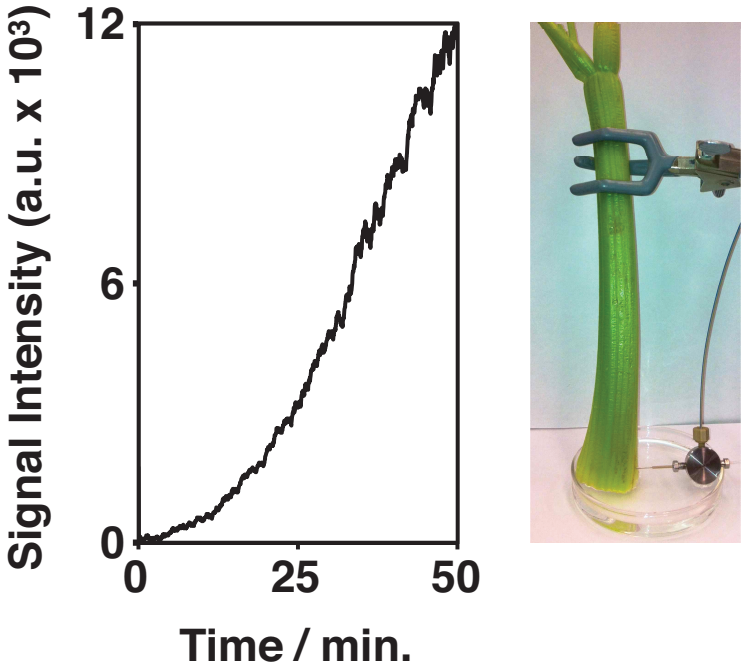

Figure 3.8: Demonstration of continuous *in-situ* / *in-vivo* monitoring using the miniature probe. The membrane end of the probe was completely inserted inside the stem of a freshly cut celery plant stalk as depicted (*Apium graveolens*), and the on-line monitoring of gemfibrozil osmotic transport up the plant stem obtained using the miniature CP-MIMS probe system is illustrated.

3.4 Conclusion

A miniature membrane sampling probe for condensed phase membrane introduction mass spectrometry (CP-MIMS) with a methanol acceptor phase and an electrospray ionization source has been developed and characterized, including the optimization of acceptor phase flow rate, sample mixing and probe washing strategies. Signal response times and detection limits are presented and compared to those obtained a larger flow cell interface design [55]. The probe demonstrates linear calibration curves in the low parts-per-billion range, and has been used to make measurements of polar, non-volatile contaminants spiked into in a variety of complex sample matrices, including artificial urine, natural water, beer and waste water effluent samples. The miniature probe was successfully employed as an *in-situ* reaction monitor to follow the loss of phenol and formation of chlorinated intermediates in response to dosing with active chlorine. A commercial autosampler was retrofitted with the probe, and used to make satisfactory automated measurements in small sample volumes. Non-exhaustive analyte depletion was observed for small sample volumes ($\sim$2 mL) with more pronounced extraction effects in smaller sample volumes. Finally, the system was successfully used in a demonstration of the *in-situ* / *in-vivo* monitoring of the osmotic transport of gemfibrozil in a celery plant stem. Future work includes further reduction of the membrane probe size and its use as part of a rapid, intelligent pre-screening autosampler methodology for high throughput sample measurements, and a systematic investigation of matrix suppression phenomena with complex sample matrices.

Chapter 4

Ionization suppression effects with condensed phase membrane introduction mass spectrometry: methods to increase the linear dynamic range and sensitivity

Reproduced in part with permission from Duncan, K.; Vandergrift, G.; Krogh, E.; Gill, C."Ionization suppression effects with condensed phase membrane introduction mass spectrometry: methods to increase the linear dynamic range and sensitivity." *J. Mass Spectrom.*, 50, 437-443 (2015). K. Duncan collected the majority of data, with contributions from G. Vandergrift. Data analysis, interpretation of results, and initial manuscript drafting was done by K. Duncan. Intellectual and editorial contributions from E. Krogh and C. Gill.

4.1 Introduction

The direct, online, trace level analysis of small polar and/or low volatility organic compounds is becoming increasingly important for both environmental and bioanalytical chemistry. Continued interest and development of progressively more sensitive analytical methodologies has resulted in the detection and quantitation of a wide range of trace level environmental contaminants such as pharmaceuticals and per-

sonal care products (PPCPs), illicit drugs, and drug metabolites in samples such as surface waters, wastewater and sewage sludge [1, 2, 76–78]. From a regulatory perspective, the need for trace analysis of illicit drugs and their respective metabolites from complex biological matrices (*e.g.,* urine) has become prevalent [79]. Additionally, small molecule biomarkers are now being utilized to help detect and diagnose specific types of diseases [80, 81].

Chromatographic methods involving manual sample preparation can be tedious and labour intensive, resulting in relatively long (and potentially costly) analysis times. As a result, many new analytical techniques have focused on achieving appropriate detection limits using online methods capable of analyzing multicomponent analyte mixtures [3]. As an example, online solid-phase extraction systems coupled with LC-MS instrumentation have led to the automation and analysis of organic micropollutants directly from complex sample matrices [82,83]. Further, Gethard and Mitra have reported the use of an online membrane distillation process to pre-concentrate aqueous environmental samples for delivery to an HPLC-MS, with detection limits in the low parts-per-billion (ppb) range for pharmaceutical residues in natural waters [84]. In a subsequent study, they further reduced detection limits by immobilizing carbon nanotubes on the membrane surface [85]. Although these online methods can reduce labour, the development of multicomponent chromatographic separations is often not trivial. Matrix effects from environmental and biological samples are common, and can quickly complicate the analysis. Taylor describes these effects as being caused by co-eluting species altering the ionization efficiency of analyte ions (either suppressing or enhancing analyte ionization) [45].

Condensed phase membrane introduction mass spectrometry (CP-MIMS) is an online technique that allows for the direct analysis of analytes in complex samples, with applications ranging from rapid screening to continuous reaction/process moni-

toring [55]. For recent trends in MIMS research (including CP-MIMS), the reader is directed towards a perspectives article [86]. The technique employs a semi-permeable membrane to separate the sample (donor phase) from a liquid (condensed) acceptor phase. Driven by gradients in chemical potential, analytes diffuse through the membrane and are solvated by a flowing acceptor phase. The permeating analyte(s) are then entrained with the acceptor phase to an atmospheric pressure ionization (API) source for identification and quantitation by mass spectrometry. Method selectivity is a function of both membrane permselectivity and unique m/z or MS/MS transitions afforded by the mass spectrometer. Previous examples of CP-MIMS variant systems in the literature include membrane systems for the online separation and preconcentration of proteins with subsequent electrospray ionization (ESI) mass spectrometry [30–33], monitoring the progress of concentrated (ppm level) pharmaceutical reaction mixtures using a polyvinylidene fluoride flat sheet membrane interfaced with an atmospheric pressure chemical ionization (APCI) mass spectrometer [34], and a polydimethylsiloxane (PDMS) hollow fibre membrane (HFM) mounted directly on an ESI capillary for the analysis of herbicides and phenols at ppb to pptr levels [35]. In addition, our group has developed and evaluated several CP-MIMS interfaces, based upon HFMs with several membrane materials and geometries, in both flow-cell and immersion probe designs [55, 87, 88].

As a consequence of using a solvent acceptor phase to transfer analytes from a membrane sampling interface, CP-MIMS can make use of the full range of API sources (*e.g.,* ESI, APCI, etc.) now available for mass spectrometry based detection. Unfortunately, ionization suppression with API sources has emerged as a major concern, especially for environmental and bioanalytical measurements. We have shown that CP-MIMS improves quantitation when compared to direct infusion analysis by ESI, as the PDMS membrane excludes many sample matrix components (*e.g.,* dis-

solved ions), which otherwise contribute to ion suppression [55]. However, samples containing high loads of co-permeating matrix species still present a challenge for quantitation via CP-MIMS by limiting the sensitivity and linear dynamic range. In early work, we observed signal differences for analytes spiked in complex sample matrices (*e.g.,* river water and artificial urine versus deionized water), and speculated that ionization suppression by co-permeating species may have been the underlying cause [55].

This study aims to further characterize these previously observed signal suppression effects, by identifying ionization suppression from membrane permeable matrix species as a concern. The linear dynamic range of CP-MIMS with both APCI and ESI is evaluated, and strategies for dynamic range extension are presented. These include the novel implementation of a continuously infused internal standard in the membrane acceptor phase, and modulation of the acceptor phase flow rate. We present results obtained for trace level analytes spiked in complex sample matrices (primary wastewater effluent and artificial urine), using both ESI and APCI. In addition, we report improved analytical sensitivity using a stopped-flow mode, with measured detection limits at low parts-per-trillion levels.

4.2 Experimental

A CP-MIMS system similar to that used in this study has been described in detail elsewhere [87,88]. Briefly, a 2 cm length of a capillary hollow fibre PDMS membrane (OD = 0.64 mm; ID = 0.30 mm; 170μm thickness) was mounted on stainless steel hypodermic supports (22 gauge, Vita Needle Co., Needham, MA, USA) to form an immersion probe type assembly (*e.g.,* J-probe [88]). The PDMS was swelled in hexane (ACS grade, Fisher Scientific, Ottawa, Ontario, Canada) to facilitate mounting,

resulting in a tight fit around the hypodermic needle following the evaporation of hexane. Methanol was pulled through the lumen of the PDMS HFM at a previously optimized flow rate of 200μL min^{-1} by a four-piston micropump (Cheminert model M6, VICI ValcoTM, Houston, TX, USA). Unless otherwise noted, the resulting CP-MIMS immersion probes were directly inserted into 40 mL samples in clear glass vials (EPA/VOA Type, Scientific Specialties Inc., Hanover, MD, USA) that were continuously mixed by a Teflon magnetic stir bar and magnetic stirrer (LABDISC S56, Fisher Scientific).

Target analytes were measured using a triple quadrupole mass spectrometer (Micromass Quattro Ultima, Waters-Micromass, Altrincham, UK) equipped with interchangeable ESI and APCI source probes. Physicochemical properties and mass spectrometer scan parameters for all target analytes are given in Table 4.1. When monitoring positive ions (*e.g.,* aniline, aniline-d_5, and 2-methylquinoline), electrospray experiments were conducted with 3.8 kV applied to the electrospray capillary, 750 L/hour nitrogen desolvation gas and 50 L/hour of nitrogen curtain gas (99.999 % N2, Praxair Nanaimo). Negative ion experiments (*e.g.,* gemfibrozil) used the same conditions, except 3.2 kV was used as the operating capillary voltage. For tandem mass spectrometry (MS/MS) experiments, the argon (99.999 % Ar, Praxair Nanaimo) collision cell pressure was $\sim$3.1 x 10^{-3} Torr. When using the APCI source, the corona discharge voltage was maintained at 4.0 kV with a desovation gas flow of 130 L/hour, and a probe temperature of 400°C.

Aniline, aniline-d_5, and gemfibrozil were obtained from Sigma Aldrich (Oakville, Ontario, Canada), and were at least 99% pure. These analytes were used as model organic micro-contaminants either containing amine or carboxylic acid functional groups. 2-Methylquinoline (Sigma Aldrich), used as a model co-permeating matrix species, was technical grade and only 95% pure. Stock solutions were gravimetrically

Table 4.1: Analyte physicochemical properties and MS scan parameters.

	Molar mass (g mol^{-1})	Vapour Pressure* (Pa @ 25^{o}C)	pK$_a$ *	Log K_{ow} *	MS scan m/z	Collision energy (eV)
Aniline	93.13	89.1	4.6	0.9	SIM 94 MS/MS 94 $\rightarrow$ 78	-
Aniline-d_5	98.13	-	-	-	SIM 99 MS/MS 99 $\rightarrow$ 83	22
2-methylquinone	143.19	1.3	5.7	2.59	SIM 144	-
Gemfibrozil	250.33	8.1 x 10^5	4.5	4.3	MS/MS 249 $\rightarrow$ 121	15

*SRC Physical Properties Database [89]

prepared using HPLC grade methanol (Fisher Scientific). Diluted aqueous standards were made using 18 MΩ de-ionized (DI) water (Model MQ Synthesis A10, Millipore Corp., Billerica, MA, USA), with less than 0.5% methanol in the final standard solutions. Samples were pH adjusted using dilute aqueous HCl or NaOH (Fisher Scientific). Ionization suppression experiments were buffered with a pH 8.5 phosphate buffer (10 ppm), to ensure the dominant surrogate matrix species (2-methylquinoline) was neutral, allowing high levels of co-permeating matrix molecules with the analyte. Likewise, the stopped-flow experiment was buffered at pH 4.0 with citrate buffer (10 ppm, adjusted to pH 4.0 with HCl) to ensure protonation of the acidic analyte being measured. Complex matrices tested include pH adjusted primary wastewater effluent from a small municipality in British Columbia, Canada, and artificial urine prepared as detailed in an earlier study [55]. All experiments were conducted under ambient conditions (25°C,101 kPa).

4.3 Results and Discussion

4.3.1 Ionization Suppression Studies

Ionization suppression has surfaced as a common problem for reproducible quantitative LC-MS/MS methods [90]. Complex matrices containing high salt loads and other matrix components can result in signal instability and the suppression of ion formation. Although hydrophobic membrane materials such as PDMS effectively reject salts and ionized matrix components, co-permeating neutral matrix species are a concern for CP-MIMS, since analytes are simultaneously monitored (as a mixture) in a continuous fashion. Fluctuations in the concentration of co-permeating matrix species may lead to significant bias in quantitation. Non-linear ionization suppression effects could also bias standard addition experiments due to altered signal intensities

for the added standards. In an effort to demonstrate these effects, 5 ppb aniline-d_5 (added directly to the acceptor phase reservoir) was monitored during the addition of 2-methylquinoline (2-MQ) to a DI water sample buffered at pH 7.4 (see Figure 4.1a).

Variations in the observed aniline-d_5 signal intensity are due to ion suppression resulting from the addition of 2-MQ in the sample, and not to membrane permeation effects (anline-d_5 is not transferred from the sample to the acceptor phase), as seen in Figure 4.1b. The addition of 1 ppm of 2-MQ to a buffered DI water sample results in a 40% decrease in the aniline-d_5 signal. There is a strong temporal correlation between the reduction of aniline-d_5 ($m/z = 99$) signal and the concomitant increase in signal for 2-MQ ($m/z = 144$). Because aniline-d_5 was continuously infused at constant concentration in the acceptor phase, decreased signal intensity is primarily due to ionization suppression in the ESI source. A second addition of 1 ppm 2-MQ to the aqueous sample resulted in further 30% reduction in the aniline-d_5 signal, presumably due to non-linear ionization suppression effects. When the membrane interface was immersed in clean DI water (sample washout), the signal for aniline-d_5 present in the acceptor phase returned to its previous level, as ionization suppression by 2-MQ was removed.

In previous work, we have shown that the concentration of analyte in the methanol acceptor phase is roughly ten times less than that in the sample in a CP-MIMS experiment with similar flow rates [87]. Realizing the flux across the membrane is analyte dependent, we estimate that a 1 ppm 2-MQ in the sample will result in roughly 100 ppb in the methanol acceptor phase. These data therefore suggest that as little as 100 ppb of co-permeating neutral matrix molecules delivered to the ESI source can result in significant reduction of analyte ionization. Although PDMS membranes act to preclude many problematic matrix species (such as salts and ionized molecules), it is apparent that co-permeating neutrals can result in suppressed analyte signals. As a

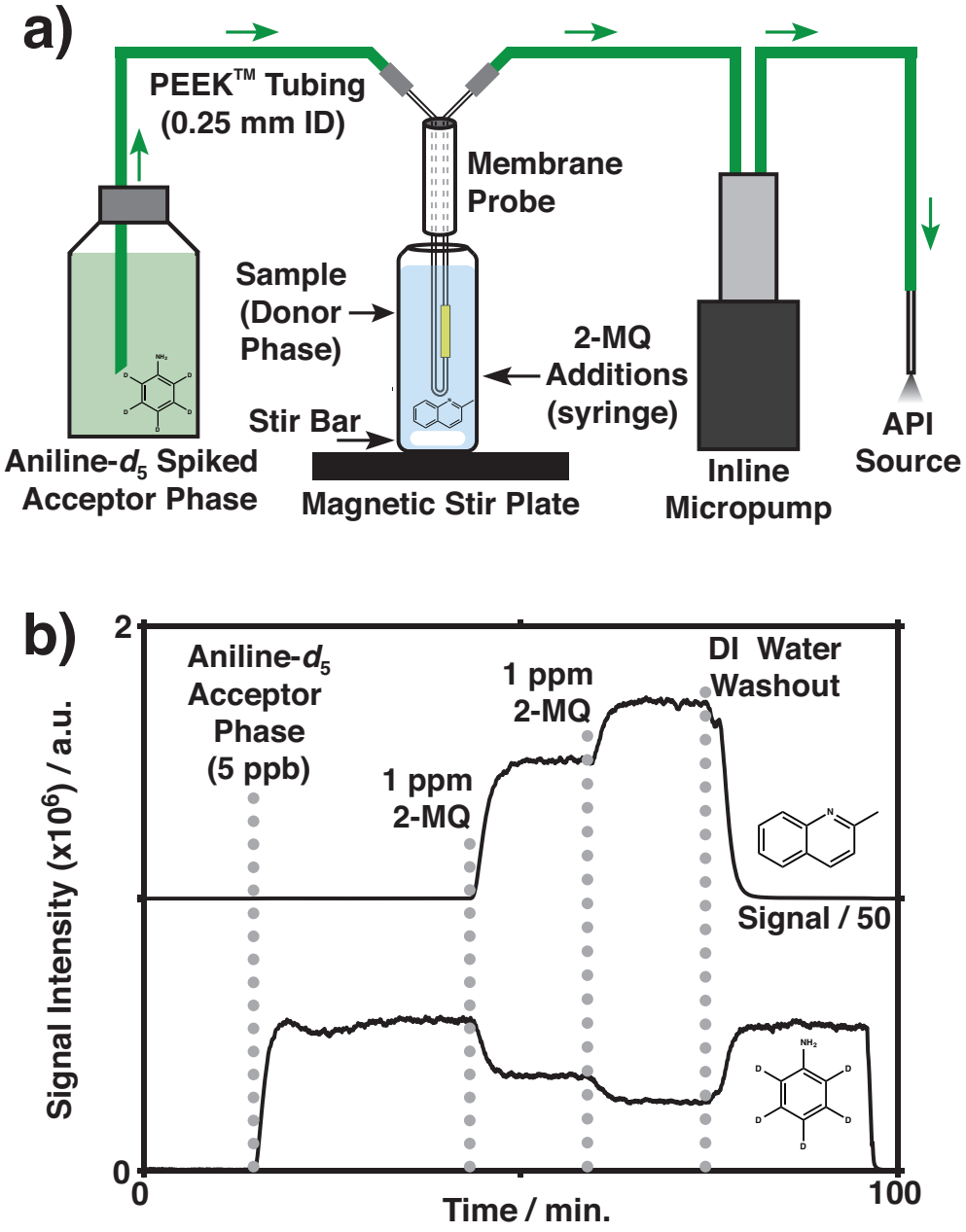

Figure 4.1: Ionization supression caused by high concentration spikes of 2-methylquinoline (2-MQ) added to the sample. As illustrated in a), aniline-d_5 (5 ppb) was added directly to the methanol (acceptor phase), followed by two additions of 2-MQ (1 ppm each) into DI water (donor phase), buffered at a pH of 7.4. Part b) shows a decrease in aniline-d_5 intensity (SIM at m/z 99) that closely follows the signal increases observed for additions of 2-MQ (SIM at m/z 144). Upon removal of 2-MQ (washout in DI water), the aniline-d_5 signal returns to original levels.

result, quantitation of analytes directly from complex samples by CP-MIMS coupled to an ESI source using direct calibration, or even with standard additions, presents a challenge.

4.3.2 Linear Dynamic Range Studies

The linear dynamic range (LDR) of CP-MIMS in conjunction with both ESI and APCI was investigated for the model compound aniline (Figure 4.2). Concentrated stock solutions of aniline were spiked into a 1 L aqueous sample, while 5 ppb aniline-d_5 was continuously infused with the methanol acceptor phase, in order to quantify and correct any effects upon ionization. Panels a) and b) in Figure 4.2 show a direct comparison of direct calibration curves for APCI and ESI under identical conditions. As anticipated, APCI was less sensitive, with the lowest limit of the LDR at ∼100 ppb. However, the APCI response was linear for aniline concentrations in excess of 500 ppm indicating that ionization suppression is less of a concern for this analyte using APCI. In contrast, ESI experiments proved more sensitive, with the lower boundary of the LDR below 1 ppb. However, ionization suppression was observed at higher concentrations, evidenced by nonlinear responses at aniline concentrations greater than ∼10 ppm (Figure 4.2b).

Varying the flow of the acceptor phase allows for modulation of the amount of methanol that solvates the permeated analytes, changing the analyte concentration in the acceptor phase before entrainment to the ion source. At higher acceptor flow rates, the analyte concentration in the acceptor phase decreases as a result of dilution. Figure 4.2c illustrates the aniline calibration curve at a methanol acceptor phase flow rate of 500 μL min^{-1} using ESI. At higher flow rates the experiment was less sensitive, but it was also less prone to ionization suppression, extending the LDR to higher sample concentrations. Although not demonstrated here, it is conceivable that on-

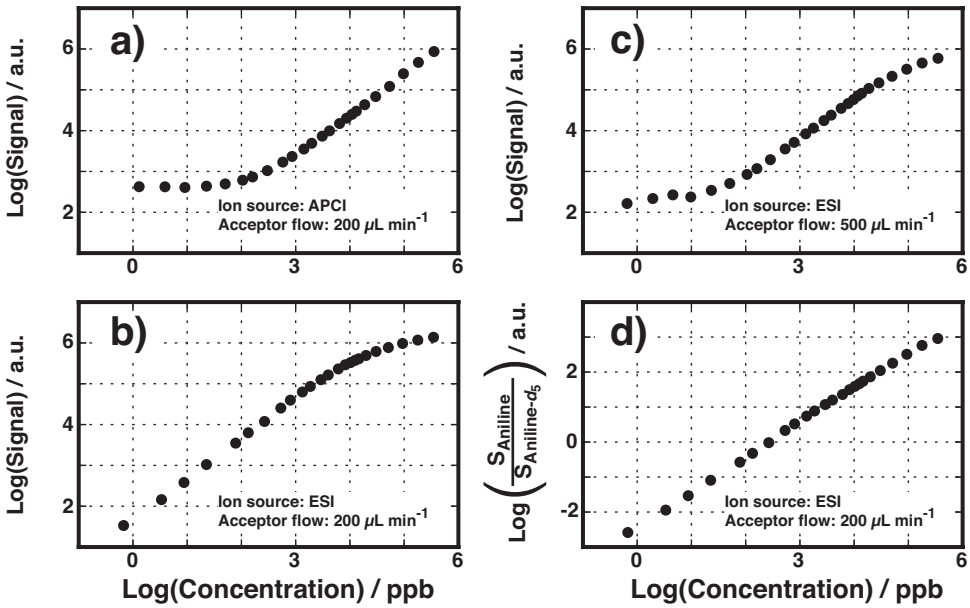

Figure 4.2: CP-MIMS calibration curves illustrating the linear dynamic range (LDR) for aniline with a) APCI and b) ESI using a 200 μL min^{-1} acceptor phase flow rate. In c) the LDR with ESI is extended to higher concentrations using an increased acceptor phase flow rate of 500 μL min^{-1}. Panel d) illustrates the ESI LDR was extended to six orders of magnitude, correcting for ion suppression at higher concentrations using the continuously infused internal standard (aniline-d_5) in the acceptor phase. Aniline and aniline-d_5 were monitored by MS/MS transitions.

the-fly acceptor phase flow rate adjustments with an automatic calibration feedback system could be useful. For example, if an observed analyte signal is too high for the measured LDR, the acceptor flow could be increased, providing an online dilution to effectively extend the methods LDR.

A second approach for extending the LDR and mitigating ionization suppression employs a continuously infused internal standard. CP-MIMS allows for two methods of adding an internal standard: i) the classical addition directly to the sample (donor phase); and ii) the addition of internal standard to the acceptor phase. By infusing the internal standard into the acceptor phase, the concentration of analyte

in the sample can be determined with minimal sample modification. This approach maintains sample integrity for future or further analysis, and has the added benefit of allowing for direct observation of any deviations in ionization efficiency. To demonstrate this strategy, as described earlier, 5 ppb of aniline-d_5 was added directly to the acceptor phase, and aniline was successively spiked into 1 L of stirred DI water (in a round bottom flask) to generate calibration data. The measured aniline signals were normalized with the internal standard signal, and plotted against aniline concentration (Figure 4.2). Excellent calibration linearity is observed for the entire concentration range examined (spanning 6 orders of magnitude). High concentrations of aniline in the sample resulted in the aniline-d_5 signal being suppressed by as much as 90% (data not shown). However, when the sample was replaced with DI water in a manner analogous to Figure 4.1, the aniline-d_5 signal quickly returned to its original level. Therefore, adding an appropriate internal standard to the acceptor phase can enable the correction of ionization suppression effects, and provide an excellent LDR when using ESI.

4.3.3 Measurements in Complex Sample Matrices

To verify the efficacy of the continuously infused internal standard present in the acceptor phase for the quantitation of trace level analytes in complex real-world sample matrices, aniline standards were spiked into three different samples (DI water, wastewater effluent and artificial urine), while 5 ppb aniline-d_5 was added directly to the methanol acceptor phase as an online internal standard. Both ESI and APCI sources were evaluated, and the results from this study summarized in Table 4.2. The ESI signal traces are illustrated in Figure 4.3. For quantitation, response factors for aniline/aniline-d_5 were first determined using the DI water sample. No notable signal suppression was observed for the aniline signal in the DI water or the wastewater

samples, however the measurement of aniline in the artificial urine sample exhibited significant signal suppression when using ESI (Figure 4.3a). The temporal features of the aniline signal indicate that the signal suppression was initially minor. However, both the aniline and the internal standard signals gradually decrease over several minutes, eventually reaching a steady state at 60% their initial levels (Figures 4.3a and b). Artificial urine is comprised of many components [55], some of which cross the membrane at differing rates. As the levels of co-permeating matrix molecules increase in the acceptor phase (*e.g.,* uric acid), the signal for aniline and aniline-d_5 will be suppressed, explaining the transient decay in signal intensities observed for the spiked artificial urine sample.

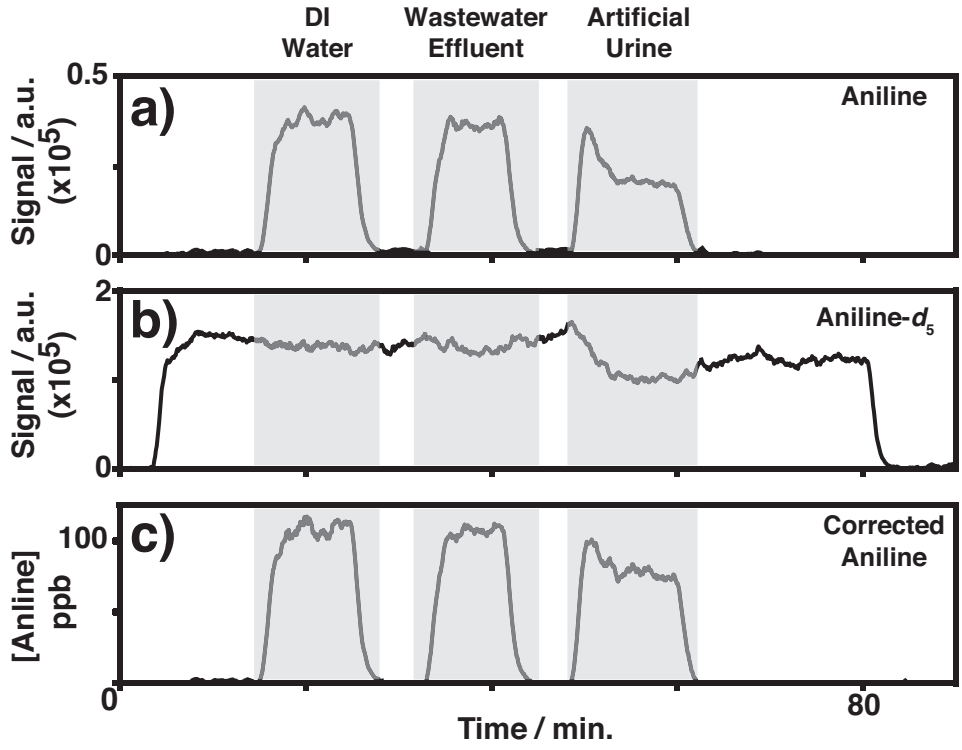

Figure 4.3: Quantitation of aniline using a CP-MIMS immersion probe in spiked water samples (DI water; wastewater effluent; and artifical urine) at pH 8.5 using a continuously infused internal standard and ESI-MS. a) aniline signal (SIM at m/z 94) for 105 ppb spiked samples, b) aniline-d_5 internal standard (SIM at m/z 99) at 5 ppb in methanol acceptor phase, c) aniline concentrations determined using an experimentally determined response factor derived from the DI water sapmle.

Using the response factor determined from the DI water sample, aniline concentrations were determined for the measured samples (Figure 4.3c). For the wastewater sample, there was minimal suppression, giving rise to a percent bias of less than one percent for both ESI and APCI (Table 4.2). The ionization suppression for the spiked artificial urine sample using ESI gives rise to an apparent aniline concentration of 72 ppb when determined using a simple, direct calibration (-28% bias). Using the correction provided by the internal standard approach, the aniline concentration was determined to be 90 ppb (-13% bias). Although the use of a continuously infused internal standard in the acceptor phase does not completely eliminate the signal suppression effects observed in the spiked artificial urine sample, the percent bias is reduced significantly. Thus, the ionization suppression resulting from co-permeating neutral matrix molecules can be at least partially mitigated using this approach.

Table 4.2: Aniline concentrations in complex aqueous samples determined by CP-MIMS, obtained using a continuously infused internal standard in the acceptor phase to correct for ionization efficiency variations.

Ionization Method	Sample Matrix	$[\text{Aniline}]_{True}$ (ppb)	$[\text{Aniline}]^{*}_{CP-MIMS}$ (ppb)	Bias (%)
ESI	Wastewater Effluent	105	105	n/a
	Artificial Urine	104	90	-13
APCI	Wastewater Effluent	398	397	<-1
	Artificial Urine	403	395	-2

* Determined with a response factor obtained using a spiked DI water sample

Because APCI demonstrated less sensitivity (vide supra), spiked aqueous samples were made up to ∼400 ppb aniline (the [aniline-d_5] in the acceptor phase remained at 5 ppb). In contrast to the results obtained using ESI, very little signal suppression was observed with APCI for all of the tested sample matrices (data not shown). Concentrations calculated utilizing the continuously infused internal standard resulted in percent bias values of less than 2% (Table 4.2). The results of these experiments suggest that although CP-MIMS using APCI may be less sensitive, matrix suppression

effects are much less of a concern when compared to ESI.

4.3.4 Stopped-Flow Quantitation

As previously described, to improve method sensitivity, CP-MIMS can operate in a stopped-flow mode where the methanol acceptor phase flow is stopped for a fixed time within the lumen of the HFM using a 4-port valve [55, 87]. During the stop-flow periods, analyte transport across the PDMS continues, allowing the accumulation of a concentrated plug of analyte in the acceptor phase volume within the HFM lumen. Following this pre-concentration step, the valve can be actuated to entrain the acceptor phase toward the ESI-MS for analysis. This results in a signal trace resembling a chromatographic peak as the analyte enriched plug is flushed through the system. The corresponding increase in sensitivity is proportional to the time the acceptor phase is stopped (until equilibrium is reached). Previous studies indicated an optimum sensitivity enhancement occurs after ∼15 minutes of stopped-flow time [55].

To demonstrate the applicability of this strategy, the membrane interface was challenged with two low level aqueous solutions of gemfibrozil (10 pptr and 100 pptr, each measured in triplicate) prepared in DI water (Figure 4.4) using MS/MS for analyte detection. The small signal spikes for blank solutions (18 MΩ DI water) were observed across all mass channels, and are attributed to acceptor phase flow pulses from the manually actuated divert valve (rather than analyte memory effects).

For data analysis, the background and noise were estimated from the mean and standard deviation of the peak areas for all six background trials. Peak areas were determined from the mass spectrometers software platform (MassLynx version 4.1). There was no observable rise in the baseline signal when the membrane interface was immersed into the 10 pptr gemfibrozil sample (*e.g.,* after ∼100 min in Figure 4.4), which suggests this sample was below the detection limit for CP-MIMS operated in

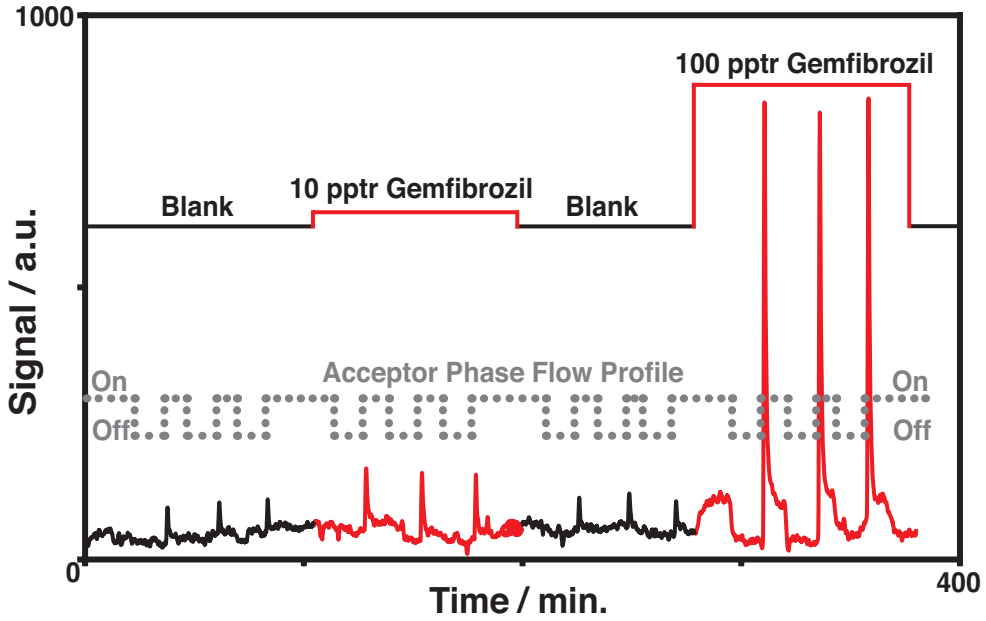

Figure 4.4: Stopped-flow mode quantitation of gemfibrozil at low pptr levels from aqueous DI samples. In order to preconcentrate analyte on the acceptor side of the membrane, the methanol acceptor phase was stopped for 15 minute intervals (depicted by the acceptor phase flow profile). Measurements were conducted in triplicate, for two blank samples and two gemfibrozil solutions (10 pptr and 100 pptr, buffered at pH 4).

continuous analysis mode. However, in stopped-flow mode, the 10 pptr sample yielded peaks that were easily distinguishable from the background trials. The corresponding (background subtracted) signal to noise (S/N) of 5 indicates that 10 pptr is very close to the detection limit for gemfibrozil using this method. When the membrane interface was submersed into the 100 pptr sample, a characteristic rise in signal was observed in continuous mode operation (*e.g.,* after ∼280 min in Figure 4.4). A resulting S/N of 6 was determined for continuous mode at 100 pptr, giving rise to a detection limit around 50 pptr. In stopped-flow mode, the 100 pptr sample exhibited peaks well above the background signal with an average S/N of 52. Therefore, by employing a stopped-flow approach, the observed detection limits were reduced by an order of magnitude. Detection limits could likely be further reduced by sample heating [35],

and/or by increasing the surface area of membrane exposed to the sample.

4.4 Conclusion

We have demonstrated that ionization suppression from high levels of co-permeating neutral matrix components are a confounding factor when making direct, quantitative measurements with CP-MIMS utilizing ESI. This suggests that direct calibration and standard addition methodologies may not be the quantitative methods of choice for CP-MIMS in conjunction with ESI. The calibration linear dynamic range (LDR) of a model analyte was evaluated by CP-MIMS using both APCI and ESI. APCI is not observed to suffer from significant suppression effects, and although less sensitive than ESI, yielded excellent calibration linearity. The LDR using ESI can be tuned by varying the flow rate of the acceptor phase through the lumen of the HFM. The novel use of an internal standard continuously infused in the membrane acceptor phase demonstrated an exceptional LDR for over 6 orders of magnitude for CP-MIMS employing ESI.

The use of an internal standard in the acceptor phase was evaluated for several complex real-world samples by CP-MIMS using both ESI and APCI. Minimal ionization suppression effects were observed for a spiked wastewater effluent sample matrix, whereas significant suppression occurred for measurements in a spiked artificial urine sample with ESI. Quantitation using response factors and a continuously infused internal standard corrected for much of the observed ionization suppression with ESI. Negligible ionization suppression was observed for any of the equivalent APCI experiments.

Using CP-MIMS in stopped acceptor phase flow mode, a S/N of 5 was observed for the direct measurement of a 10 pptr gemfibrozil standard, which corresponds to

a detection limit of ∼5 pptr. This is roughly a 10× sensitivity improvement from continuous acceptor flow mode experiments. Future work will includes the evaluation of longer/bundled membrane systems and heating strategies aimed at decreasing detection limits, as well as automation to provide real-time acceptor phase control and switching. We are currently examining the applicability of non-labeled internal standards as viable alternatives when isotopically labeled molecules are not readily available.

Chapter 5

Semi-quantitative sceening and mass profiling of Naphthenic acids

Reproduced with permission from Duncan, K.; D. Letourneau; Vandergrift, G.; Jobst, K.; Reiner, E.; Gill, C.; Krogh, E."A semi-quantitative approach for the rapid screening and mass profiling of naphthenic acids directly in contaminated aqueous samples." *J. Mass Spectrom.*, 51, 44-52 (2016). K. Duncan collected the majority of data for low resolution MS experiments, with minor contributions from D. Letourneau, and G. Vandergrift. K. Duncan and K. Jobst collected high resolution MS data. Initial drafting of the paper was done by K. Duncan, with E. Krogh providing major editorial oversight. Additional editorial contributions were from C. Gill, E. Reiner, K. Jobst.

5.1 Introduction

Classical naphthenic acids (NAs) are a complex mixture of alkyl-substituted carboxylic acids described by the general formula: $C_nH_{2n+z}O_x$, where n represents the number of carbon atoms, z is the hydrogen deficiency, and x is the number of oxygen atoms. Historically, attention towards NAs was directed towards pipeline and oil processing facility corrosion, however, more recently, NAs have emerged as toxic, persistent environmental contaminants in the northern Alberta Athabasca oil fields. Several reviews nicely summarize the properties, toxicity, measurement, and treatment of oil sands naphthenic acids [91, 92].

Mass spectrometry has surfaced as the most common tool used to characterize

complex NA mixtures. Selectivity arises from both the ionization method used and *m/z* discrimination. Headley *et al.* present a review detailing the recent advances in mass spectrometric characterization of NAs from oil sand, environmental samples, and crude oil [93]. It is apparent that high resolution Fourier Transform Mass Spectrometry (FTMS) is among the most popular techniques for NA profiling. When coupled with negative electrospray ionization (ESI), FTMS facilitates the accurate mass determination of $[M\text{-}H]^-$ ions [94–96]. Further, by varying the ionization technique employed in conjunction with FTMS, Barrow *et al.* were able to more broadly characterize NA samples that also contain compounds with poor electrospray ionization efficiencies [97]. In addition to atmospheric pressure ionization (API) sources, a recent study showcased the characterization of NAs by derivatization followed by GC, coupled to ultra-high resolution MS [98]. Electron ionization, CH_4 chemical ionization, and NH_3 chemical ionization were evaluated, correlating compound elemental composition with respect to retention time. Recent advances in two dimensional gas chromatography - time of flight mass spectrometry have further characterized derivatized NA mixtures and have been useful in the identification of individual molecular components [99].

Quantitative techniques for NAs include liquid chromatographic separation coupled to mass spectrometry. Ross and co-workers quantified acid extracted organics from natural waters surrounding the Canadian oil sands by liquid chromatography in conjunction with negative electrospray ionization high resolution time of flight mass spectrometry [100]. Total NA quantitation was based on the integration of signal intensities at observed *m/z* values that matched theoretical homologue groups present in a refined Merichem standard (a commercially available, complex mixture of NAs), and concentrations were assigned based on a four point refined Merichem direct calibration. An innovative approach utilizing liquid chromatographic separation

entails NA derivatization with N-(3-dimethylaminoprophyl)-N-ethylcarbodiimide followed by tandem MS analysis of a common fragment for all derivitized carboxylate groups with positive electrospray ionization [101]. Rather than quantify NAs as an equivalent concentration of refined Merichem, Woudneh *et al.* elected to report total NAs as equivalents of the surrogate standard pyrenebutyric acid. While these methods are sensitive and quantitative, sample cleanup, handling, and chromatography contribute to greater analysis time and cost.

High-throughput rapid screening techniques better facilitate large-scale monitoring campaigns, and could be employed in conjunction with more sensitive and quantitative techniques by positively identifying contaminated samples. Shang *et al.* demonstrated a rapid LC-MS screening method with for total NAs from contaminated aqueous samples, with method detection limits of 10 ppb [102]. The method centrifuged aqueous samples to precipitate particulate matter, and injected a large volume (1 mL) of supernatant into the LC-MS system for detection by full scan negative ion ESI. Further work, with the addition of high resolution MS, yielded a method for high-throughput analysis of total NAs, and improved detection limits by an order of magnitude [103]. While these techniques require little sample preparation, highly complex samples (*e.g.,* oil sands process waters) would prove challenging. Matrix effects and high salt concentrations can interfere with chromatography as well as suppress ionization, and high level samples may introduce sample memory effects. Differential ion mobility has surfaced as a technique for rapidly characterizing NA samples in conjunction with negative ESI [104,105], however few studies have demonstrated quantitative results without chromatographic separation. As an alternative, several spectroscopic strategies (*e.g.,* FT-IR, UV-Vis, Fluorescence) have been utilized for the direct analysis of NAs in oil sands process waters (OSPW) and other environmental samples [106,107]. Although robust and simple, these optical methods

suffer from modest detection limits and poor specificity. Further, these methods do not provide any information on the relative distribution of NA isomer classes afforded by mass spectrometry.

Condensed phase membrane introduction mass spectrometry (CP-MIMS) has been established as a technique for the online analysis of trace level organic micropollutants directly from contaminated aqueous samples, including carboxylated analytes [55, 86, 87, 108]. A semi-permeable membrane (*e.g.,* polydimethylsiloxane, PDMS) separates the sample from a flowing solvent acceptor phase, which entrains membrane permeants to the MS for detection. The membrane acts to preclude salts and polar species, reducing matrix effects often observed from the direct injection of complicated samples. As outlined in a previous study, NAs can be directly monitored from real-world OSPWs with very little sample preparation [88]. The selectivity of the method is a function of membrane perm-selectivity, negative ion ESI, and the m/z of the molecular components.

The goals of the presented study are to demonstrate CP-MIMS as a semi-quantitative technique for the rapid screening of NAs directly from environmental and industrial samples, to utilize the method to obtain m/z profiles for sample characterization, and to demonstrate its utility as an on-line, continuous monitoring approach. The effects of sample pH upon the membrane permeability of carboxylic acids were explored. High resolution MS was used to establish which compound classes present in a refined Merichem NA standard permeated the PDMS membrane for detection. Several real-world NA contaminated samples were analyzed by CP-MIMS using both selected ion monitoring and full scan experiments, and were compared to results obtained by solid phase extraction liquid chromatography tandem mass spectrometry (SPE-LC-MS/MS) [101]. Lastly, CP-MIMS was evaluated for the online monitoring of NA adsorption in heterogeneous solutions containing activated biochar [109]. In

addition to providing direct observation of temporal changes of NA concentrations in aqueous solution, this method provides useful information on the relative changes in the mass distribution of naphthenic acid components [88]. We demonstrate the use of CP-MIMS for the rapid screening and mass profiling of NAs directly from contaminated samples.

5.2 Experimental

5.2.1 Condensed phase membrane introduction mass spectrometry

In-house constructed membrane interfaces were used for this work in the immersion J-probe configuration as outlined in a previous study [88]. Briefly, hexane (HPLC grade, Fisher Scientific, Ottawa, Ontario, Canada) was used to swell a 2 cm piece of PDMS hollow fibre membrane (Dow Corning Silastic tubing, OD = 0.64 mm; ID = 0.30 mm; 170 μ thickness, Midland, MI, USA), which was subsequently mounted on stainless steel hypodermic tubing supports (22 gauge, Vita Needle Co., Needham, MA, USA). Thin film composite membranes (0.5 μm PDMS film deposited on a 263 μm OD and 209 μm ID polypropylene support, neoMecs Inc., Eden Prairie, MN, USA) and 35 μm PDMS membranes (237 μm OD and 167 μm ID, Permselect, MedArray Inc., MI, USA) were mounted with epoxy potting as described elsewhere [88]. A methanol acceptor phase solvent was pulled through the lumen of the PDMS membrane at 200 μL min^{-1} by a low internal volume four piston micropump (Cheminert Model M6, VICI ValcoTM, Houston, TX, USA). Sample measurements were made by immersing the membrane probe directly into continuously mixed aqueous samples in 40 mL glass sample vials (Scientific Specialties Inc., Hanover,MD, USA). Sample mixing was accomplished using a magnetic stir plate. Naphthenic acids were analyzed

after adjusting the sample pH with small additions of 6 M HCl (Fisher Scientific) to a value below the pK_a of typical organic carboxylic acids (*i.e.,* pH ∼4), protonating carboxylate ions (to their neutral form) to facilitate membrane transport across the PDMS membrane. Control experiments to observe neutral compounds present in the sample, conducted at pH ∼8, consisted of raising the sample pH with 6 M NaOH (Fisher Scientific) prior to measurement. Sample pH was monitored with a pH meter (Accumet AR25, Fisher Scientific) and/or pH indicator strips (Sigma-Aldrich, Oakville, ON, Canada). All experiments were conducted under ambient conditions (25°C,101 kPa).

5.2.2 Mass spectrometry

Nominal resolution mass spectrometry experiments were performed using a Micromass Quattro LC triple quadrupole mass spectrometer (Waters-Micromass, Altrincham, UK). Negative ion ESI was used for NA analysis with a capillary voltage of -3.2 kV and an entrance cone voltage of 30 V, in conjunction with full scan MS (m/z 80–600, 1 s scan time). Selected ion monitoring experiments utilized a 0.5 s dwell time for each m/z monitored. Desolvation gas (UHP grade nitrogen, Praxair, Nanaimo, Canada) was maintained at a flow of 750 L hr^{-1} and heated to 300°C.

High resolution mass spectrometry experiments were performed using an IonSpec Fourier transform ion cyclotron resonance mass spectrometer (FTICR-MS), equipped with a 9.4 T superconducting magnet. The ESI source (capillary voltage: -3.0 kV, entrance cone voltage: 30 V) was operated in the negative mode. Ion collection and transient times ranged from 1 to 3 seconds, and were used to generate full scan mass spectra from m/z 100 to 1000 with resolution between 200 000 and 400 000. Internal mass calibration was accomplished using ubiquitous background ions at m/z 255.23295 and m/z 283.26425. Full scan mass spectra were exported as peak lists

and elemental compositions were assigned using a combination of custom macros for Microsoft Excel as well as Elemental Composition Calculator (Varian Inc.) [98]. For the calculations, 0–100 of the elements C,H,N,O and S were considered. All assignments were within 5 ppm of the theoretical values. A cluster of peaks $\sim m/z$ 400–450 was observed in the pH 3 CP-MIMS Kendrick mass defect plot (Figure 5.3b), which we have attributed to sodium bound dimers; for clarity, these peaks were not included in the figure.

5.2.3 Standard solutions and real world samples

Refined Merichem (Merichem Company, Houston, Texas) stock solutions were prepared gravimetrically with HPLC grade methanol (Fisher Scientific), and subsequent standard solutions were diluted in deionized (DI) water (Model MQ Synthesis A10, Millipore Corp., Billerica, MA, USA). Care was taken to ensure that there was less than 0.1% methanol in all measured aqueous solutions.

Real-world samples were collected from northern Alberta and include two oil sands processed waters (OSPW), two groundwaters (GW), and two surface waters (SW). Selected water quality parameters are summarized in Table 5.1. Surface waters were collected from a natural river several kilometers away from any industrial activity or other anthropogenic inputs. Surface waters were well oxygenated, with relatively low total dissolved solids, and dominated by dissolved $CaCO_3$. The total organic carbon measured as non-purgeable organic carbon (Shimadzu TOC-VCPH, Shimadzu Corporation, Tokyo, Japan) was around 15 mg/L C and almost entirely in the dissolved form. Groundwater samples (GW1 and GW2) were collected from two independent aquifers, one a deep saline water source (GW1) and the other a shallow potable water supply (GW2). These waters were anoxic and had elevated total dissolved solid content, dominated by dissolved sodium. The total organic carbon was 8 and 17 mg/L

C for GW1 and GW2, respectively. The oil sands processed waters were basic (pH 10 11), with elevated total dissolved solids content with 7.6 and 50 mS/cm for OSPW1 and OSPW2, respectively. These samples also had elevated TOC content at 420 and 2500 mg/L C, respectively. All water samples were collected in June 2012, filtered through glass microfibre filters (GF/C, Whatman, Fisher Scientific) and stored at 4 °C until analyzed by CP-MIMS. SPE-LC-MS/MS analysis for NAs was provided by a commercial laboratory (AXYS Analytical Services) [101] and reported as pyrene butryric acid (PyBA) equivalents.

Table 5.1: Selected water quality parameters for samples analyzed.

	SW1	SW2	GW1	GW2	OSPW1	OSPW2
pH	8.2	7.7	8.8	7.2	9.5	11.3
Sp. Cond. / μS cm^{-1}	260	200	2300	870	7600	50,000
DOC/TOC / ppm C	15/16	16/16	14/17	8/8	400/400	2500/2500
NA / ppm PyBA	0.006	0.004	0.099	0.022	26	150

* quantified as pyrene butryric acid equivalents [101]

5.2.4 Biochar adsorption studies

Adsorption studies were carried out by continuously monitoring naphthenic acids directly in buffered aqueous solutions. Activated biochar samples were added in doses ranging from ∼20–2000 mg/L with constant stirring. Two distinct biochar samples were used for comparison purposes. Sample A was prepared by pyrolysis of Aspen wood under nitrogen at 600°C [109]. Sample B is commercially available (ColorSorb G5, Jacobi, Kalmar, Sweden). These biochars were chosen for their availability and observed differences in adsorptive properties (Layzell, personal communication). After achieving stable baseline signals in DI water, the CP-MIMS membrane probe was immersed in an aqueous solution containing 4.1 ppm of Merichem buffered at pH = 3.60 ± 0.05 with glycine/HCl (0.12 M glycine, Fisher Scientific). After obtaining at

least five minutes of steady-state NA signal, a dose of solid biochar was added to the Merichem/buffer solution (doses ranged from 25–700 mg/L). Signal decay due to NA adsorption was monitored via the full scan total ion current (TIC) as well as appropriate NA SIM values (*e.g., m/z* 185, 223, 231, 237 and 263). Final full scan mass spectra were background-subtracted, and filtered to eliminate minor peaks under 5% total intensity. To ensure that that observed changes in the mass spectra were not a result of any undesired pH changes in the sample induced by biochar dosing exhausting the buffer capacity, the sample pH was continuously monitored during adsorption experiments using a pH meter immersed in the sample during the experiment. To eliminate any potential interference between experiments from biochar adhering to the membrane surface, the membranes were either replaced or washed thoroughly by immersing in methanol between samples.

5.3 Results and Discussion

5.3.1 CP-MIMS verses dilution and direct infusion

Mass spectrometric characterization of samples (both low and high resolution) can be as simple as diluting a sample with a volatile solvent and directly infusing it into an API source (*e.g.,* ESI, APCI, or APPI) [110]. Very little sample preparation is involved, and substantial compositional information can be ascertained from full scan or targeted MS experiments (*e.g.,* SIM or MS/MS). However, complex samples with high levels of matrix species (*e.g.,* salts) can lead to significant ionization suppression, requiring higher dilution ratios. Unfortunately, this can reduce less abundant analyte concentrations below instrumental detection limits.

Online membrane sampling techniques involving PDMS membranes preclude salts and charged molecules from reaching the ion source and mass spectrometer. This

reduces ionization suppression and noise associated with matrix components often encountered in electrospray ionization [108]. As a result, the signal to noise ratio of permeable analytes can be significantly increased over direct infusion experiments. To demonstrate this, a real-world Athabasca oil sands contaminated sample (OSPW2) was diluted into methanol for direct infusion and into DI water (pH 4) for analysis by CP-MIMS using ESI and a triple quadruple mass spectrometer. Figure 6.5 shows the negative ion mass spectra $[M\text{-}H]^-$ for a 100× and 200× diluted sample. The top panels display the spectra resulting from CP-MIMS, and demonstrate the typical naphthenic acid profile for C_{12}–C_{20} acids centered around m/z 250 [91, 92, 96]. It should be noted that in addition to naphthenic acids, the MIMS spectra may also contain additional ionizable organics that are permeable to the membrane at pH 4 (*e.g.,* alcohols or phenols). In contrast, the spectra resulting from the direct infusion at the same dilution ratios does not resemble a typical naphthenic acid profile and is dominated by several peaks associated with other matrix components. There are relatively few peaks in the expected naphthenic acid window (m/z 200–300) for the more concentrated direct infusion sample (100×) suggesting that matrix components are suppressing naphthenic acids present in the sample. While further dilution results in a more comparable NA mass spectra, this will inevitably lower the concentration of less abundant NAs below the limit of detection. Furthermore, the CP-MIMS spectra show the expected reduction in signal intensity resulting from the two-fold difference in dilution, whereas the intensity of most peaks in the spectra resulting from direct infusion actually increase upon dilution from 100× to 200×. The latter is consistent with ionization suppression and limits the quantitative interpretation of signal intensities resulting from direct infusion experiments. Therefore, by rejecting salts and confounding matrix components, CP-MIMS has been shown to reduce ionization suppression of naphthenic acid molecules and facilitate the direct quantitative analysis

of NAs in contaminated OSPWs.

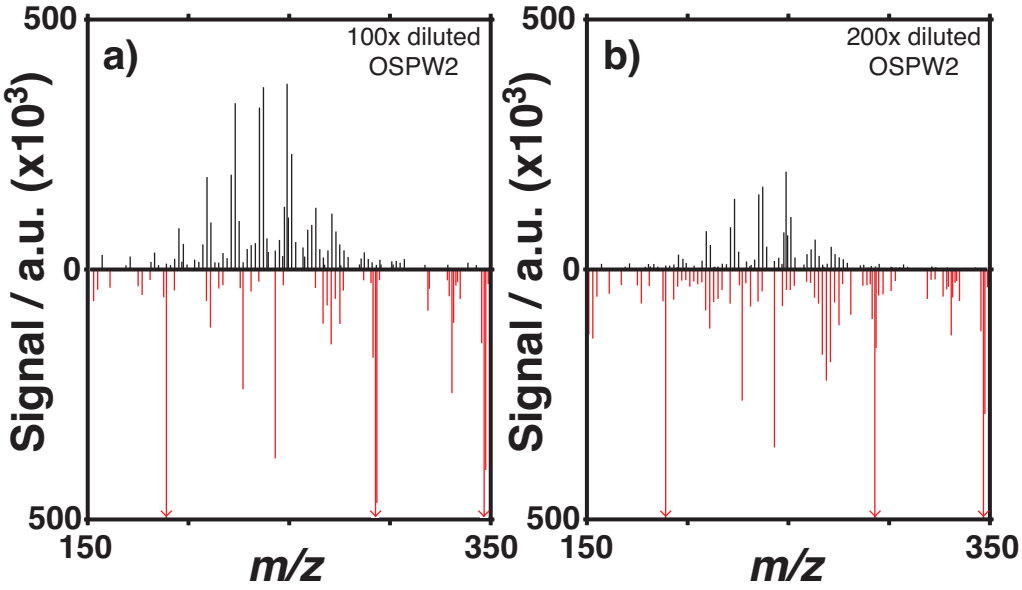

Figure 5.1: Full scan negative ion mass spectrum of OSPW2 sample diluted a) 100× and b) 200×. Top panels show the spectra resulting from an acidified aqueous sample by CP-MIMS whereas the inverted spectra in the bottom panels are from the direct infusion of the same sample diluted in methanol.

5.3.2 Qualitative characterization of membrane permeable species in NA samples

Given that typical aliphatic and aromatic carboxylic acids have pK_as in the 4–5 range, they are extensively ionized at neutral pH, and because analytes must be in a neutral form to permeate PDMS membranes, the analysis of naphthenic acids by CP-MIMS is dependent on the sample pH. We demonstrate the effect of pH on the signal/noise ratio for a number of model carboxylic acids in Figure 5.2. Maximum signals for decanoic acid, cyclohexanebutyric acid, and pyrenebutyric acid are observed at sample pH values less than 4. As the pH of the solution increases, these compounds become increasingly ionized to their corresponding carboxylates, which are impermeable to the PDMS membrane. Therefore, in order to maximize NA sensitivity using

CP-MIMS, all subsequent samples were adjusted to pH $\leq$ 4 prior to measurement. While Figure 5.2 clearly shows that all carboxylic acids become membrane permeable in their acidic form, it also illustrates differing sensitivity for the three model compounds depicted measured at comparable concentrations. Overall sensitivity in CP-MIMS is a function of intrinsic molecular properties that govern membrane permeation (*i.e.,* relative solubility and diffusivity) as well as those influencing ionization efficiency. Although the difference in sensitivity for each acid could complicate the quantitative analysis of NAs using a surrogate standard (*e.g.,* PyBA), this issue is not unique to CP-MIMS [101]. Thus, we have used both PyBA equivalents and total NA concentration (as Merichem) for quantitative purposes.

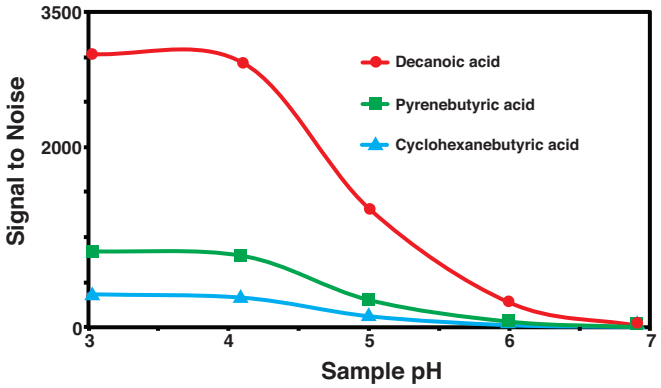

Figure 5.2: CP-MIMS derived signal to noise ratios for three representative carboxylic acids (50 ppb) as a function of the sample pH between pH 3 and 7 monitored in negative ion mode as the $[M\text{-}H]^-$ ions. Cyclohexane butyric, decanoic, and pyrene butyric acid were monitored at m/z 169, 171 and 287, respectively.

To further characterize membrane permeation and the effects of sample pH, 1 ppm of Merichem naphthenic acid mixture was introduced to an ESI FTICR-MS by both direct infusion (in methanol) and using a CP-MIMS interface (with aqueous sample pH values of 3 and 8). The resulting Kendrick Mass Defect plots with accurate mass assigned compound classes are displayed in Figure 5.3. While at least ten compound classes and several hundred exact mass molecular formulae are observed in the direct

infusion experiment (panel a), far fewer compounds are permeating the membrane at pH 3 (panel b). Many more compounds are present when the sample is directly infused into the mass spectrometer, compared to CP-MIMS experiments. In particular, fewer sulfur containing species (most notably SO_3 and SO_4 compound classes) appear in the CP-MIMS experiments. This is consistent with the much lower pK_a values of species such as sulfonic acids, which will remain ionized at pH 3. Sulfur-containing compounds detected by CP-MIMS likely contain sulfur atoms in moieties such as sulfoxides, sulfones, thiols, or thioethers.

Peaks identified as containing O_2, which could in principle include carboxylic acids, esters and/or some combination of alcohols, ketones or ethers appear to dominate the plots for both CP-MIMS experiments. However, since ESI is relatively inefficient at ionizing esters, ketones and ethers, we expect that most of the observed O_2 species are in fact carboxylic acids and/or hydroxylated species [93]. The observation that considerably more compound classes are detected at pH 3 (panel b) than at pH 8 (panel c) is consistent with the presence of protonated carboxylic acids in acidic solution. We propose that O_2 species detected at pH 8 do not contain carboxylic acid functionalities, and are composed of hydroxylated compounds. The fact that some of the O_2 species appearing in the direct infusion experiment are not observed by CP-MIMS at pH 3 is likely due to the roughly ten-fold analyte dilution between the aqueous sample and flowing methanol acceptor phase, previously characterized for this system [87]. This is consistent with the high resolution full scan mass spectrum for Merichem (Figure A.1), which indicates the peaks at m/z <200 and m/z >400 are minor contributors. We also observe that some of the O_2 peaks from $\sim$ m/z 200–250 present at pH 3 are not apparent at pH 8. This is consistent with other experiments conducted with Merichem at unit mass resolution, where the distribution of peaks at elevated pH ($\sim$7–8) is centred at $\sim m/z$ 300. When the sample pH is dropped to 4, the

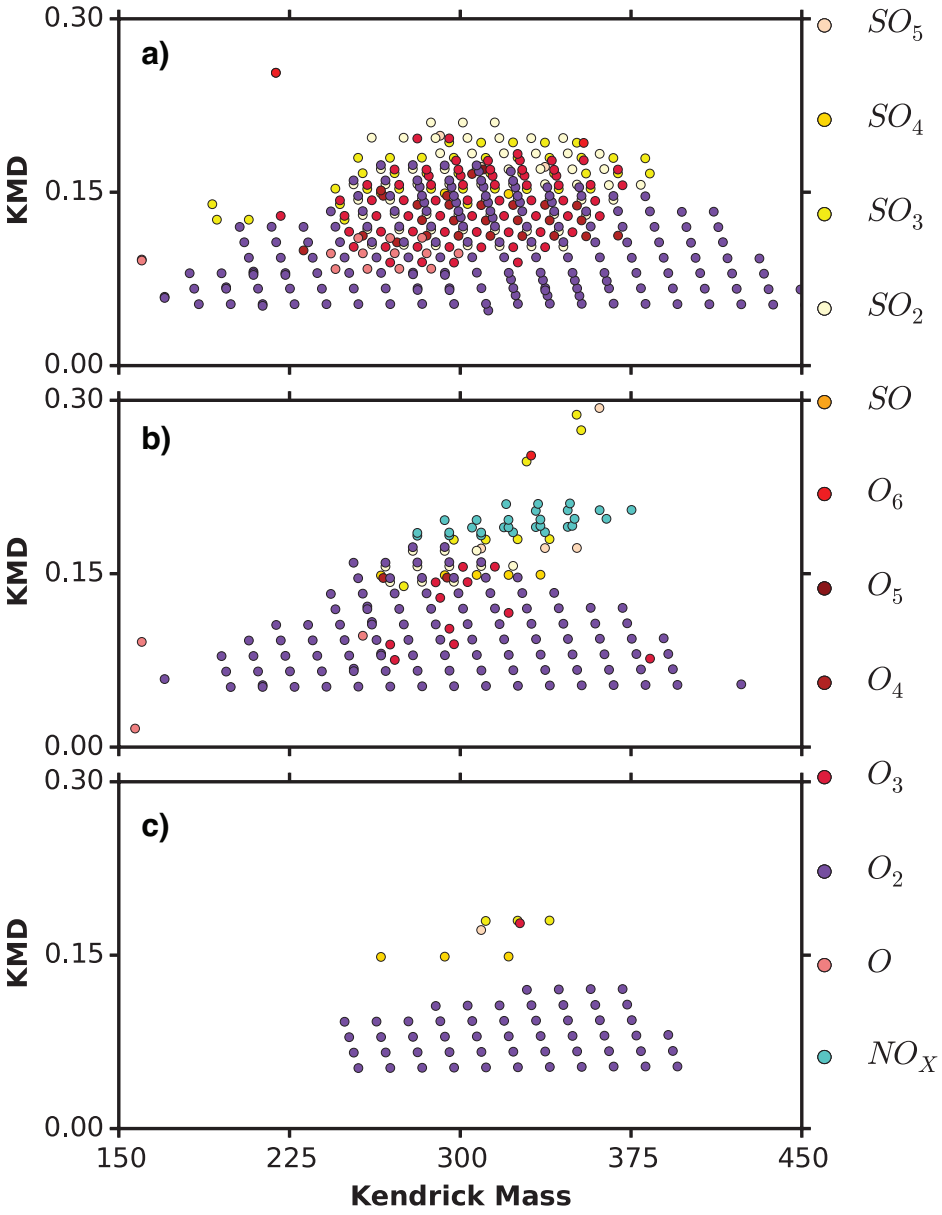

Figure 5.3: Kendrick mass defect plots of a standard Merichem naphthenic acid mixture a) direct infusion showing multiple compound classes including SO_3 and SO_4 species, b) CP-MIMS spectra at sample pH 3 showing a predominance of O_2 species which we primarily attribute to carboxylic acids and diols and c) CP-MIMS spectra at sample pH 8 showing a predominance of O_2 species which we attribute primarily to diols. All mass spectra obtained in methanol solution on high resolution FT-ICR with electrospray ionization in negative ion mode.

higher mass peaks ($\sim$ *m/z* 270–330) tend to decrease in relative abundance, while those in the lower mass range *m/z* 200–250 start to dominate the mass spectrum (data not shown). This suggests that for Merichem, NAs are predominantly centred around C_{14} - C_{16} isomer classes (*m/z* 200–250), whereas the alcohols and other O_2 containing species are predominantly in the higher mass O_2 peaks. We also observe several minor unassigned nitrogen containing peaks in Figure 5.3b with classifications of N_2O_2 or N_2O_4 (labelled N_2O_x). It is conceivable that carboxylic acids containing less basic nitrogen moieties such as pyroles and/or amides, are crossing the PDMS membrane at pH $\sim$3 (in neutral form), but not when the sample pH was raised to 8 and the ionized carboxylates preclude membrane transport.

Because the analysis of NAs by CP-MIMS is carried out by lowering the pH below that of the pK_a of carboxylic acids, their neutral forms partition into and permeate through the hydrophobic PDMS membrane into the methanol acceptor phase. Many more peaks and compound classes appear when the sample is directly infused to the MS, however, the membrane employed in the CP-MIMS experiment both selects for carboxylic acids, while sulfonic acids (and other charged species at pH 4) are not measured by the described CP-MIMS method. Nonetheless, it can be envisioned that contaminated samples can be rapidly screened for NAs by CP-MIMS without chromatographic separation, directly in an acidified sample. The technique provides both signal intensities and mass spectra, which allows for simultaneous quantitative and qualitative assessments.

5.3.3 Membrane performance characteristics

Naphthenic acid analysis by CP-MIMS requires very little sample preparation (pH adjustment and possible dilution for high NA concentrations). The analytical duty cycle is dictated primarily by membrane transport kinetics, which are dependent on

membrane thickness [9, 72]. Three different PDMS membranes were evaluated with Merichem NA mixtures, with membrane response times and estimated detection limits for several representative isomer classes reported in Table 5.2. Naphthenic acid response times range from 10–20 minutes for a HFM with a 170 μm wall thickness, with the larger NAs taking longer due to their greater hydrodynamic volume and correspondingly smaller diffusivity. This is the most robust and easily handled membrane material of those presented here. The 35 μm membrane and 0.5 μm thin film composite membrane (TFCM) have shorter lifespans, and are more difficult to construct. Response times for representative NAs were roughly 10$\times$ faster on the TFCM compared to the 170 μm membrane. In addition to thickness, the density and degree of crosslinking in the PDMS preparation affects the diffusivity of permeants. We have previously reported that the 35 μm thick PDMS is less permeable than expected and only leads to a slight improvement in response times [88]. In general, sensitivity can be improved by increasing the surface area of the membrane in contact with the sample and is a function of the ratio of inner/outer diameter of the HFM.

Table 5.2: Comparison of membrane geometries, response times, and detection limit estimates for selected NA isomer classes.

m/z	Response Time t_{10-90} / min PDMS Membrane			Detection Limit* ppb PDMS Membrane		
	0.5 μm	35 μm	170 μm	0.5 μm	35 μm	170 μm
213	0.6	10	10	20	10	10
223	0.6	15	15	20	5	5
237	0.6	15	25	40	20	5
251	0.7	20	25	30	20	5
305	3	20	20	30	20	10

* based on S/N = 3

5.3.4 Semi-quantitative analysis of real world samples

Six representative samples, including two OSPWs, two GWs, and two SWs were selected in order to test the efficacy of CP-MIMS (using the 170 μm thick HFM) for the semi-quantitative rapid screening of real-world samples. For comparison, each sample was also analyzed by a commercial laboratory using solid phase extraction, chemical derivatization, liquid chromatography, and tandem mass spectrometry (SPE-LC-MS/MS) [101]. The total naphthenic acid concentrations for these samples ranged from 4 ppb to 150 ppm as pyrenebutyric acid equivalents (Table 5.1). Figure 5.4 shows the time course chronogram monitoring three representative NA isomer classes at m/z 221, 223 and 235. The membrane probe was sequentially immersed into each of six samples (pH adjusted <4) and rinsed in methanol between samples. It should be noted that data for only three NA isomer classes are displayed, and that other

characteristic NA m/z exhibited similar chronograms. In order to bring high concentration OSPW samples into range, they were diluted 250×. The signal intensity easily distinguishes each of the three sample types from one another. The two SW samples with $[NA]_T < 10$ ppb are near the detection limits for the method, whereas the GW samples with $[NA]_T$ at 20 and 100 ppb provide easily measureable signals by CP-MIMS. The OSPWs containing substantial naphthenic acid loads with $[NA]_T$ of 26 and 150 ppm respectively yield significant signals (even after 250× dilution) as shown in Figure 5.4. These data suggest that CP-MIMS is capable of screening samples in the ppb to ppm concentration range for individual NA isomer classes. Although samples were exposed to the membrane interface for ∼20 mins to generate the data in Figure 5.4, the duty cycle can be improved by using a thinner membrane, heating of the membrane interface or sample and/or using non-steady-state signals (*e.g.,* short sample exposure times) [87]. The thicker 170 μm membrane used was chosen for ease of construction and high durability: from experience, one HFM interface has the potential to last for months of operation before replacement.

An alternative strategy to targeted screening, as presented above, is to utilize the full scan mass spectrum in negative ESI to screen for the total concentration of all naphthenic acids present, rather than dwell on SIM scans for particular ions. This methodology could reduce bias for samples from different sources that contain different NA profiles (which may be missed by the above targeted method). To demonstrate the use of this method for semi-quantitative analysis of total NAs in a sample by CP-MIMS, the mass spectrum obtained from OSPW2 (diluted 250×) at pH >7 (mainly due to hydroxylated compounds that permeate the membrane and are readily ionized in negative ion mode) was subtracted from that obtained for the sample at pH <4, which detects both hydroxylated and carboxylated compounds. The resulting difference spectrum peak intensities were then converted to pyrenebutyric

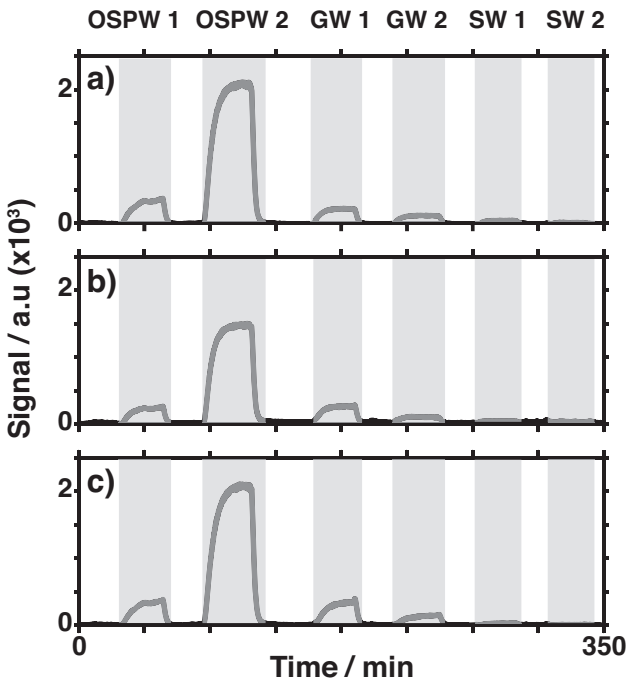

Figure 5.4: Selected ion monitoring chronogram of six water samples (shaded) as $[M\text{-}H]^-$ at m/z 221 (a), 223 (b) and 235 (c) separated by a methanol wash between samples (unshaded). OSPW1 and OSPW2 were diluted 250× before analysis.

acid equivalents with a direct calibration curve (y = 3650x +15580, r^2= 0.997, n=4, where y is the signal intensity at m/z 287 and x is the [PyBA] in ppb), and scaled by the sample dilution factor. The results are displayed in Figure 5.5(a), and are compared to a reconstructed mass profile of NAs derived from analysis by SPE-LC-MS/MS, given in Figure 5.5(b). The use of PyBA equivalents was employed here for comparison purposes only, and there is nothing inherent in CP-MIMS that precludes other quantitation approaches. We have, for example also used direct calibrations to total NA concentration as Merichem (Figure A.2) similar to the work of Ross and coworkers [100]. We generally observe relative standard deviations (RSD) of less than 30% for replicate samples in the ppb–ppm range (*e.g.,* OSPW2, n = 3) when analyzed by CP-MIMS using an external PyBA calibration curve. The RSD on the analysis by SPE-LC-MS/MS is reported as <17% RSD for samples measured in the pptr–ppm

range [101].

In addition to the similar m/z profiles observed for both techniques, the total NA concentration (estimated by summing the observed signals) was 160 ppm using CP-MIMS and 150 ppm by SPE-LC-MS/MS, which are indistinguishable given the precision inherent in both methods. Lower concentration samples analyzed by CP-MIMS displayed considerably greater variance, suggesting that other interferences are confounding quantitation at lower concentrations (*e.g.,* $[\mathrm{NA}]_T < 0.1$ ppm). We have observed the linear dynamic range for total Merichem standards to be roughly 0.1–5 ppm using CP-MIMS in full scan mode (Figure A.2, a) and 0.01–5 ppm using the targeted SIM approach (Figure A.2, b). It should be noted that after 250× dilution, OSPW2 has a total concentration of 0.6 ppm (as PyBA), which is easily detected by CP-MIMS. Diluted OSPW1 and undiluted GW1 both have total NA concentrations of roughly 0.1 ppm (as PyBA), which is at the lower end of our LDR, which may (in part) explain the larger observed biases for these samples. We are currently exploring several methods to increase CP-MIMS sensitivity for NAs, including decreasing the acceptor phase flow rate [108], heating the membrane interface, increasing the surface area of the membrane interface, and the use of base (*e.g.,* sodium acetate) within the acceptor phase to enhance ionization. Samples that have total NA concentrations in the low parts-per-billion may be better suited to targeted SIM methods for common reoccurring NA isomer classes present within the majority of contaminated samples. Nonetheless, these data suggest that CP-MIMS can be used for the semi-quantitative analysis of NAs directly in contaminated samples. Further, with the advent of field portable ESI mass spectrometers [111, 112], CP-MIMS may provide an avenue to directly screen samples for NAs in the field or at the source. Contaminated samples may be quickly identified for subsequent lab-based quantitative analysis, when greater accuracy or precision is required.

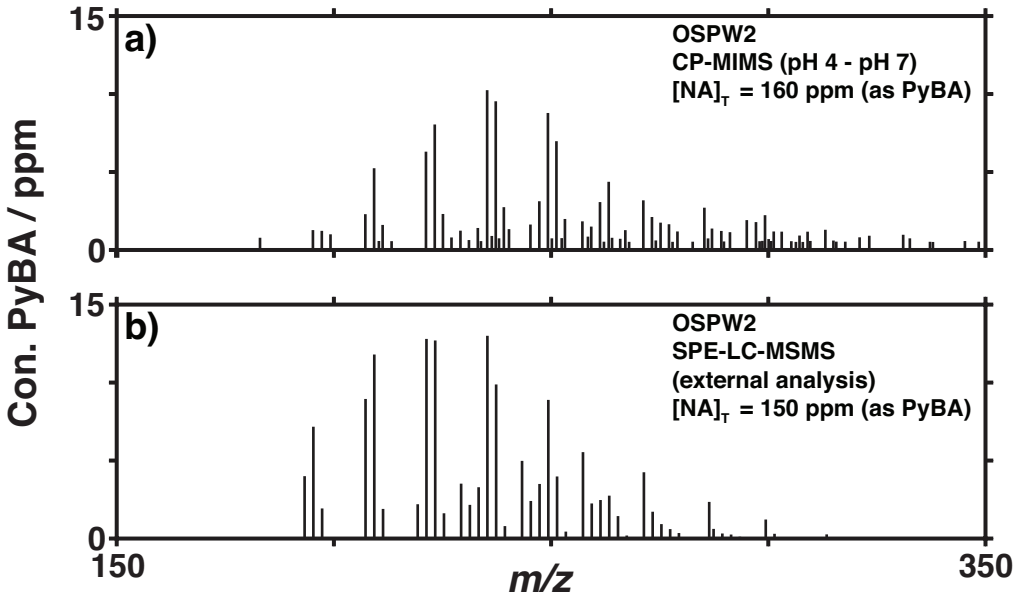

Figure 5.5: Comparison of full scan mass spectra of naphthenic acids in OSPW2 displayed as pyrene butyric acid (PyBA) equivalent concentrations by a) CP-MIMS spectra at pH 4 minus spectra at pH 7 (both background subtracted) converted to [PyBA] using four point calibration curve and b) reconstructed from analysis of naphthenic acid isomer classes from AXYS Analytical Services based on acid extraction, chemical derivatization, liquid chromatography and tandem mass spectrometry.

5.3.5 Continuous monitoring of NAs in dynamic systems

To illustrate the use of the technique to monitor the changes in the full scan mass spectrum over time in a dynamic system, a CP-MIMS probe was immersed in a glycine buffered aqueous solution at pH 3.60. A mixture of naphthenic acids from a Merichem standard was injected to achieve a final concentration of 4.1 ppm. After steady state signals were obtained, a dose of activated biochar was added as a sorbent to form a stirred suspension. Figure 5.6 shows mass spectra of Merichem solutions before (top panels) and after (shown as inverted spectra for ease of comparison in the bottom panels) the addition of two different biochar samples. Sample A (shown on the left) shows relatively little sorptive activity, even at doses up to 700 mg/L,

whereas Sample B (right) demonstrates a much higher sorptive capacity, even with 25× less biochar sorbent added. Whereas Sample A shows little change in the mass profile of naphthenic acid isomer classes before and after addition, Sample B appears to be somewhat more effective at removing the lighter components in the naphthenic acid mixture. The inset chronograms display the time course of several representative isomer classes, illustrating the extent and rate of removal of various naphthenic acid isomer classes. When Sample B is added at a dose of 700 mg/L, all of the peaks in the spectra disappear on the order of 20 mins, indicating complete NA adsorption and removal from aqueous solution (Figure A.3). Although membrane performance in these heterogeneous mixtures appeared to degrade over time as some biochar adheres to the PDMS surface, membranes were either replaced or washed between experiments to improve reproducibility.

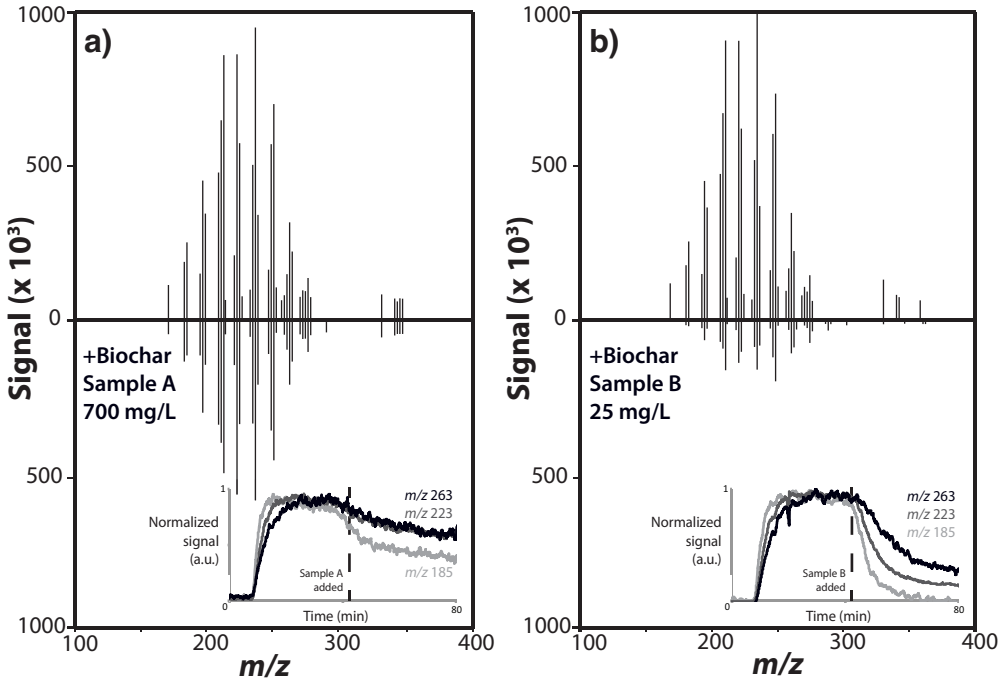

Figure 5.6: Adsorption of Merichem naphthenic acids on aqueous suspensions of biochar samples A and B. Top panels display the steady state full scan mass spectra for 4.1 ppm Merichem in 0.12 M glycine buffer, pH = 3.65 ± 0.02. Bottom panels display the mass spectra of the same solution after a) 700 mg/L of biochar Sample A or b) 25 mg/L of biochar Sample B have been added and allowed to decay to a steady state. Full scan mass spectra are background subtracted and filtered to remove minor peaks contributing less than 5%. The inset chronograms display the normalized signals for selected isomer classes of naphthenic acid ions $[M\text{-}H]^-$. Merichem is added at time ∼10 mins and biochar is added at time ∼40 mins.

5.4 Conclusion

Condensed phase membrane introduction mass spectrometry has been demonstrated as a proof-of-concept approach for both qualitative and quantitative analysis of NAs directly in contaminated samples. Method specificity is derived from selective membrane permeability of protonated NAs at sample pH $<$ pK_a, ionization efficiency, and *m/z* discrimination. Since negative ion ESI affords the concurrent ionization of hydroxylated and carboxylated analytes, ionization alone may not provide sufficient

selectivity for NAs present within complex samples. However, monitoring samples before and after pH adjustment to pH <4, provides a means to discriminate hydroxylated and carboxylated compounds. The technique was used to rapidly screen real-world samples by monitoring selected NA ions as $[M\text{-}H]^-$. The results compared well with analysis by SPE-LC-MS/MS, easily distinguishing high, medium and low concentration samples containing NAs in the ppb-ppm range. The use of CP-MIMS as an on-line continuous monitor of dynamic concentration changes during the adsorption of NAs onto activated carbon directly in heterogeneous suspensions at environmentally relevant levels has also been demonstrated. We are currently working on mobilization of the technique on a portable platform for on-site assessments, rapid screening and process monitoring.

Chapter 6

Selective ionization and tandem mass spectrometric rapid screening of carboxylic acids from complex aqueous samples

Reproduced with permission from Duncan, K.; Volmer, D.; Gill, C.; Krogh, E."Rapid screening of carboxylic acids from waste and surface waters by ESI-MS/MS using barium ion chemistry and on-line membrane sampling" *J. Am. Soc. Mass Spectrom.*, in press (2015). Project conceived, designed, and carried out by K. Duncan. Data analysis and manuscript preparation by K. Duncan, with additional intellectual contributions from E. Krogh, C. Gill, and D. Volmer.

6.1 Introduction

Rapid screening methodologies offer researchers the option of surveying large numbers of samples prior to comprehensive targeted analysis (*e.g.,* GC-MS or LC-MS). Further, with the advent of field portable miniature mass spectrometers [111–113] and ambient ionization sources [114,115], mass spectrometry is a viable option for the direct analysis of environmental and/or bioanalytical samples. Many biomolecules and organic pollutants contain carboxylic acid functional groups [116]. In particular, naphthenic acids (NAs) have emerged as persistent environmental contaminants [92,117]. NAs are classically defined as aliphatic carboxylic acids with the general formula $C_nH_{2n+z}O_x$,

where n represents the number of carbon atoms, z the hydrogen deficiency, and x the number of oxygen atoms. Moreover, they exist as complex mixtures of hundreds to thousands of different molecules within contaminated samples [97, 110]. These analytes are often readily ionized by electrospray ionization (ESI) to yield predominantly $[M\text{-}H]^-$ ions. While an abundant deprotonated molecule is beneficial for tandem MS, many aliphatic carboxylic acids (*e.g.,* fatty acids and naphthenic acids) generate very few or no structurally diagnostic product ions, which makes developing selective tandem MS methods virtually impossible [110, 118]. Consequently, selective direct MS analysis of aliphatic carboxylic acids remains difficult, in particular without the use of chromatography. In addition, negative mode electrospray ionization is effective at ionizing both hydroxylated and carboxylated analytes.

The use of metal ions for the cationization of carboxylated analytes facilitates analysis by positive ion MS. In conjunction with collision induced dissociation (CID), cation adducts fragment via charge remote fragmentation mechanisms to form structure-specific product ions [119]. Examples of metal-carboxylate adducts used for mass spectrometry in the literature include di-lithium [120, 121], copper [122], and alkaline earth metal complexes [119]. In particular, several studies have focused on the cationization of fatty acids with barium [121, 123, 124]. Zehethofer *et al.* were able to screen 29 free fatty acids (saturated, unsaturated, and polyunsaturated) using unique tandem mass spectrometric transitions [124]. Interestingly, each mass spectrum that was displayed in their study had common product ions at m/z at 139 and 155, attributed to and $[BaH]^+$ and $[BaOH]^+$, respectively. We exploit the use of this barium chemistry for the online complexation of carboxylates for subsequent mass spectral analysis. We report the utilization of these product ions for rapid screening of carboxylated analytes directly from complex aqueous samples using condensed phase membrane introduction mass spectrometry (CP-MIMS).

CP-MIMS is a direct sampling mass spectrometric method that utilizes a membrane interface to separate an aqueous sample from a flowing solvent acceptor phase. Several recent studies establish CP-MIMS as a relevant method for the rapid quantitative analysis of pharmaceuticals, environmental contaminants, and biomolecules from real-world matrices (*e.g.,* surface water, wastewater effluent, and artificial urine) [55,87,88,108]. The membrane precludes transport of ionized species within the sample (*e.g.,* salts), whereas hydrophobic analytes partition into the membrane, diffuse through it, and are solvated by a flowing acceptor solvent. The signal to noise ratio is increased over direct infusion methods by reducing the noise and ionization suppression related to ionized matrix species in the sample [55]. In general, both the selectivity and sensitivity of CP-MIMS can be affected at the membrane (permselectivity), ion source (ionization efficiency) and mass spectrometry level.

We report the combination of selective ionization and tandem mass spectrometry (via barium-carboxylate complexes) in positive ion mode with CP-MIMS for online rapid screening of carboxylated analytes in complex aqueous samples. A series of structurally related compounds were analyzed by direct infusion to identify the source of hydrogen present within the common $[BaOH]^+$ and $[BaH]^+$ product ions, to elucidate a mechanism and establish structural criteria for carboxylic acid detection by this method. In addition, both carboxylated and hydroxylated analytes were examined to identify possible isobaric interferences. Direct calibration of several model analytes is presented, demonstrating method linearity and limits of detection. Lastly, we apply positive ion tandem MS methods for the screening of naphthenic acids with unknown molecular structures in spiked surface waters from northern Alberta. This method can be used for non-targeted screening, where selectivity for carboxylic acids in complex samples arises in part from the barium ion affinity [125] in the flowing acceptor as well as positive ion tandem MS to yield common product ions [124].

6.2 Experimental

6.2.1 Standard solutions and sample preparation

All stock solutions were prepared gravimetrically in methanol using compounds with 99.99% purity (Sigma Aldrich, Oakville, ON, Canada), unless otherwise noted. Barium acetate (99.99%, Fisher Scientific, Ottawa, ON, Canada) stock solutions were prepared in deionized 18 MΩ water (Model MQ Synthesis A10, Millipore Corp., Billerica, MA, USA). Solutions used for obtaining CID spectra were prepared at 500 ppb of the desired analyte in methanol with 0.1 mM barium acetate (final water concentration of 2.5% v/v). Perfluoroctyl ethanoic acid was obtained as a 50 ± 2.5 μg/mL solution in isopropanol (Wellington Laboratories, Guelph, ON, Canada). Wastewater effluent was collected from a small municipality in British Columbia, and surface water was collected from a river in northern Alberta; both were stored at 4°C and raw samples were used without filtration for CP-MIMS analysis. Refined Merichem naphthenic acid standard (Merichem company, Houston, TX, USA), a complex mixture of naphthenic acid isomer classes, was supplied from Environment Canada and stored at 4°C prior to dilution.

6.2.2 Mass Spectrometry method development

A syringe pump (Econoflow, Harvard Apparatus, St. Laurent, QC, Canada) was employed to directly infuse solutions at 200 μL/min (for direct comparison to CP-MIMS experiments) to a triple quadrupole mass spectrometer (Quattro LC, Waters, Altrincham, UK) with positive electrospray ionization. Desolvation gas was maintained at 700 L/hour at 300°C, with a 50 L/hour curtain gas setting. Relatively high cone voltages were required to maximize the abundance of desired carboxylate-barium adduct species, with the entrance cone set at 50 V and the extractor cone set at 10 V. A high

collision cell pressure was utilized (∼8 mTorr) for CID (collision energy, 60 eV), which displayed the greatest intensity for desired product ions. Product ion scans with a 1 s scan time over m/z 100 to 500 in Q3 were used to obtain CID mass spectra, which were averaged for >30 scans.

6.2.3 Condensed phase membrane introduction mass spectrometry

CP-MIMS experiments were conducted using polydimethylsiloxane (PDMS) hollow fibre membrane (HFM) (Dow Corning Silastic tubing, OD = 0.64 mm; ID = 0.30 mm; 170μm thickness, Midland, MI, USA) membrane immersion probes constructed in-house as previously described [88, 108]. A syringe pump was used to push acceptor phase solvent through the lumen of the HFM at 200 μL/min. The membrane interface probes were directly immersed into well-mixed aqueous samples acidified to pH < pK_a (typically pH ∼4), and rinsed with clean methanol (HPLC grade, Fisher Scientific) between samples. Aqueous sample pH was adjusted to < 4 via small additions of 6 M HCl (Fisher Scientific), and verified via pH test strips (Sigma Aldrich).

Both methanol and acetonitrile were evaluated as acceptor phase solvents, with methanol giving the lowest background intensities for peaks in the spectral region of interest (m/z 300-500). Barium acetate was added directly to the acceptor phase reservoir to a final concentration of 0.1 mM, as previously published [124]. Experiments were conducted with 0.05, 0.1 and, 0.2 mM barium acetate, with the greatest signal to noise resulting from 0.1 mM (data not shown). Data for CP-MIMS experiments were collected using multiple reaction monitoring for $[M\text{-}H+Ba]^+$ ions fragmenting to m/z 155 and 139 (0.5 s dwell time each). Signal intensities displayed in the figures correspond to the sum of intensities for both m/z 155 and 139 for each precursor ion. All experiments were conducted at room temperature and atmospheric

pressure (∼25°C and 101 kPa).

6.3 Results and Discussion

6.3.1 Confirmation of diagnostic ions for quantitative screening purposes

Previous work by Volmer and coworkers employing barium ions as cationization reagent for fatty acids by tandem MS displayed major product ions at *m/z* 155 and 139, attributed to $[BaOH]^+$ and $[BaH]^+$ [124]. To elucidate the source of hydrogen in these product ions, several model carboxylic acids were prepared as dilute methanol solutions with 0.1 mM aqueous barium acetate (2.5% v/v). To establish whether α hydrogen transfer was taking place, lauric acid, 2,2-lauric acid-d_2, and perfluorooctylethanoic acid solutions were directly infused into the mass spectrometer and product ions *m/z* 139 and 155 produced from teh precurser ion $[M\text{-}H+Ba]^+$ were monitored. Figure 6.1 displays the resulting CID mass spectra. The lauric acid CID spectrum (Figure 6.1a) exhibits several diagnostic ions, and compares well with analogous spectra from the literature [124]. Interestingly, the spectra obtained for lauric acid-d_2 (panel b) displays a strong signal for the same product ions at *m/z* = 139 and 155, as depicted in Scheme 1. However, the peak occurring at *m/z* 196 from lauric acid, now appears at *m/z* 198. We attribute this ion to $[C_2H_2O_2Ba]^+$ (or $[C_2D_2O_2Ba]^+$ in case of lauric acid-d_2), which results from bond cleavage between the α and β carbons (Scheme 1). Secondly, the signal at *m/z* 209 has shifted to 210. The ion at *m/z* 209 has been previously attributed to charge remote fragmentation between β and γ carbons, resulting in formation of an alkene after loss of H_2 [126]. This is further supported by the shift of *m/z* 209 to 210 for CID of lauric acid-d_2, where a deuterium atom is lost from the α position. We propose the ion to have the

formula $[C_3H_2DO_2Ba]^+$. Since no mass shift was observed for m/z 155 or 139, the source of hydrogen in $[BaOH]^+$ and $[BaH]^+$ is not the α position. Furthermore, when perfluorooctylethanoic acid (which only contains hydrogen atoms in α position) was directly infused under the same conditions (see Figure 6.1c), no signal was observed for m/z 155 and 139. This observation confirms the hypothesis that hydrogen transfer from the α position was not responsible for formation of $[BaOH]^+$ and $[BaH]^+$ product ions.

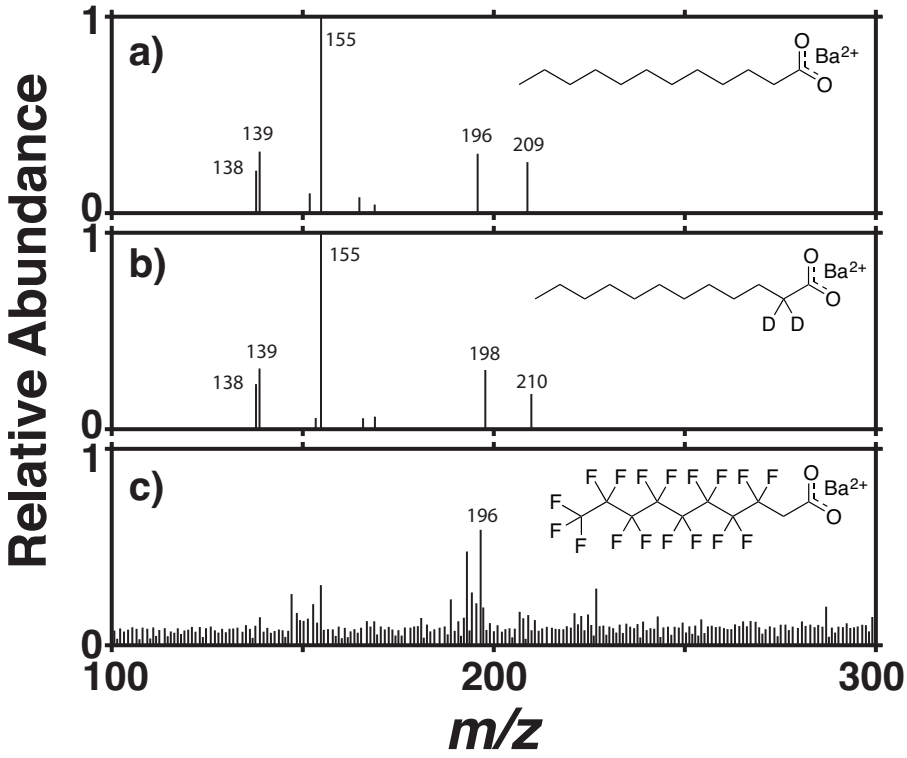

Figure 6.1: CID mass spectra for (a) lauric acid, (b) lauric acid-d_2, and (c) perfluorooctylethanoic acid in the presence of barium acetate. The noise seen in panel (c) is the result of considerably lower absolute intensities.

A homologous series of phenyl-substituted aliphatic carboxylic acids were investigated to determine if the hydrogen atom from β or γ carbons was transferred to form the product ions at m/z 155 and 139. The CID spectra for 2-phenylethanoic acid, 3-phenylpropanoic acid, and 4-phenylbutanoic acid are displayed in Figure 6.3. As ex-

Scheme 1:

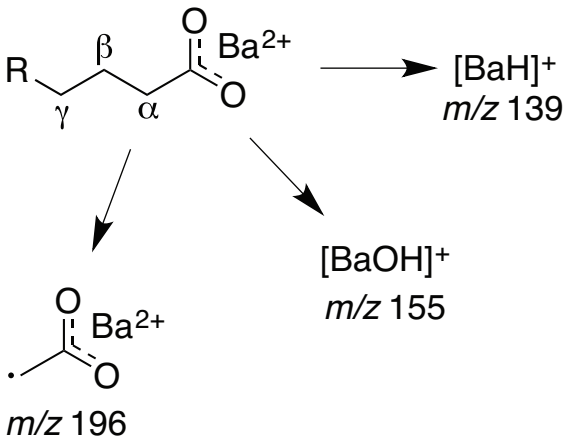

pected, no discernable signals were observed for *m/z* 155 and 139 for 2-phenylethanoic acid, which only has α carbon hydrogen atoms. Conversely, the desired product ions were readily observed by CID of 3-phenylpropanoic acid (Figure 6.3b), which has β carbon hydrogen atoms. Signal intensity for *m/z* 155 and 139 increased when hydrogen atoms were present on the γ carbon, as illustrated by CID of 4-phenylbutanoic acid (Figure 6.3c). The results suggest that hydrogen atoms on β and/or γ carbons can lead to formation of both $[BaOH]^+$ and $[BaH]^+$. Further, the increase of signal intensity observed for 4-phenylbutanoic acid could indicate a combination of two competing mechanisms. Thus, prospective carboxylic acids analyzed by this method must contain hydrogen atoms on either β or γ carbons in order to be detected. A proposed mechanism for formation of $[BaOH]^+$ and $[BaH]^+$ from $[M\text{-}H+Ba]^+$ precursor ions is shown in Scheme 2. It is conceivable that a similar mechanism exists for γ hydrogen transfer. However, as no compounds were available to us that contained exclusively γ hydrogens, we are unable to confirm this mechanistic variant. It should be noted, that the final product structures in Scheme 2 are not directly observed, and their inclusion here is merely for reasons of completeness.

To evaluate method selectivity, several model compounds were directly infused

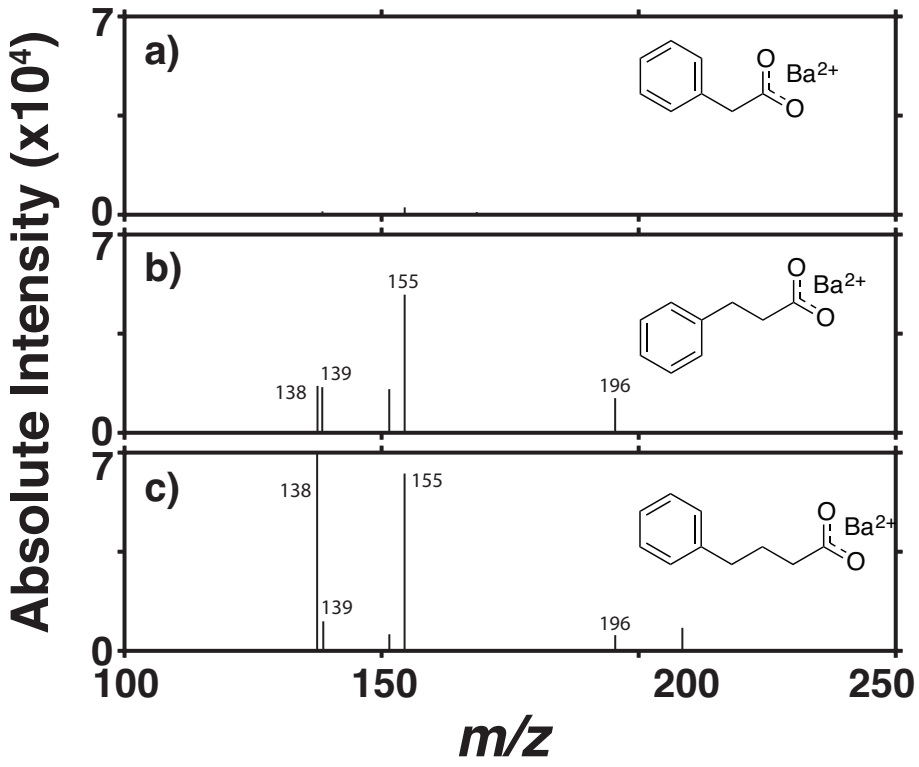

Figure 6.3: CID mass spectra of (a) 2-phenylethanoic acid, (b) 3-phenylpropanoic acid, and (c) 4-phenylbutanoic acid in the presence of barium acetate.

into the ESI source, monitoring the product ions at m/z 139 and 155 from [M-H+Ba]$^+$. Figure 6.4 displays the resulting signal intensities from four different carboxylic acids (50 ppb) and four different alcohols (250 ppb). Strong signals were observed for the carboxylated analytes, except for perfluorodecanoic acid (which does not contain C-H bonds). Perfluorodecanoic acid was added as a control to ensure that m/z 155 and 139 were not products of hydrogen/hydride transfer from background moisture within the collision cell. It is quite apparent that no signal was observed from hydroxylated species, even at the higher concentrations tested. We attribute this to the much weaker affinity of barium ions for alcohols within the acceptor solvent phase and/or the liquid/gas phase of the ESI source.

Although no signals were observed for monohydroxylated molecules, we observed

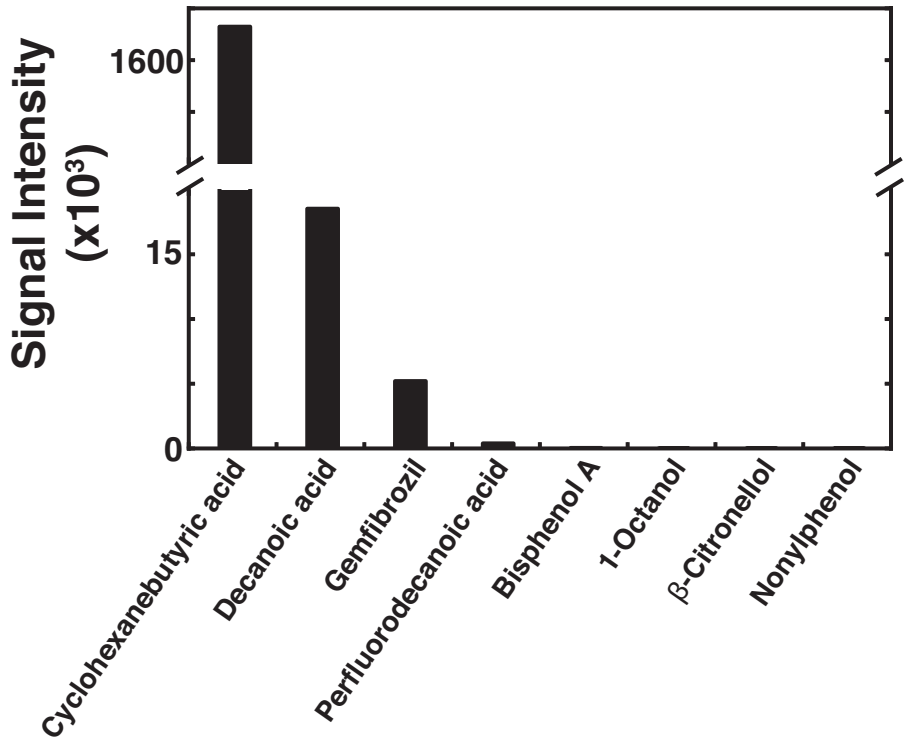

Figure 6.4: Direct infusion of several carboxylated and hydroxylated compounds. The signal intensity displayed represents the sum of the product ions m/z 139 and 155 for the CID analysis of each corresponding $[M\text{-}H+Ba]^+$ ion. The first three compounds also exhibit the qualifier ion at m/z 196.

barium adducts for a 1,3-diol (2-ethyl-1,3-hexanediol), generating product ions at m/z 155 and 139 (CID spectrum shown in Figure A.4). However, this compound did not give rise to the qualifier ion at m/z 196 (Scheme 1 and Figure A.4). Cleavage between the α and β carbon for 1,2-diol ions with the formula $[M\text{-}H+Ba]^+$ would result in m/z 197 product ions, and the same process for 1,3-diols would yield product ions with 3 carbon atoms ($m/z > 196$). In summary, the tandem MS method used for subsequent experiments selects for a $[M\text{-}H+Ba]^+$ precursor ion and monitors the sum of $[BaOH]^+$ and $[BaH]^+$ product ions. Analytes with unknown molecular structures

Scheme 2:

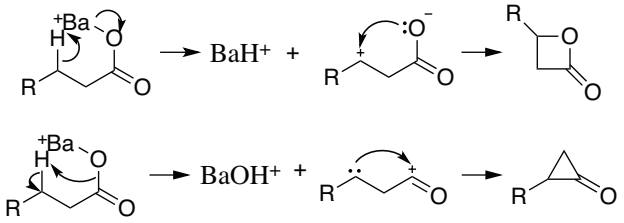

can be identified as carboxylic acids via this method, provided the CID spectrum also contains the qualifying ion at m/z 196.

6.3.2 Direct analysis in wastewater effluent

Combining the selectivity of barium adduct formation and tandem MS with CP-MIMS allowed for the continuous on-line direct measurement of carboxylic acids in complex aqueous samples. By simply adding barium acetate to the methanol acceptor phase solvent reservoir, CP-MIMS was readily adapted [108]. The addition of barium acetate facilitated both the complexation of barium to carboxylates in the acceptor phase solution (by raising the pH above the pK_a value of the carboxylic acids) and cationization of carboxylates during the ESI process. To demonstrate the utility of this method, a CP-MIMS probe was immersed directly into wastewater effluent spiked with increasing levels of lauric acid and gemfibrozil. Representative calibration curves plotting the sum of product ion intensities (m/z 139 and 155) versus concentration are presented in Figure 6.6. Excellent linearity was observed, with r^2 values for lauric acid and gemfibrozil at 0.997 and 0.999. Experiments in deionized water yielded a linear dynamic range (LDR) for gemfibrozil of three orders of magnitude with concentrations up to 1200 ppb. Although Zehethofer *et al.* observed considerably wider LDR for similar analytes using LC-MS with the same barium acetate concentrations [124], we attributed the smaller range observed here to ion suppression effects from co-permeating matrix molecules, particularly in complex dirty samples.

Although the membrane in CP-MIMS precluded any charged species from entering the acceptor phase, co-permeating matrix molecules have been previously demonstrated to contribute to ionization suppression in ESI [108]. In this earlier study, we presented several strategies for increasing the LDR for CP-MIMS-ESI, including: i) using a continuously infused internal standard to provide correction factors to account for variations in ionization efficiency and ionization suppression; and ii) adjusting the flow of acceptor solvent to increase or decrease the effective concentration of permeating analyte species in the acceptor phase solvent. The same methods could also be employed here to extend the LDR, if necessary.

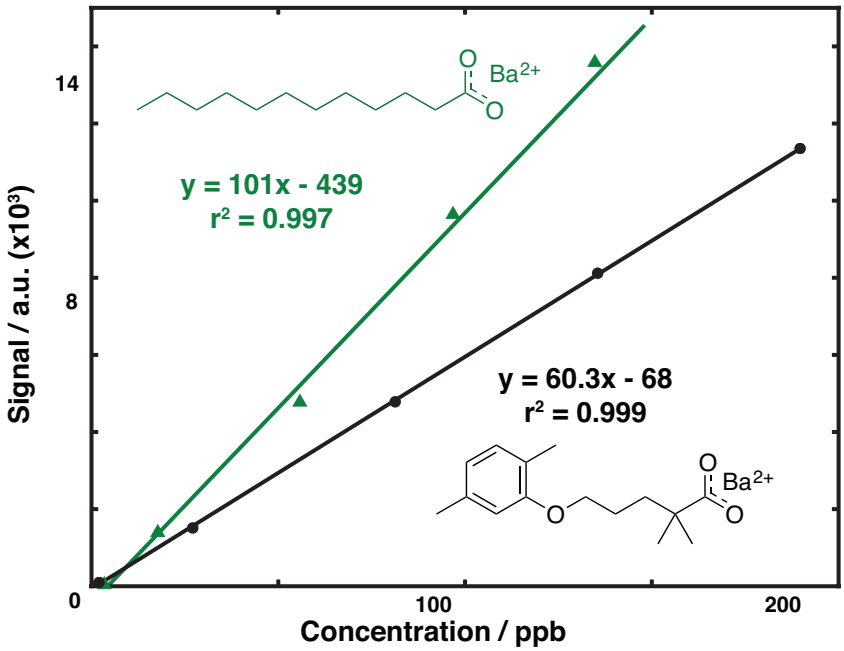

Figure 6.6: Calibration of model compounds in wastewater effluent. The signal displayed represents the sum of both m/z 139 and 155 product ions from each [M-H+Ba]$^+$ precursor ion.

Table 6.1 summarizes calculated detection limits for gemfibrozil and lauric acid by CP-MIMS in both negative ion ESI mode using [M-H]$^-$ ions and tandem MS of

barium adducts in positive ion mode. As can be seen, both model analytes exhibited detection limits of 1 ppb with the barium cationization method, which is ~ 10 higher than for the negative ion experiments. Given that gemfibriozil has distinctive CID transitions in negative ion ESI (m/z 249 $\rightarrow$ 121), barium cationization in a targeted screening method offers few advantages. However, lauric acid does not fragment to any diagnostic ions in negative ESI mode. The higher detection limits observed may therefore be an acceptable sacrifice for gaining improved selectivity of targeted tandem MS screening amenable to aliphatic carboxylated analytes. This is particularly important for fast, direct sampling methods that preclude chromatography such as CP-MIMS.

Table 6.1: Comparison of detection limits between negative mode ESI and positive tandem MS method or analytes in deionized water.

Analyte	Ionization method			
	Negative ESI CP-MIMS		Barium adduct CP-MIMS	
	MS	DL* / ppb	MS	DL* / ppb
Lauric acid	SIM 199	0.1	MS/MS 337 $\rightarrow$ 139 + 155	1
Gemfibrozil	SIM 249 $\rightarrow$ 121	0.05 [108]	MS/MS 387 $\rightarrow$ 139 + 155	1

* Detection limits based on S/N = 3

6.3.3 Non-targeted tandem MS screening of naphthenic acids

The analytical method presented here can be used for targeted or non-targeted screening of carboxylic acids in contaminated aqueous samples. Given that the product ions are common for the barium carboxylate adducts ([M-H+Ba]$^+$), unknown carboxy-

lated analytes can be identified through CID spectra, and functional group confirmation can be ascertained through the presence of *m/z* 196 ($[C_2H_2O_2Ba]^+$). We have previously demonstrated CP-MIMS as a potential rapid screening methodology for naphthenic acids from contaminated aqueous samples [88]. Further, recent work has shown that hydroxylated compounds contribute signal to CP-MIMS quantification of NAs using negative ion ESI (Chapter 5).

To demonstrate proof of concept, the method was used for on-line monitoring of naphthenic acids in a natural water sample. Figure 6.7 displays the time evolution (chronogram) of the MS/MS signal intensity from the continuous monitoring of a surface water from northern Alberta. At ∼5 min, a spike of a Merichem NA mixture was added to yield a resulting total NA concentration of 1 ppm. While this sample is extremely complex, containing many individual NAs and other compounds [92, 93], we have exploited the barium ion adduct formation and the CID qualifier ion at *m/z* 196 to increase the specificity for NAs. Figure 6.7 displays the signals at *m/z* 139 + 155 arising from four selected $[M\text{-}H+Ba]^+$ precursor ions at *m/z* 359, 387, 417, and 445, corresponding to NA isomer classes $C_{14}H_{22}O_2$ ($[M\text{-}H]^-$, *m/z* 221), $C_{16}H_{26}O_2$ ($[M\text{-}H]^- = m/z$ 249), $C_{18}H_{32}O_2$ ($[M\text{-}H]^- = m/z$ 279), and $C_{20}H_{36}O_2$ ($[M\text{-}H]^- = m/z$ 307), respectively. Ions from negative ion ESI are included to facilitate comparisons with other studies [101]. At nominal mass resolution, only the NA isomer class is known (*i.e.,* there will generally be several individual NAs at each *m/z* with varying chemical structure). The concentration of each monitored ion (isomer class) is in the low parts-per-billion range. In excellent work by Woudneh et al. using solid phase extraction, chemical derivatization and liquid chromatography-mass spectrometry, abundances for all naphthenic acid isomer classes present in a Merichem mixture were provided [101].

Using these data for the composition of Merichem, the estimated concentrations of

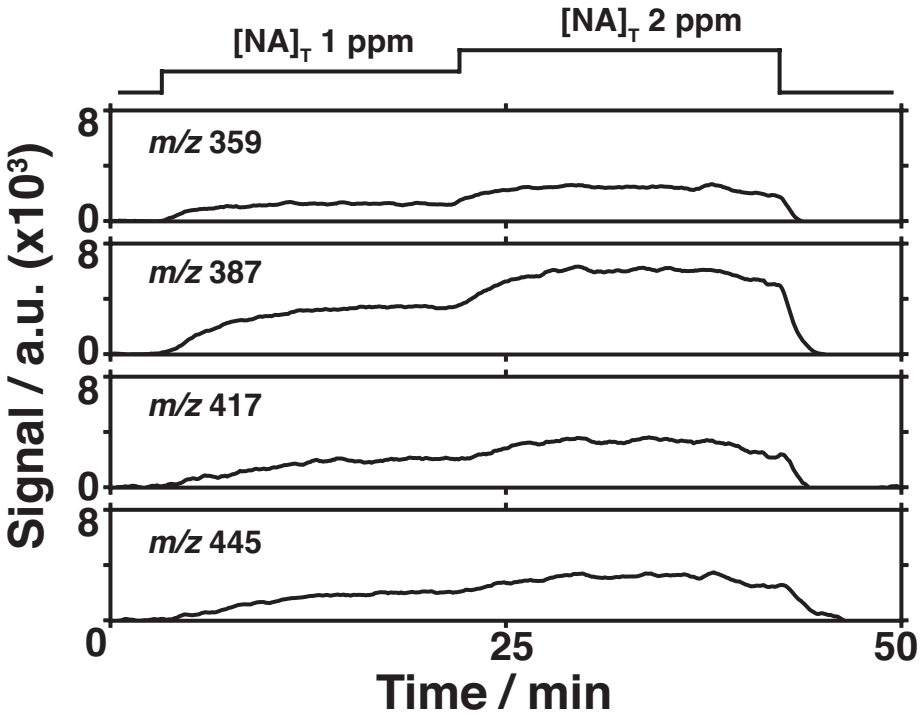

Figure 6.7: On-line tandem MS analysis of Merichem naphthenic acids spiked to a natural river water sample. The signals represent the sum of m/z 139 + 155 ions arising from $[M\text{-}H+Ba]^+$ precursor ions (indicated), with the qualifying ion at m/z 196 present in the CID spectrum.

each NA isomer class for each spike correspond to 53, 75, 15 and 4 ppb for the signals displayed in Figure 6.7 at m/z 359, 387, 417 and 445, respectively. This suggests that we were able to monitor trace levels of NAs with unknown molecular structures directly in surface waters. However, the authors note that the ionization efficiencies of individual analytes may vary, and in the case of non-targeted analysis, this method could suffer from inherent biases in quantitation. This challenge is not unique to the presented method, and is common whenever analytical standards are not available. This assay also excluded signals from hydroxylated species present in the contaminated samples, which could otherwise contribute to the signals in negative ion ESI, resulting in positive bias. Improved selectivity is particularly relevant for continuous online methods where sample clean-up and chromatographic separations

are not possible or problematic. Further, with the growing interest for field portable ESI mass spectrometers [111, 113], this method could offer increased selectivity for in-field analysis of carboxylic acids, while maintaining the analytical robustness that is inherent to CP-MIMS.

6.4 Conclusion

We have demonstrated a method for selective ionization and tandem mass spectrometric identification of carboxylic acids directly in aqueous samples. The method employs common product ions for all barium complexed carboxylate precursor ions ($[M\text{-}H+Ba]^+$). Use of isotopically labeled standards and a homologous series of phenyl-substituted carboxylic acids suggests the source of hydrogen present within the common product ions $[BaOH]^+$ and $[BaH]^+$ is not from an α carbon, but rather from the β and/or γ positions. Possible method interferences including 1,3-diols can be eliminated by the use of *m/z* 196 ($[C_2H_2O_2Ba]^+$) as diagnostic qualifier ion, which only occurs for barium carboxylates. We have paired this new tandem MS method with CP-MIMS for direct analysis of carboxylated analytes in complex aqueous samples (*e.g.,* wastewater effluent and northern Alberta surface water). The observed linear dynamic range is roughly two to three orders of magnitude and may be extended using corrections from a continuously infused standard and/or modulating the acceptor phase flowrate. Detection limits calculated for model analytes are in the low ppb range, which is approximately 10× higher than those observed for negative ESI. However, the lower sensitivity is offset by greater selectivity, which is particularly important for fast direct sampling methods that preclude chromatography such as CP-MIMS. Lastly, we demonstrate the use of this method for non-targeted screening of naphthenic acids at the ppb level with directly spiked surface water samples.

In combination with conventional techniques (*e.g.,* LC-MS), rapid screening methods can be used to increase the number of samples analyzed, while minimizing the time and cost of analysis. The method described can be elaborated for both qualitative and quantitative screening of carboxylated analytes in bioanalytical and/or environmental samples, with the potential for in-field analysis.

Chapter 7

Conclusions

7.1 Summary

The purpose of this thesis was to develop a high precision on-line sampling approach, coupled with mass spectrometry, for the continuous analysis of small organic molecules directly in aqueous samples. This technique was developed for the rapid screening of environmental and/or bioanalytical samples, enabling greater data density, and potentially reducing the number inconsequential samples to be analyzed by more rigorous conventional analytical methods (*e.g.,* LC-MS). Sample duty cycle for CP-MIMS is limited by membrane permeation, and therefore can be controlled with different membrane materials and/or geometries. Moreover, method selectivity can be tuned at the membrane, ionization source, and mass spectrometric level, offering high method versatility for a wide range of analytes.

Chapter 2 demonstrates our groups first attempt at a liquid|membrane|liquid interface for the analysis of a range of analytes from complicated samples (*e.g.,* river water and artificial urine). A methanol acceptor phase was pulled through the lumen of 10 cm hollow fibre polydimethylsiloxane membrane and directed towards an ESI

source, while sample was recirculated over the outside of the hollow fibre. Method detection limits were in the low parts-per-billion for most analytes tested, and response times ranged from 1 to 10 minutes ($t_{10-90\%}$). Additional sensitivity was gained through stopping the flow of acceptor phase within the membrane interface for a given interval of time, prior to MS measurement.

One major limitation for the previously mentioned flow cell interface design was the need to recirculate the sample at relatively high flow rates ($\sim$ 300 mL min^{-1}), which avoided laminar flow in the sample side of the membrane interface. As a result, relatively large sample sizes had to be used in order to interface with our sample peristaltic pumping system ($>$ 100 mL). Many biological and environmental samples require smaller volumes, therefore Chapter 3 focused on the miniaturization of the earlier CP-MIMS flow cell interface. Comparable detection limits were achieved with the developed miniature membrane probe, and analytes were measured from samples with volumes down to 400 μL. It was noted that significant analyte depletion was observed in samples under 2 mL. This problem may be circumvented by quantifying using short, reproducible membrane exposure times. The construction of the immersion probes was especially useful for the direct analysis of dirty samples, where the probe could be easily washed by immersion into a wash solvent.

Results from Chapters 2 and 3 indicated that when working with complicated sample matrices (*e.g.,* artificial urine) co-permeating matrix species caused suppression of analyte signal. Chapter 4 explored this issue and presented several strategies to mitigate ionization suppression observed with electrospray ionization. The linear dynamic range for a model analyte was extended to over 6 orders of magnitude using a continuously infused internal standard. As an alternative, modulation of the acceptor phase flow rate extended both the low and high end of the linear dynamic range, providing greater analytical versatility.

Chapter 5 applied the previously developed technology to a real-world scenario involving aqueous samples contaminated with complicated mixtures of analytes: Naphthenic acids, a class of water soluble aliphatic carboxylic acids linked to the extraction of bitumen from the northern Alberta tar sands. CP-MIMS was applied as a semi-quantitative method for the rapid screening and mass profiling of naphthenic acids directly in complicated aqueous solutions (*e.g.,* oil sands process waters). The sample pH was reduced to below 4 to ensure membrane transport of neutral carboxylic acid species, while negative ion mode electrospray ionization yielded $[M\text{-}H]^{-1}$ ions for mass spectrometric identification. Two methods of quantitation were discussed, including targeted SIM scans, and a non-targeted full scan approach.

Negative ESI, was unable to discriminate between hydroxylated and carboxylated species, leading to a potential bias for NA quantitation (Chapter 5). Chapter 6 further enhanced the selectivity for carboxylated analytes with the addition of barium acetate to the acceptor phase solvent — facilitating the formation of $[M-H+Ba]^{+}$ ions with ESI. These precursor ions were then fragmented using high energy collision induced dissociation to common peaks at *m/z* 155 and 139, attributed to $[BaOH]^{+}$ and $[BaH]^{+}$, respectively. The CID mechanisms for the formation of *m/z* 155 and 139 were investigated, and hydrogen transfer was found to occur from hydrogens on β and γ carbons. This method was used for the tandem mass spectrometric characterization of naphthenic acids (with unknown molecular structures), directly from spiked natural waters.

This thesis details the initial development and characterization of a CP-MIMS interface for the direct analysis of real-world samples. The range of analytes has been expanded from those previously reported for similar systems in the literature, while maintaining comparable or improved detection limits. Further, the work embodied in this thesis represents the first attempt to quantitatively analyze real-world

samples using CP-MIMS. The simplistic interface design allows for differentiation between membrane and ionization effects, with the ability to directly infuse analytes to the ion source (bypassing the membrane). Therefore, attention can be directed towards understanding and/or improving either/both component(s) individually. This approach can not be easily accomplished using MIMS with a gaseous acceptor phase.

7.2 Recommendations for Future Work

Significant work has been made in the development of a liquid|membrane|liquid interface for the continuous sampling of analytes in aqueous samples. However, much new ground remains, and future work should aim to decrease response times, while improving method sensitivity and selectivity. CP-MIMS allows the user to customize the setup at the membrane, ionization source, and MS level, in order to accommodate the analyte(s) of interest. As such, attention should be drawn to these areas for future work.

The majority of work to date has utilized hydrophobic PDMS membranes for interface construction. Many other polymer materials exist, which may facilitate transport of analytes not amenable to PDMS. This thesis has presented some preliminary data with Nafion (cation permeable polymer) membranes, but only scratched the surface in terms of applicability. Early work not presented in this thesis, has observed the transport of zwitterionic species through the conductive polymer. Applications for such an interface could include continuous on-line sampling of small peptide and/or amino acids from aqueous samples. Further, many fresh and salt water toxins (*e.g.,*kainic acid, domoic acid) are charged at nearly every pH, and therefore cannot be detected by CP-MIMS. Use of Nafion and/or other ion exchangeable membranes with transport of zwitterionic speices or highly polar neutrals could facilitate these analyses.

Furthermore, nearly all of the work to date using CP-MIMS has relied on passive diffusion. Future work should consider the use of facilitated transport (*e.g.,* potentially driven) through cation and/or anion permeable membranes. Collecting through both polarities of ion permeable membranes allows the researcher to isolate positive and negative ions for separate MS analyses, with the option for preconcentration.

In addition to alternative membrane materials, versatility at the ionization source may widen the range analytes amenable to CP-MIMS. Current PDMS membranes select for hydrophobic molecules, while ESI shows greatest ionization efficiencies for charged and/or easily ionizable species. As such, proper care must be made to ensure the analyte is neutral in the sample solution, but ionized in the acceptor phase solvent. Some work in this thesis (and by others) has attempted to use APCI to analyze molecules not responsive to ESI, however ionization by APCI remains to be dominated by acid/base chemistry, similar to ESI. The conjunction of CP-MIMS to atmospheric pressure photoionization (APPI) would better facilitate the ionization of non-polar molecules (*e.g.,* polyaromatic hydrocarbons and polychlorinated biphenyls). Preliminary data (not presented in this thesis) shows promise for the analysis of polyaromatic hydrocarbons by CP-MIMS interfaced to an APPI source. Having ESI, APCI, and APPI sources available would allow the user to optimize the CP-MIMS system for a given set of analytes.

Preliminary work with highly hydrophobic molecules such as PAHs and long chain fatty acids, has however, presented a challenge not foreseen in the previous chapters. It is well understood that CP-MIMS measures the free and available concentration of analyte present in the sample. That is, any analyte bound to something in the sample (*e.g.,* particulate material), will not be observed by our method of analysis. While this can be advantageous, as the free and available concentration may be a desirable quantity (particularly in binding and uptake studies), CP-MIMS analysis of highly

complex samples may underestimate the total concentration of analyte in the sample. For example, the maximum signal observed for pyrenebutyric acid corresponds to $\sim$ 150 ppb, where after, the signal begins to decrease — likely due to aggregation within the solution. Future work should investigate and characterize this phenomenon further, perhaps comparing the free and available concentration of samples measured by CP-MIMS to the total extracted concentration by more conventional methods (*e.g.,* LC-MS).

Ultimately, the technology developed in this thesis might be best suited as a rapid sample pre-screen prior to comprehensive chromatographic analysis. The developed membrane probe is small and robust, and has been previously fitted to an autosampler (Chapter 2). Further, if the volume of the sample is large enough, the integrity of the sample is largely unchanged though analysis by CP-MIMS. Therefore, once a sample is confirmed to be a 'hit', the sample can then be flagged for subsequent SPE-LC-MS analysis. In addition to lab settings, the ruggedness and durability of membrane interfaces could allow the pairing of CP-MIMS with mobile and/or field deployable mass spectrometers equipped with atmospheric pressure ionization sources. In field adaptive sampling may allow users to pre-screen samples at the source, and only send samples confirmed to contain analytes off for external analysis. This approach could greatly minimize the cost of field campaigns, and allow better understanding of the spatial distribution of analytes in the natural environment.

Appendix A

Supplementary Figures

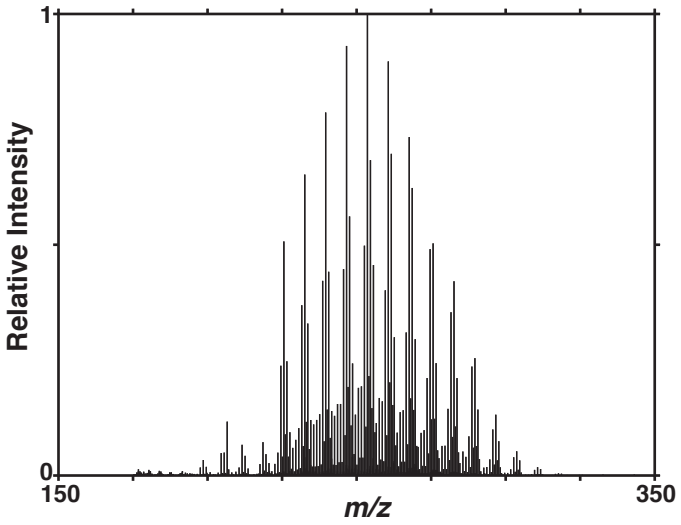

Figure A.1: High resolution full scan mass spectrum for direct infusion of 1 ppm refined Merichem (in methanol).

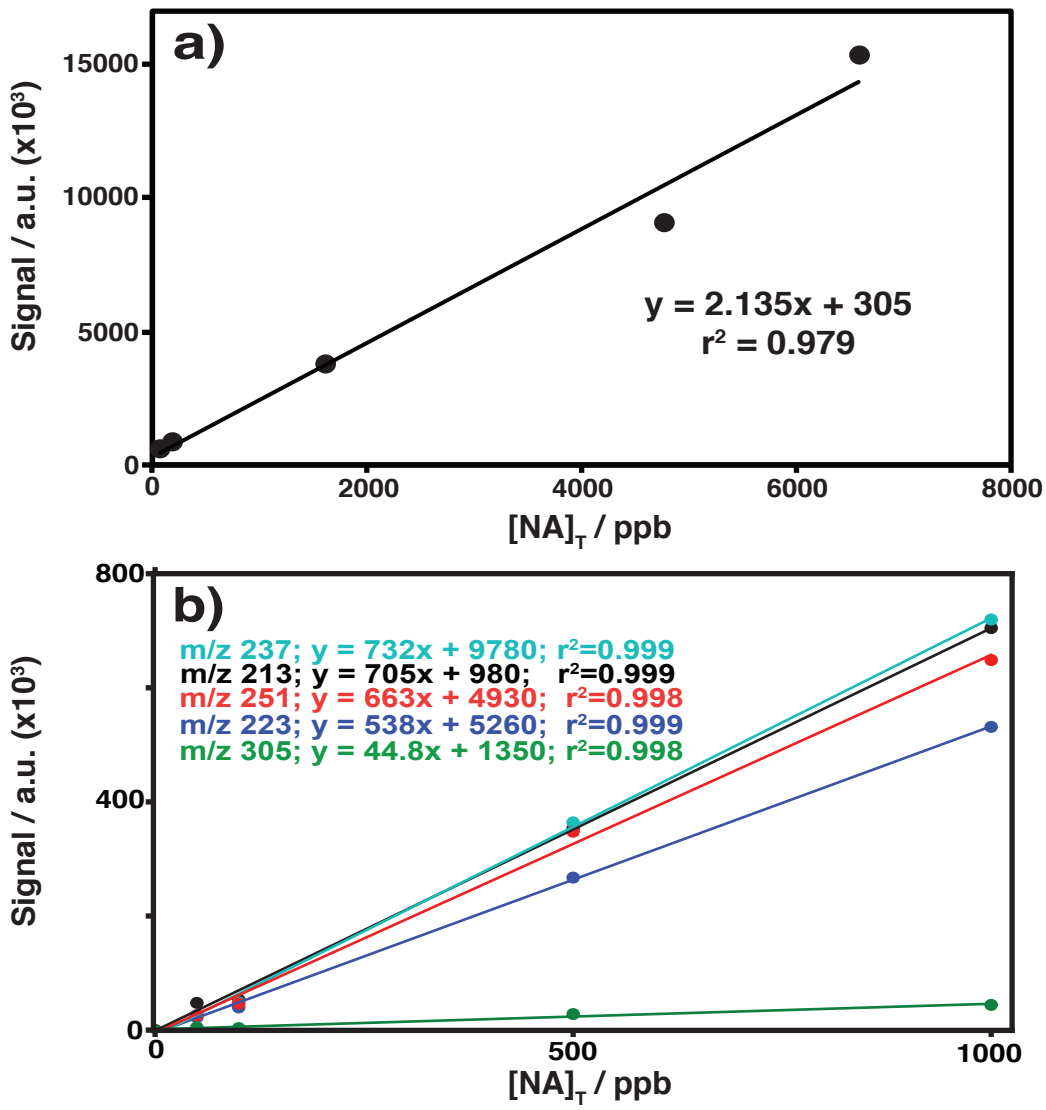

Figure A.2: Calibration curves for Merichem naphthenic acid mixture in aqueous solution, a) Calibration curve generated from fullscan TIC b) Calibration curve generated from five SIMs at masses typical of common peaks in the Merichem mass spectrum. Sample pH was adjusted to ∼4. Total NA concentration reported as Merichem equivalents.

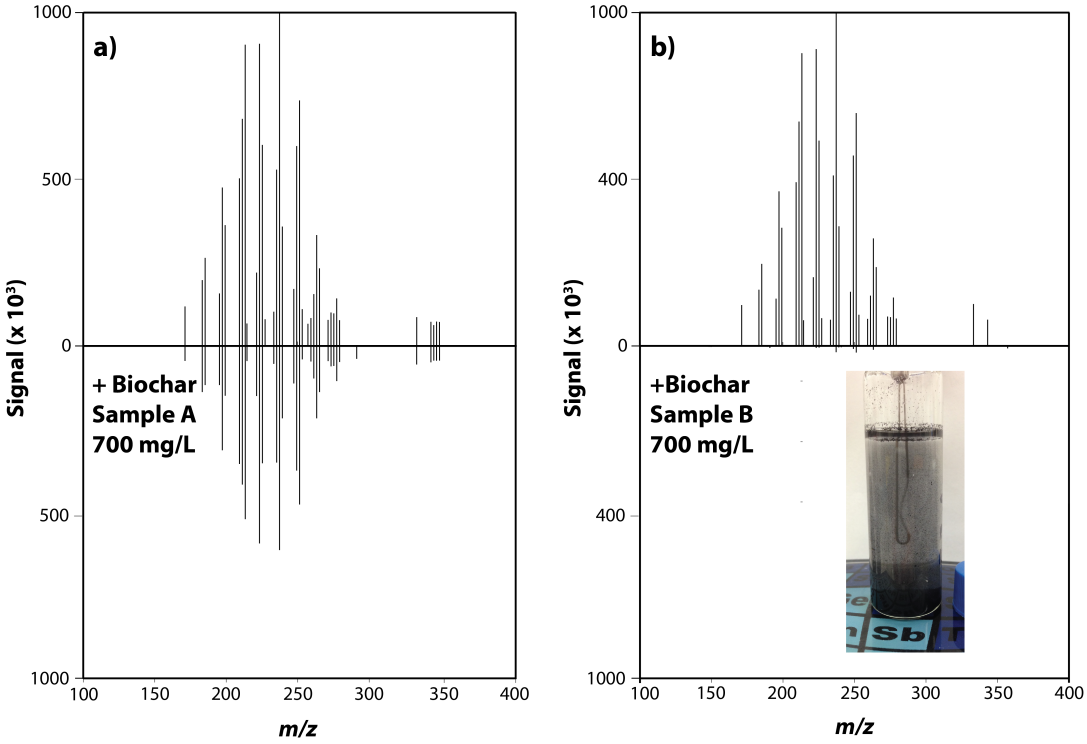

Figure A.3: Adsorption of Merichem naphthenic acids on aqueous suspensions of biochar samples A and B. Top panels display the normalized mass spectra for 4.1 ppm Merichem in 0.12 M glycine buffer (pH = 3.65 ± 0.02). Bottom panels display the mass spectra of the same solution after 700 mg/L of biochar Sample A or Sample B have been added and allowed to decay to a steady state. Inset photo shows the CP-MIMS J-probe immersed in a biochar suspension. Full scan mass spectra are background subtracted and filtered to remove minor peaks contributing less than 5%.

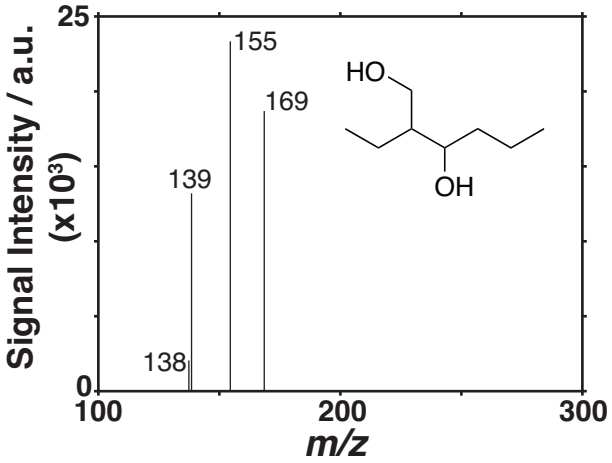

Figure A.4: CID mass spectra of 2-ethyl-1,3-hexanediol in the presence of barium acetate.

Bibliography

[1] D. Fatta-Kassinos, S. Meric, and A. Nikolaou, "Pharmaceutical residues in environmental waters and wastewater: current state of knowledge and future research," *Anal. Bioanal.Chem.*, vol. 399, no. 1, pp. 251–275, 2011.

[2] S. L. Bartelt-Hunt, D. D. Snow, T. Damon, J. Shockley, and K. Hoagland, "The occurrence of illicit and therapeutic pharmaceuticals in wastewater effluent and surface waters in nebraska," *Environ. Pollut.*, vol. 158, no. 8, pp. 2790–2791, 2010.

[3] S. D. Richardson, "Water analysis: Emerging contaminants and current issues," *Anal. Chem.*, vol. 79, no. 12, pp. 4295–4324, 2007.

[4] R. A. Ketola, T. Kotiaho, M. E. Cisper, and T. M. Allen, "Environmental applications of membrane introduction mass spectrometry," *J. Mass Spectrom.*, vol. 37, no. 5, pp. 457–476, 2002.

[5] G. Hoch and B. Kok, "A mass spectrometer inlet system for sampling gases dissolved in liquid phases," *Arch. Biochem. Biophys.*, vol. 101, pp. 160–70, 1963.

[6] L. B. Westover, J. C. Tou, and J. H. Mark, "Novel mass spectrometric sampling device-hollow fiber probe," *Anal. Chem.*, vol. 46, no. 4, pp. 568–571, 1974.

[7] R. C. Johnson, R. G. Cooks, T. M. Allen, M. E. Cisper, and P. H. Hemberger, "Membrane introduction mass spectrometry: trends and applications," *Mass Spectrom. Rev.*, vol. 19, no. 1, pp. 1–37, 2000.

[8] A. M. Llamas, C. B. Ojeda, and F. S. Rojas, "Process analytical chemistry - application of mass spectrometry in environmental analysis: An overview," *Appl. Spectrosc. Rev.*, vol. 42, no. 4, pp. 345–367, 2007.

[9] M. A. LaPack, J. C. Tou, and C. G. Enke, "Membrane mass spectrometry for the direct trace analysis of volatile organic compounds in air and water," *Anal. Chem.*, vol. 62, pp. 1265–1271, 1990.

[10] A. J. Thompson, A. S. Creba, R. M. Ferguson, E. T. Krogh, and C. G. Gill, "A coaxially heated membrane introduction mass spectrometry interface for the

rapid and sensitive on-line measurement of volatile and semi-volatile organic contaminants in air and water at parts-per-trillion levels," *Rapid Commun. Mass Spectrom.*, vol. 20, no. 13, pp. 2000–8, 2006.

[11] L. Riter, Z. Takats, L. Charles, and R. G. Cooks, "High surface area membrane introduction mass spectrometry for analysis of volatile and semi-volatile organic compounds in air," *Rapid Commun. Mass Spectrom.*, vol. 15, pp. 1520–24, 2001.

[12] C. S. Creaser and D. J. Weston, "In-membrane preconcentration/membrane inlet mass spectrometry of volatile and semivolatile organic compounds," *Anal. Chem.*, vol. 72, no. 13, pp. 2730–6, 2000.

[13] M. Leth and F. R. Lauritsen, "A fully integrated trap-membrane inlet mass spectrometry system for the measurement of semivolatile organic compounds in aqueous solution," *Rapid Commun. Mass Spectrom.*, vol. 9, pp. 591–596, 1995.

[14] F. R. Lauritsen and R. A. Ketola, "Quantitive determination of semivolatile organic compounds in solution using trap-and-release membrane inlet mass spectrometry," *Anal. Chem.*, vol. 69, no. 23, pp. 4917–4922, 1997.

[15] R. Haddad, M. A. Mendes, N. F. Hoehr, and M. N. Eberlin, "Amino acid quantitation in aqueous matrices via trap and release membrane introduction mass spectrometry: homocysteine in human plasma," *Analyst*, vol. 126, no. 8, pp. 1212–5, 2001.

[16] M. A. Mendes and M. N. Eberlin, "Trace level analysis of vocs and semi-vocs in aqueous solution using a direct insertion membrane probe and trap and release membrane introduction mass spectrometry," *Analyst*, vol. 125, pp. 21–24, 2000.

[17] C. S. Creaser, D. G. Lamarca, L. M. dos Santos, A. P. New, and P. A. James, "A universal temperature controlled membrane interface for the analysis of volatile and semi-volatile organic compounds," *Analyst*, vol. 128, no. 9, pp. 1150–6, 2003.

[18] M. H. Soni, J. H. Callahan, and S. W. McElvany, "Laser desorption-membrane introduction mass spectrometry," *Anal. Chem.*, vol. 70, p. 3103, 1998.

[19] T. Aggerholm and F. R. Lauritsen, "Direct detection of polyaromatic hydrocarbons, estrogenic compounds and pesticides in water using desorption chemical ionisation membrane inlet mass spectrometry," *Rapid Commun. Mass Spectrom.*, vol. 15, no. 19, pp. 1826–31, 2001.

[20] F. R. Lauritsen, M. A. Mendes, and T. Aggerholm, "Direct detection of large fat-soluble biomolecules in solution using membrane inlet mass spectrometry and desorption chemical ionization," *Analyst*, vol. 125, no. 1, pp. 211–5, 2000.

[21] R. Haddad, R. Sparrapan, T. Kotiaho, and M. N. Eberlin, "Easy ambient sonic-spray ionization-membrane interface mass spectrometry for direct analysis of solution constituents," *Anal. Chem.*, vol. 80, no. 3, pp. 898–903, 2008.

[22] C. Xu, J. Patrick, and R. G. Cooks, "Affinity membrane introduction mass spectrometry," *Anal. Chem.*, vol. 67, p. 724, 1995.

[23] C. S. Creaser, D. G. Lamarca, J. Brum, C. Werner, A. P. New, and D. Freitas, "Reversed-phase membrane inlet mass spectrometry applied to the real-time monitoring of low molecular weight alcohols in chloroform," *Anal. Chem.*, vol. 74, no. 1, pp. 300–4, 2002.

[24] M. Gernatova, P. Janderka, A. Marcinkova, and P. Ostrizek, "Use of nafion as a membrane separator in membrane introduction mass spectrometry," *Eur. J. Mass Spectrom.*, vol. 15, no. 5, pp. 571–577, 2009.

[25] R. M. Alberici, R. Sparrapan, W. F. Jardim, and M. N. Eberlin, "Selective trace lever analysis of phenolic compounds in water by flow injection analysis - membrane introduction mass spectrometry," *Environ. Sci. Technol.*, vol. 35, no. 10, pp. 2084–2088, 2001.

[26] R. Sparrapan, M. N. Eberlin, and R. M. Alberici, "Quantitation of trace phenolic compounds in water by trap-and-release membrane introduction mass spectrometry after acetylation," *Rapid Commun. Mass Spectrom.*, vol. 22, no. 24, pp. 4105–4108, 2008.

[27] A. S. Creba, A. N. Weissfloch, E. T. Krogh, and C. G. Gill, "An enzyme derivatized polydimethylsiloxane (pdms) membrane for use in membrane introduction mass spectrometry (mims)," *J. Am. Soc. Mass Spectrom.*, vol. 18, no. 6, pp. 973–9, 2007.

[28] T. R. Covey, B. A. Thomson, and B. B. Schneider, "Atmospheric pressure ion sources," *Mass Spectrom. Rev.*, vol. 28, no. 6, pp. 870–897, 2009.

[29] T. Fyles, *Principles of Artificial Membrane Transport by Synthetic Ionophores.* Inclusion Aspects of Membrane Chemistry, Dordrecht: Kluwer Academic Publishers, 1991.

[30] A. J. Tomlinson and S. Naylor, "Systematic development of on-line membrane preconcentration capillary electrophoresis mass spectrometry for the analysis of peptide mixtures," *J. Capillary. Electrophor.*, vol. 2, no. 5, pp. 225–233, 1995.

[31] Y. Jiang and C. S. Lee, "On-line coupling of micro-enzyme reactor with micro-membrane chromatography for protein digestion, peptide separation, and protein identification using electrospray ionization mass spectrometry," *J. Chromatogr. A*, vol. 924, no. 1-2, pp. 315–322, 2001.

[32] Y. Li, J. W. Cooper, and C. S. Lee, "Miniaturized membrane-based reversed-phase chromatography and enzyme reactor for protein digestion, peptide separation, and protein identification using electrospray ionization mass spectrometry," *J. Chromatogr. A*, vol. 979, no. 1-2, pp. 241–247, 2002.

[33] J. W. Cooper, J. Z. Chen, Y. Li, and C. S. Lee, "Membrane-based nanoscale proteolytic reactor enabling protein digestion, peptide separation, and protein identification using mass spectrometry," *Anal. Chem.*, vol. 75, no. 5, pp. 1067–1074, 2003.

[34] R. Clinton, C. S. Creaser, and D. Bryant, "Real-time monitoring of a pharmaceutical process reaction using a membrane interface combined with atmospheric pressure chemical ionisation mass spectrometry," *Anal. Chim. Acta*, vol. 539, no. 1-2, pp. 133–140, 2005.

[35] E. VanHassel and M. E. Bier, "An electrospray membrane probe for the analysis of volatile and semi-volatile organic compounds in water," *Rapid Commun. Mass Spectrom.*, vol. 21, no. 3, pp. 413–420, 2007.

[36] J. H. Nelson, E. T. Krogh, C. G. Gill, and D. A. Friesen, "Monitoring the tio2-photocatalyzed destruction of aqueous environmental contaminants at parts-per-trillion levels using membrane introduction mass spectrometry (mims)," *J. Environ. Sci. Health A: Tox. Hazard Subst. Environ. Eng.*, vol. 39, no. 9, pp. 2307–17, 2004.

[37] SRC Physical Properties Database. http://www.srcinc.com/what-we-do/product.aspx?id=133. Accessed November 2010.

[38] A. C. D. Inc., "Acd/chemsketch v10.04," 2007.

[39] T. Brooks and C. W. Keevil, "A simple artificial urine for the growth of urinary pathogens," *Lett. Appl. Microbiol.*, vol. 24, no. 3, pp. 203–206, 1997.

[40] A. W. Martinez, S. T. Phillips, E. Carrilho, S. W. Thomas, H. Sindi, and G. M. Whitesides, "Simple telemedicine for developing regions: Camera phones and paper-based microfluidic devices for real-time, off-site diagnosis," *Anal. Chem.*, vol. 80, no. 10, pp. 3699–3707, 2008.

[41] A. Eaton, L. Clesceri, and A. Greenberg, *Standard Methods for the Examination of Water and Wastewater*. Washington, DC: American Public Health Association, 1995.

[42] M. A. Hickner, "Ion-containing polymers: new energy & clean water," *Mater. Today*, vol. 13, no. 5, pp. 34–41, 2010.

[43] A. Randova, L. Bartovska, S. Hovorka, M. Poloncarzova, Z. Kolska, and P. Izak, "Application of the group contribution approach to nafion swelling," *J. Appl. Polym. Sci.*, vol. 111, no. 4, pp. 1745–1750, 2009.

[44] M. N. Eberlin, "Electrospray ionization mass spectrometry: a major tool to investigate reaction mechanisms in both solution and the gas phase," *Eur. J. Mass Spectrom.*, vol. 13, no. 1, pp. 19–28, 2007.

[45] P. J. Taylor, "Matrix effects: the achilles heel of quantitative high-performance liquid chromatography-electrospray-tandem mass spectrometry," *Clin. Biochem.*, vol. 38, no. 4, pp. 328–334, 2005.

[46] R. V. Rios, L. L. da Rocha, T. G. Vieira, R. M. Lago, and R. Augusti, "On-line monitoring by membrane introduction mass spectrometry of chlorination of organics in water. mechanistic and kinetic aspects of chloroform formation," *J. Mass Spectrom.*, vol. 35, no. 5, pp. 618–24, 2000.

[47] J. A. Jonsson and L. Mathiasson, "Membrane-based techniques for sample enrichment," *J. Chromatogr. A*, vol. 902, pp. 205–225, 2000.

[48] S. Zhao, L. Zou, C. Y. Tang, and D. Mulcahy, "Recent developments in forward osmosis: Opportunities and challenges," *J. Membr. Sci.*, vol. 396, pp. 1–21, 2012.

[49] Q. Zhao, Q. F. An, Y. Ji, J. Qian, and C. Gao, "Polyelectrolyte complex membranes for pervaporation, nanofiltration and fuel cell applications," *J. Membr. Sci.*, vol. 379, no. 1-2, pp. 19–45, 2011.

[50] L. Wang, J.-P. Corriou, C. Castel, and E. Favre, "A critical review of cyclic transient membrane gas separation processes: State of the art, opportunities and limitations," *J. Membr. Sci.*, vol. 383, no. 1-2, pp. 170–188, 2011.

[51] L. Steller, M. Kreir, and R. Salzer, "Natural and artificial ion channels for biosensing platforms," *Anal. and Bioanal. Chem.*, vol. 402, no. 1, pp. 209–230, 2012.

[52] G. Merle, M. Wessling, and K. Nijmeijer, "Anion exchange membranes for alkaline fuel cells: A review," *J. Mem. Sci.*, vol. 377, no. 1-2, pp. 1–35, 2011.

[53] A. Antony, J. H. Low, S. Gray, A. E. Childress, P. Le-Clech, and G. Leslie, "Scale formation and control in high pressure membrane water treatment systems: A review," *J. Membr. Sci.*, vol. 383, no. 1-2, pp. 1–16, 2011.

[54] N. G. Davey, E. T. Krogh, and C. G. Gill, "Membrane introduction mass spectrometry (mims)," *Trends Anal. Chem.*, vol. 30, no. 9, pp. 1477– 1485, 2011.

[55] K. D. Duncan, E. P. B. McCauley, E. T. Krogh, and C. G. Gill, "Characterization of a condensed-phase membrane introduction mass spectrometry (cp-mims) interface using a methanol acceptor phase coupled with electrospray ionization for the continuous on-line quantitation of polar, low-volatility analytes at trace levels in complex aqueous samples," *Rapid Commun. Mass Spectrom.*, vol. 25, no. 9, pp. 1141–1151, 2011.

[56] J. D. Tammam, A. G. Williams, J. Banks, G. Cowie, and D. Lloyd, "Membrane inlet mass spectrometric measurement of o_2 and co_2 gradients in cultures of lactobacillus paracasei and a developing cheddar cheese ecosystem," *Int. J. Food Microbiol.*, vol. 65, no. 1-2, pp. 11–22, 2001.

[57] G. Cowie and D. Lloyd, "Membrane inlet ion trap mass spectrometry for the direct measurement of dissolved gases in ecological samples," *J. Microbiol. Methods*, vol. 35, no. 1, pp. 1–12, 1999.

[58] D. Jolly and P. Vezina, "In vivo microdialysis in the rat: Low cost and low labor construction of a small diameter, removable, concentric-style microdialysis probe system," *J. Neurosci. Methods*, vol. 68, no. 2, pp. 259–267, 1996.

[59] C. U. Ungerstedt, "Dialysis probe," *US Patent*, vol. 4694832, 1987.

[60] D. Remane, D. K. Wissenbach, M. R. Meyer, and H. H. Maurer, "Systematic investigation of ion suppression and enhancement effects of fourteen stable-isotope-labeled internal standards by their native analogues using atmospheric-pressure chemical ionization and electrospray ionization and the relevance for multi-analyte liquid chromatographic/mass spectrometric procedures," *Rapid Commun. Mass Spectrom.*, vol. 24, no. 7, pp. 859–867, 2010.

[61] C. R. Mallet, Z. L. Lu, and J. R. Mazzeo, "A study of ion suppression effects in electrospray ionization from mobile phase additives and solid-phase extracts," *Rapid Commun. Mass Spectrom.*, vol. 18, no. 1, pp. 49–58, 2004.

[62] R. King, R. Bonfiglio, C. Fernandez-Metzler, C. Miller-Stein, and T. Olah, "Mechanistic investigation of ionization suppression in electrospray ionization," *J. Am. Soc. Mass Spectrom.*, vol. 11, no. 11, pp. 942–950, 2000.

[63] J. P. Antignac, K. de Wasch, F. Monteau, H. De Brabander, F. Andre, and B. Le Bizec, "The ion suppression phenomenon in liquid chromatography-mass spectrometry and its consequences in the field of residue," *Anal. Chim. Acta*, vol. 529, no. 1-2, pp. 129–136, 2005.

[64] I. Cotte-Rodriguez, E. Handberg, R. J. Noll, D. P. A. Kilgour, and R. G. Cooks, "Improved detection of low vapour pressure compounds in air by serial combination of single-sided membrane introduction with fiber introduction mass spectrometry," *Analyst*, vol. 130, pp. 679–86, 2005.

[65] R. C. da Silva, V. G. Zuin, J. H. Yariwake, M. N. Eberlin, and F. Augusto, "Fiber introduction mass spectrometry: determination of pesticides in herbal infusions using a novel sol-gel pdms/pva fiber for solid-phase microextraction," *J. Mass Spectrom.*, vol. 42, no. 10, pp. 1358–1362, 2007.

[66] J. Pawliszyn, *Handbook of Solid Phase Microextraction.* China: Chemical Industry Press of China, 1 ed., 2009.

[67] J. Manso, T. Garcia-Barrera, and J. L. Gomez-Ariza, "New home-made assembly for hollow-fibre membrane extraction of persistent organic pollutants from real world samples," *J. Chromatogr. A*, vol. 1218, no. 44, pp. 7923–7935, 2011.

[68] I. Rodriguez and R. Cela, "Combination of solid-phase extraction procedures with gas chromatographic hyphenated techniques for chlorophenol determination in drinking water," *Trends Anal. Chem.*, vol. 16, no. 8, pp. 463–475, 1997.

[69] A. Dupuis, V. Migeot, A. Cariot, M. Albouy-Llaty, B. Legube, and S. Rabouan, "Quantification of bisphenol a, 353-nonylphenol and their chlorinated derivatives in drinking water treatment plants," *Environ. Sci. Pollut. Res.*, vol. 19, no. 9, pp. 4193–4205, 2012.

[70] N. Veldhoen, R. C. Skirrow, H. Osachoff, H. Wigmore, D. J. Clapson, M. P. Gunderson, G. Van Aggelen, and C. C. Helbing, "The bactericidal agent triclosan modulates thyroid hormone-associated gene expression and disrupts postembryonic anuran development," *Aquat. Toxicol.*, vol. 80, no. 3, pp. 217–227, 2006.

[71] S. J. Robins, D. Collins, J. T. Wittes, V. Papademetriou, P. C. Deedwania, E. J. Schaefer, J. R. McNamara, M. L. Kashyap, J. M. Hershman, L. F. Wexler, H. B. Rubins, and V.-H. S. Grp, "Relation of gemfibrozil treatment and lipid levels with major coronary events - va-hit: A randomized controlled trial," *J. Am. Med. Assoc.*, vol. 285, no. 12, pp. 1585–1591, 2001.

[72] D. W. Janes, C. J. Durning, D. M. van Pel, M. S. Lynch, C. G. Gill, and E. T. Krogh, "Modeling analyte permeation in cylindrical hollow fiber membrane introduction mass spectrometry," *J. Membr. Sci.*, vol. 325, no. 1, pp. 81–91, 2008.

[73] W. Koehler and H.-H. Geppert, "Method and device for vibration during solid phase microextraction," *US Patent*, vol. 569322, 1997.

[74] X. Ma, S. Zhang, and X. Zhang, "An instrumentation perspective on reaction monitoring by ambient mass spectrometry," *Trends Anal. Chem.*, vol. 35, no. 0, pp. 50–66, 2012.

[75] P. Nandi and S. M. Lunte, "Recent trends in microdialysis sampling integrated with conventional and microanalytical systems for monitoring biological events: A review," *Anal. Chim. Acta*, vol. 651, no. 1, pp. 1–14, 2009.

[76] A. L. N. van Nuijs, B. Pecceu, L. Theunis, N. Dubois, C. Charlier, P. G. Jorens, L. Bervoets, R. Blust, H. Neels, and A. Covaci, "Cocaine and metabolites in waste and surface water across belgium," *Environ. Pollut.*, vol. 157, no. 1, pp. 123–129, 2009.

[77] M. R. Boleda, M. T. Galceran, and F. Ventura, "Monitoring of opiates, cannabinoids and their metabolites in wastewater, surface water and finished water in catalonia, spain," *Water Res.*, vol. 43, no. 4, pp. 1126–1136, 2009.

[78] E. Zuccato, S. Castiglioni, R. Bagnati, C. Chiabrando, P. Grassi, and R. Fanelli, "Illicit drugs, a novel group of environmental contaminants," *Water Res.*, vol. 42, no. 4-5, pp. 961–968, 2008.

[79] C. D. R. de Oliveira, M. Roehsig, R. M. de Almeida, W. L. Rocha, and M. Yonamine, "Recent advances in chromatographic methods to detect drugs of abuse in alternative biological matrices," *Curr. Pharm. Anal.*, vol. 3, no. 2, pp. 95–109, 2007.

[80] W. H. A. de Jong, E. G. E. de Vries, and I. P. Kema, "Current status and future developments of lc-ms/ms in clinical chemistry for quantification of biogenic amines," *Clin. Biochem.*, vol. 44, no. 1, pp. 95–103, 2011.

[81] A. Roux, D. Lison, C. Junot, and J.-F. Heilier, "Applications of liquid chromatography coupled to mass spectrometry-based metabolomics in clinical chemistry and toxicology: A review," *Clin. Biochem.*, vol. 44, no. 1, pp. 119–135, 2011.

[82] R. Lopez-Serna, S. Perez, A. Ginebreda, M. Petrovic, and D. Barcelo, "Fully automated determination of 74 pharmaceuticals in environmental and waste waters by online solid phase extraction-liquid chromatography-electrospray-tandem mass spectrometry," *Talanta*, vol. 83, no. 2, pp. 410–424, 2010.

[83] M. J. Garcia-Galan, T. Garrido, J. Fraile, A. Ginebreda, M. S. Diaz-Cruz, and D. Barcelo, "Application of fully automated online solid phase extraction-liquid chromatography-electrospray-tandem mass spectrometry for the determination of sulfonamides and their acetylated metabolites in groundwater," *Anal. Bioanal.Chem.*, vol. 399, no. 2, pp. 795–806, 2011.

[84] K. Gethard and S. Mitra, "Membrane distillation as an online concentration technique: application to the determination of pharmaceutical residues in natural waters," *Anal. Bioanal.Chem.*, vol. 400, no. 2, pp. 571–575, 2011.

[85] K. Gethard and S. Mitra, "Carbon nanotube enhanced membrane distillation for online preconcentration of trace pharmaceuticals in polar solvents," *Analyst*, vol. 136, no. 12, pp. 2643–2648, 2011.

[86] E. T. Krogh and C. G. Gill, "Membrane introduction mass spectrometry (mims): a versatile tool for direct, real-time chemical measurments," *J. Mass Spectrom.*, vol. 49, pp. 1205–1213, 2014.

[87] K. D. Duncan, M. D. Willis, E. T. Krogh, and C. G. Gill, "A miniature condensed-phase membrane introduction mass spectrometry (cp-mims) probe for direct and on-line measurements of pharmaceuticals and contaminants in small, complex samples," *Rapid Commun. Mass Spectrom.*, vol. 27, no. 11, pp. 1213–1221, 2013.

[88] M. D. Willis, K. D. Duncan, E. T. Krogh, and C. G. Gill, "Delicate polydimethylsiloxane hollow fibre membrane interfaces for condensed phase membrane introduction mass spectrometry (cp-mims)," *Rapid Commun. Mass Spectrom.*, vol. 28, no. 7, pp. 671–681, 2014.

[89] SRC Physical Properties Database. http://www.srcinc.com/what-we-do/product.aspx?id=133. Accessed November 2014.

[90] M. J. Avery, "Quantitative characterization of differential ion suppression on liquid chromatography/atmospheric pressure ionization mass spectrometric bioanalytical methods," *Rapid Commun. Mass Spectrom.*, vol. 17, no. 3, pp. 197–201, 2003.

[91] D. M. Grewer, R. F. Young, R. M. Whittal, and P. M. Fedorak, "Naphthenic acids and other acid-extractables in water samples from alberta: What is being measured?," *Sci. Total Environ.*, vol. 408, no. 23, pp. 5997–6010, 2010.

[92] L. D. Brown and A. C. Ulrich, "Oil sands naphthenic acids: A review of properties, measurement, and treatment," *Chemosphere*, vol. 127, no. 127, pp. 276–290, 2015.

[93] J. V. Headley, K. M. Peru, and M. P. Barrow, "Advances in mass spectrometric characterization of naphthenic acids fraction compounds in oil sands environmental samples and crude oil - a review," *Mass Spectrom. Rev.*, p. 10.1002/mas.21472, 2015.

[94] J. V. Headley, K. M. Peru, D. W. McMartin, and M. Winkler, "Determination of dissolved naphthenic acids in natural waters by using negative-ion electrospray mass spectrometry," *J. AOAC Int.*, vol. 85, no. 1, pp. 182–187, 2002.

[95] J. V. Headley, K. M. Peru, M. P. Barrow, and P. J. Derrick, "Characterization of naphthenic acids from athabasca oil sands using electrospray ionization: The significant influence of solvents," *Anal. Chem.*, vol. 79, no. 16, pp. 6222–6229, 2007.

[96] J. V. Headley, M. P. Barrow, K. M. Peru, B. Fahlman, R. A. Frank, G. Bickerton, M. E. McMaster, J. Parrott, and L. M. Hewitt, "Preliminary fingerprinting of athabasca oil sands polar organics in environmental samples using electrospray ionization fourier transform ion cyclotron resonance mass spectrometry," *Rapid Commun. Mass Spectrom.*, vol. 25, no. 13, pp. 1899–1909, 2011.

[97] M. P. Barrow, M. Witt, J. V. Headley, and K. M. Peru, "Athabasca oil sands process water: Characterization by atmospheric pressure photoionization and electrospray ionization fourier transform ion cyclotron resonance mass spectrometry," *Anal. Chem.*, vol. 82, no. 9, pp. 3727–3735, 2010.

[98] X. Ortiz, K. J. Jobst, E. J. Reiner, S. M. Backus, K. M. Peru, D. W. McMartin, G. O'Sullivan, V. Y. Taguchi, and J. V. Headley, "Characterization of naphthenic acids by gas chromatography-fourier transform ion cyclotron resonance mass spectrometry," *Anal. Chem.*, vol. 86, no. 15, pp. 7666–7673, 2014.

[99] S. J. Rowland, A. G. Scarlett, D. Jones, C. E. West, and R. A. Frank, "Diamonds in the rough: Identification of individual naphthenic acids in oil sands process water," *Environ. Sci. Technol.*, vol. 45, no. 7, pp. 3154–3159, 2011.

[100] M. S. Ross, A. d. S. Pereira, J. Fennell, M. Davies, J. Johnson, L. Sliva, and J. W. Martin, "Quantitative and qualitative analysis of naphthenic acids in natural waters surrounding the canadian oil sands industry," *Environ. Sci. Technol.*, vol. 46, no. 23, pp. 12796–12805, 2012.

[101] M. B. Woudneh, C. M. Hamilton, J. P. Benskin, G. Wang, P. McEachern, and J. R. Cosgrove, "A novel derivatization-based liquid chromatography tandem mass spectrometry method for quantitative characterization of naphthenic acid isomer profiles in environmental waters," *J. Chromatogr. A*, vol. 1293, pp. 36–43, 2013.

[102] D. Shang, M. Kim, M. Haberl, and A. Legzdins, "Development of a rapid liquid chromatography tandem mass spectrometry method for screening of trace naphthenic acids in aqueous environments," *J. Chromatogr. A*, vol. 1278, pp. 98–107, 2013.

[103] P. Brunswick, D. Shang, G. van Aggelen, R. Hindle, L. M. Hewitt, R. A. Frank, M. Haberl, and M. Kim, "Trace analysis of total naphthenic acids in aqueous environmental matrices by liquid chromatography/mass spectrometry-quadrupole time of flight mass spectrometry direct injection," *J. Chromatogr. A*, vol. 1405, pp. 49–71, 2015.

[104] W. Gabryelski and K. L. Froese, "Characterization of naphthenic acids by electrospray ionization high-field asymmetric waveform ion mobility spectrometry mass spectrometry," *Anal. Chem.*, vol. 75, no. 17, pp. 4612–4623, 2003.

[105] M. R. Noestheden, J. V. Headley, K. M. Peru, M. P. Barrow, L. L. Burton, T. Sakuma, P. Winkler, and J. L. Campbell, "Rapid characterization of naphthenic acids using differential mobility spectrometry and mass spectrometry," *Environ. Sci. Technol.*, vol. 48, no. 17, pp. 10264–10272, 2014.

[106] M. H. Mohamed, L. D. Wilson, J. V. Headley, and K. M. Peru, "Screening of oil sands naphthenic acids by uv-vis absorption and fluorescence emission spectrophotometry," *J. Environ. Sci. Health. Part A Toxic/Hazard. Subst. Environ. Eng.*, vol. 43, no. 14, pp. 1700–1705, 2008.

[107] R. J. Kavanagh, B. K. Burnison, R. A. Frank, K. R. Solomon, and G. Van Der Kraak, "Detecting oil sands process-affected waters in the alberta oil sands region using synchronous fluorescence spectroscopy," *Chemosphere*, vol. 76, no. 1, pp. 120–126, 2009.

[108] K. D. Duncan, G. W. Vandergrift, E. T. Krogh, and C. G. Gill, "Ionization suppression effects with condensed phase membrane introduction mass spectrometry: methods to increase the linear dynamic range and sensitivity," *J. Mass Spectrom.*, vol. 50, no. 3, pp. 437–443, 2015.

[109] A. Veksha, W. Zaman, D. B. Layzell, and J. M. Hill, "Enhancing biochar yield by co-pyrolysis of bio-oil with biomass: Impacts of potassium hydroxide addition and air pretreatment prior to co-pyrolysis," *Bioresour. Technol.*, vol. 171, pp. 88–94, 2014.

[110] J. V. Headley, K. M. Peru, and M. P. Barrow, "Mass spectrometric characterization of naphthenic acids in environmental samples: A review," *Mass Spectrom. Rev.*, vol. 28, no. 1, pp. 121–134, 2009.

[111] C. Janfelt, R. Grsbll, and F. R. Lauritsen, "Portable electrospray ionization mass spectrometry (esi-ms) for analysis of contaminants in the field," *Int. J. Environ. Anal. Chem.*, vol. 92, no. 4, pp. 397–404, 2011.

[112] N. Sanders, E. Sokol, R. Perry, G. Huang, R. Noll, J. Duncan, and R. Cooks, "Hand-held mass spectrometer for environmentally relevant analytes using a variety of sampling and ionization methods," *Eur. J. Mass Spectrom.*, vol. 16, no. 1, pp. 11–20, 2010.

[113] C. C. Mulligan, N. Talaty, and R. G. Cooks, "Desorption electrospray ionization with a portable mass spectrometer: in situ analysis of ambient surfaces," *Chem. Commun.*, no. 16, pp. 1709–1711, 2006.

[114] R. G. Cooks, Z. Ouyang, Z. Takats, and J. M. Wiseman, "Ambient mass spectrometry," *Science*, vol. 311, no. 5767, pp. 1566–1570, 2006.

[115] C.-C. Hsu and P. C. Dorrestein, "Visualizing life with ambient mass spectrometry," *Curr. Opin. Biotechnol.*, vol. 31, pp. 24–34, 2015.

[116] S. D. Richardson, "Environmental mass spectrometry: Emerging contaminants and current issues," *Anal. Chem.*, vol. 84, no. 2, pp. 747–778, 2012.

[117] J. S. Clemente and P. M. Fedorak, "A review of the occurrence, analyses, toxicity, and biodegradation of naphthenic acids," *Chemosphere*, vol. 60, no. 5, pp. 585–600, 2005.

[118] J. L. Kerwin, A. M. Wiens, and L. H. Ericsson, "Identification of fatty acids by electrospray mass spectrometry and tandem mass spectrometry," *J. Mass Spectrom.*, vol. 31, no. 2, pp. 184–192, 1996.

[119] E. Davoli and M. Gross, "Charge remote fragmentation of fatty acids cationized with alkaline earth metal ions," *J. Am. Soc. Mass Spectrom.*, vol. 1, no. 4, pp. 320–324, 1990.

[120] S. Trimpin, D. E. Clemmer, and C. N. McEwen, "Charge-remote fragmentation of lithiated fatty acids on a tof-tof instrument using matrix-ionization," *J. Am. Soc. Mass Spectrom.*, vol. 18, no. 11, pp. 1967–1972, 2007.

[121] J. Crockett, M. Gross, W. Christie, and R. Holman, "Collisional activation of a series of homoconjugated octadecadienoic acids with fast atom bombardment and tandem mass spectrometry," *J. Am. Soc. Mass Spectrom.*, vol. 1, no. 2, pp. 183–191, 1990.

[122] C. Afonso, A. Riu, Y. Xu, F. Fournier, and J.-C. Tabet, "Structural characterization of fatty acids cationized with copper by electrospray ionization mass spectrometry under low-energy collision-induced dissociation," *J. Mass Spectrom.*, vol. 40, no. 3, pp. 342–349, 2005.

[123] J. Zirrolli, E. Davoli, L. Bettazzoli, M. Gross, and R. Murphy, "Fast atom bombardment and collision-induced dissociation of prostaglandins and thromboxanes: Some examples of charge remote fragmentation," *J. Am. Soc. Mass Spectrom.*, vol. 1, no. 4, pp. 325–335, 1990.

[124] N. Zehethofer, D. M. Pinto, and D. A. Volmer, "Plasma free fatty acid profiling in a fish oil human intervention study using ultra-performance liquid chromatography/electrospray ionization tandem mass spectrometry," *Rapid Commun. Mass Spectrom.*, vol. 22, no. 13, pp. 2125–2133, 2008.

[125] R. K. Cannan and A. Kibrick, "Complex formation between carboxylic acids and divalent metal cations," *J. Am. Chem. Soc.*, vol. 60, no. 10, pp. 2314–2320, 1938.

[126] N. J. Jensen, K. B. Tomer, and M. L. Gross, "Gas-phase ion decomposition occurring remote to a charge site," *J. Am. Chem. Soc.*, vol. 107, no. 7, pp. 1863–1868, 1985.